



SCUOLA INTERNAZIONALE SUPERIORE DI STUDI AVANZATI - INTERNATIONAL SCHOOL FOR ADVANCED STUDIES
I-34014 Trieste ITALY - Via Beirut 4 - Tel. [+39-40-37871 - Telex:460269 SISSA I - Fax: [+39-40-3787528

SISSA Lecture notes on Numerical methods for strongly correlated electrons

Sandro Sorella and Federico Becca

Academic year 2014-2015, 5th draft, printed on June 21, 2016

Summary

In these lectures we review some of the most recent computational techniques for computing the ground state of strongly correlated systems. All methods are based on projection techniques and are generally approximate. There are two different types of approximations, the first one is the truncation of the huge Hilbert space in a smaller basis that can be systematically increased until convergence is reached. Within this class of methods we will describe the Lanczos technique, modern Configuration Interaction schemes, aimed at improving the simplest Hartee-Fock calculation, until the most recent Density Matrix Renormalization Group. Another branch of numerical methods, uses instead a Monte Carlo sampling of the full Hilbert space. In this case there is no truncation error, but the approximation involved are due to the difficulty in sampling exactly the signs of a non trivial (e.g., fermionic) ground state wavefunction with a statistical method: the so called "sign problem". We will review the various techniques, starting from the variational approach to the so called "fixed node scheme", and the the most recent improvements on a lattice.

Contents

1	Introduction	7
1.1	Matrix formulation	8
1.2	Projection techniques	8
1.3	Variational principle	10
I	From Hartree-Fock to exact diagonalization methods	13
2	Hartree-Fock theory	15
2.1	Many-particle basis states for fermions and bosons.	15
2.2	Second quantization: brief outline.	18
2.2.1	Changing the basis set.	22
2.2.2	The field operators.	22
2.2.3	Operators in second quantization.	23
2.3	Why a quadratic hamiltonian is easy.	24
2.4	The Hartree-Fock equations.	24
2.5	Hartree-Fock in closed shell atoms: the example of Helium.	28
2.5.1	Beyond Hartree-Fock: Configuration Interaction.	31
2.6	Hartree-Fock fails: the H_2 molecule.	32
3	Exact diagonalization and Lanczos algorithm	37
3.1	Hubbard model	37

3.2	Two-site Hubbard problem: a toy model.	40
3.3	Lanczos algorithm	42
II Monte Carlo methods		47
4	Probability theory	49
4.1	Introduction	49
4.2	A bit of probability theory	50
4.2.1	Events and probability	50
4.2.2	Random variables, mean value and variance	52
4.2.3	The Chebyshev's inequality	53
4.2.4	The law of large numbers: consistency of the definition of probability . . .	54
4.2.5	Extension to continuous random variables and central limit theorem	55
5	Quantum Monte Carlo: The variational approach	59
5.1	Introduction: importance of correlated wavefunctions	59
5.2	Expectation value of the energy	60
5.3	Zero variance property	61
5.4	Markov chains: stochastic walks in configuration space	62
5.5	Detailed balance	63
5.6	The Metropolis algorithm	66
5.7	The bin technique for the estimation of error bars	68
6	Langevin molecular dynamics for classical simulations at finite T.	71
6.1	Discrete-time Langevin dynamics	71
6.2	From the Langevin equation to the Fokker-Planck equation	73
6.3	Langevin dynamics and Quantum Mechanics	74
6.4	Harmonic oscillator: solution of the Langevin dynamics	75
6.5	Second order Langevin dynamic	76

6.6	The Born-Oppenheimer approximation	77
6.7	Dealing with Quantum Monte Carlo noise	77
6.8	Canonical ensemble by Generalized Langevin Dynamics	79
6.9	Integration of the second order Langevin dynamics and relation with first order dynamics	80
7	Stochastic minimization	83
7.1	Wave function optimization	83
7.2	Stochastic reconfiguration method	84
7.2.1	Stochastic reconfiguration versus steepest descent method	86
7.2.2	Statistical bias of forces	88
7.2.3	Structural optimization	89
8	Green's function Monte Carlo	93
8.1	Exact statistical solution of model Hamiltonians: motivations	93
8.2	Single walker technique	93
8.2.1	Correlation functions	96
8.2.2	Convergence properties of the Markov process	97
8.3	Importance sampling	98
8.4	The limit $\Lambda \rightarrow \infty$ for the power method, namely continuous time approach	100
8.4.1	Local operator averages	101
8.5	Many walkers formulation	102
8.5.1	Carrying many configurations simultaneously	103
8.5.2	Bias control	105
8.6	The GFMC scheme with bias control	106
9	Reptation Monte Carlo	109
9.1	motivations	109
9.2	A simple path integral technique	109

9.3	Sampling $W(R)$	111
9.3.1	Move RIGHT $d = 1$	111
9.3.2	Move LEFT $d = -1$	111
9.4	Bounce algorithm	112
10	Fixed node approximation	115
10.1	Sign problem in the single walker technique	115
10.2	An example on the continuum	115
10.3	Effective hamiltonian approach for the lattice fixed node	119
11	Auxiliary field quantum Monte Carlo	123
11.1	Trotter approximation	123
11.2	Auxiliary field transformation	124
11.3	A simple path integral technique	125
11.4	Some hint for an efficient and stable code	127
11.4.1	Stable imaginary time propagation of a Slater Determinant	127
11.4.2	Sequential updates	128
11.4.3	Delayed updates	130
11.4.4	No sign problem for attractive interactions, half-filling on bipartite lattices	131
A	Re-sampling methods	135
A.1	Jackknife	135
B	A practical reconfiguration scheme	137
B.1	An efficient implementation of the single walker algorithm	138
B.1.1	Second step: computation of correlation functions	138
C	O is a semipositive definite operator	141
D	E_γ^{FN} is a convex function of γ	143

Chapter 1

Introduction

The study of strongly correlated systems is becoming a subject of increasing interest due to the realistic possibility that in many physical materials, such as High-Tc superconductors, strong correlations between electrons may lead to an unexpected physical behavior, that cannot be explained within the conventional schemes, such as, for instance, mean-field or Fermi liquid theories.

Within standard textbook free-electron or quasi-free-electron theory it is difficult to explain insulating behavior when the number of electron per unit cell is odd. There are several examples of such "Mott insulators", especially within the transition metal oxides, like MnO. Ferromagnetism and antiferromagnetism, also, cannot be fully understood within a single particle formulation.

One of the most important models in strongly correlated systems, and today also relevant for High-Tc superconductors (the undoped compounds are antiferromagnetic), is the so-called Heisenberg model

Heisenberg
model

$$H = J \sum_{\langle i,j \rangle} \vec{S}_i \cdot \vec{S}_j = J \sum_{\langle i,j \rangle} [S_i^z S_j^z + \frac{1}{2}(S_i^+ S_j^- + \text{H.c.})] \quad (1.1)$$

where J is the so-called superexchange interaction ($J \approx 1500K > 0$ for the High-Tc), $\langle i, j \rangle$ denotes nearest-neighbor summation with periodic boundary conditions on a 2d square-lattice, say, and $\vec{S}_j = (S_j^x, S_j^y, S_j^z)$ are spin 1/2 operators on each site. Indeed on each site there are two possible states: the spin is up ($\sigma = 1/2$) or down ($\sigma = -1/2$) along the z-direction, thus implying $S_j^z |\sigma\rangle_j = \sigma |\sigma\rangle_j$. In this single-site basis (described by vectors $|\sigma\rangle_j$ with $\sigma = \pm 1/2$), the non-diagonal operators $S_j^+ = S_j^x + iS_j^y$ and $S_j^- = S_j^x - iS_j^y$ (i here is the imaginary unit) flip the spin on the site j , namely $S_j^\pm |\mp 1/2\rangle_j = |\pm 1/2\rangle_j$. More formally, the above simple relations can be derived by using the canonical commutation rules of spin operators, i.e., $[S_j^x, S_k^y] = i\delta_{j,k} S_j^z$ and antisymmetric permutations of x, y, z components. These commutation rules hold also for larger spin S ($2S + 1$ states on each site, with $S_j^z = -S, -S + 1, \dots, S$), and the Heisenberg model can be simply extended to larger spin values. (Such an extension is also important because, for many materials, the electron spin on each atomic site is not restricted to be 1/2, essentially due to many-electron multiplets with high spin, according to Hund's first rule.)

1.1 Matrix formulation

Having defined the single site Hilbert space, the hamiltonian H is defined for an arbitrary number of sites, in the precise sense that the problem is mapped onto a diagonalization of a finite square matrix. All the states $|x\rangle$ can be labeled by an integer x denoting the rows and columns of the matrix. A single element $|x\rangle$ denotes a particular configuration where the spins are defined on each site:

$$|x\rangle = \prod_j |\sigma_j(x)\rangle_j$$

For a two-site system, for instance, we can define:

$$\begin{aligned} |1\rangle &= |\uparrow, \downarrow\rangle \\ |2\rangle &= |\downarrow, \uparrow\rangle \\ |3\rangle &= |\uparrow, \uparrow\rangle \\ |4\rangle &= |\downarrow, \downarrow\rangle \end{aligned}$$

and the matrix elements $H_{x,x'} = \langle x|H|x'\rangle$ can be easily computed:

$$H_{x,x'} = \begin{pmatrix} -J/4 & J/2 & 0 & 0 \\ J/2 & -J/4 & 0 & 0 \\ 0 & 0 & J/4 & 0 \\ 0 & 0 & 0 & J/4 \end{pmatrix} \quad (1.2)$$

The diagonalization is therefore simple and does not require any computer.

What happens, however, when we increase the number of sites? The problem becomes complex as the dimension of the Hilbert space, and consequently the size of the matrix, increases *exponentially* with the number of sites N , precisely as 2^N in the Heisenberg case.. In this case even for writing the matrix elements of a $2^N \times 2^N$ square matrix, the computational time and memory required is prohibitive large already for $N = 16$ (the memory required is ≈ 10 Gygabytes).

At present, there is no method that allows the general solution of a generic many-body hamiltonian with a computational effort scaling polynomially with the system size N . The complexity of the many-body problem is generally exponential, and this is the main reason why strong correlation is such a difficult task.

1.2 Projection techniques

In order to reduce the difficulty of the numerical task, one can notice that the matrix (1.2) has many zeros. We will assume, henceforth, for simplicity that the ground state is unique. Although the number of possible configurations $|x\rangle$ is exponential large, whenever the Hamiltonian acts on a single configuration $|x\rangle \rightarrow H|x\rangle$, it generates only a relatively small number, of order $\simeq N$, of new configurations. In the Heisenberg model case (1.1), the number of possible new configurations

is equal to the number of possible spin flips on $|x\rangle$ which is limited to DN , where D is the dimensionality and N the number of electrons. The $2^N \times 2^N$ matrix $H_{x',x}$ is therefore very *sparse*, as there are at most $DN2^N$ non-zero elements over 2^{2N} entries. In such a case methods that are based on iterations, rather than explicit diagonalization of the hamiltonian, are by far more efficient. Sparse matrix

Let us take an initial wavefunction $\psi_0(x) = \psi_G(x)$ with non-zero overlap with the exact ground state $\phi_0(x)$, e.g., a randomly generated vector in the 2^N Hilbert space. The exact ground state can be filtered out iteratively by applying, for instance, the so-called *power method*: Power method

$$\psi_{n+1}(x) = \sum_{x'} (\Lambda \delta_{x,x'} - H_{x,x'}) \psi_n(x') \quad (1.3)$$

Due to the sparseness of the matrix, each iteration (1.3) is relatively cheap, computationally, as only the knowledge of the non vanishing matrix elements are required.

It is simple to show that for large number of iterations n the iterated wavefunction ψ_n converges to the ground state $\phi_0(x)$ for a large enough constant Λ . Indeed, we can expand the initial wavefunction in the basis of eigenstates ϕ_i of H , with corresponding energies E_i , E_0 being the ground state energy:

$$|\psi_G\rangle = \sum_i a_i |\phi_i\rangle \quad (1.4)$$

with $a_i = \langle \phi_i | \psi_G \rangle$, and the normalization condition:

$$\sum_i a_i^2 = 1. \quad (1.5)$$

Thus at the iteration n :

$$\psi_n = \sum_i a_i (\Lambda - E_i)^n |\phi_i\rangle. \quad (1.6)$$

It is clear that, by increasing n , the ground state component in expansion (1.6) is growing much faster than all the other ones, provided

$$\text{Max}_i |\Lambda - E_i| = |\Lambda - E_0|, \quad (1.7)$$

which is generally verified for large enough Λ , namely, as it is easy to verify, for $\Lambda > \Lambda_{\text{Min}} = \frac{E_{\text{Max}} + E_0}{2}$, where E_{Max} is the maximum eigenvalue of H , and Λ_{min} is the minimum possible Λ to achieve convergence to the ground state. Finally, apart for an irrelevant normalization factor $(\Lambda - E_0)^n$, the convergence of ψ_n to ϕ_0 is obtained with an exponentially increasing accuracy in n , namely with an error proportional to p^n , where $p = \text{Max}_{i \neq 0} \frac{|\Lambda - E_i|}{|\Lambda - E_0|}$. It is not important to know exactly the value of Λ_{Min} , as the method works for any larger Λ , and indeed the choice of $\Lambda = \Lambda_{\text{Min}}$ is not the most efficient one. In fact in this case, both the ground state and the eigenstate corresponding to E_{Max} are filtered out by the power method.

A remarkable improvement in the convergence of the power method is obtained with the so called *Lanczos technique*, which will be described in the forthcoming lectures.

Exercise 1.1 The power method when the Ground State is not unique. Suppose that the ground state is not unique, i.e., there are many states with the lowest possible energy E_0 (e.g.,

in the ferromagnetic case). Is the convergence of the power method exponential also in this case? Does the final state $\psi_n(x)$ for large n depends on the initial wavefunction? How can one remedy to this drawback of the power-method and determine **all** the degenerate ground states?

1.3 Variational principle

In general, even with exact projection methods the problem of exponential complexity 2^N is not solved, and for generic model hamiltonian H it is impossible to work with system sizes of order $N > \sim 30$, which is far from being satisfactory for delicate questions like existence or non existence of antiferromagnetic long-range-order in the 2D antiferromagnetic Heisenberg model: this issue was indeed highly debated in the early stage of High-Tc.

All reliable approximate techniques are based on the variational principle and will be described in details in the forthcoming sections. Here we want to recall the basis of the variational principle.

Given any approximate state ψ_G for the ground state ϕ_0 , the variational energy E_V is defined by:

$$E_V = \langle \psi_G | H | \psi_G \rangle . \quad (1.8)$$

Using the expansion (1.4) it is readily obtained that

$$\epsilon \stackrel{def}{=} E_V - E_0 = \sum_{i \neq 0} |a_i|^2 (E_i - E_0) \geq 0 . \quad (1.9)$$

Thus, any trial state ψ_G provides an upper bound of the exact energy.

The relation (1.9) is the basis of approximate techniques. Essentially, given any approximation ψ_G of ϕ_0 , all computational effort is devoted to minimizing the variational energy E_V consistently with the chosen approximation (truncation of Hilbert space or whatever).

In this section we analyze in what sense an approximate wavefunction with given “distance” in energy ϵ from the exact ground state one, can be considered as a good approximation of the many-body ground state ϕ_0 . A crucial role is played by the gap $\Delta = E_1 - E_0 > 0$ (always finite and non-vanishing in a finite system with N electrons) to the first excited state. From the relation (1.9) and the fact that $E_i \geq E_0 + \Delta$, by definition of Δ , it simply follows that

$$\epsilon = \sum_{i \neq 0} |a_i|^2 (E_i - E_0) \geq \Delta \sum_{i \neq 0} |a_i|^2 . \quad (1.10)$$

From the normalization condition (1.5), we finally find

$$\eta = 1 - |a_0|^2 \leq \frac{\epsilon}{\Delta} . \quad (1.11)$$

This relation tells us that in order to have an accurate approximation of the ground state, namely $\eta = 1 - |a_0|^2 \ll 1$, a sufficient condition is that the error ϵ in the variational energy has to be much smaller than the gap Δ to the first excited state. If we consider that the gap Δ for a system

of N electron is typically decreasing with N , we can easily understand how difficult it is to fulfill (1.11) with a numerical approach.

This difficulty is further amplified when estimating the maximum error that we can expect in calculating correlation functions, i.e., generally speaking, expectation values of Hermitian operators \hat{O} (say, the value of the spin $\hat{O} = S_i^z$ at site i) on the state ϕ_0 . Given that (1.11) is satisfied with rather good accuracy, say $\eta \approx 10^{-4}$, what we can expect for $\langle \psi_G | \hat{O} | \psi_G \rangle$? Defining λ to be the maximum eigenvalue (in modulus) of the operator \hat{O} (for instance, $\lambda = 1/2$ for $\hat{O} = S_i^z$), we can denote by $O_{i,j} = \langle \phi_i | \hat{O} | \phi_j \rangle$ the matrix elements of the operator \hat{O} in the basis of eigenstates of H , $O_{0,0}$ being the exact ground state expectation value. Using again the expansion (1.6), and a bit more complicated bounds (left for exercise), we find:

$$|\langle \psi_G | \hat{O} | \psi_G \rangle - O_{0,0}| \leq \eta O_{0,0} + \lambda \sqrt{\eta} \sqrt{|a_0|^2 + 1}. \quad (1.12)$$

This relation shows that the accuracy in correlation functions is more problematic than that on the ground state energy, with a term proportional to $\sqrt{\eta}$. Summarizing, we have shown that with a given accuracy in energy ϵ/Δ , we can expect only *the square root of this accuracy for correlation functions*. This is the most important drawback of all approximate techniques. However, in some cases it has been possible to obtain such an accuracy and have a good control of correlation functions (not more than half of the significant digits obtained for the energy).

Part I

From Hartree-Fock to exact diagonalization methods

Chapter 2

Hartree-Fock theory

Dealing with a system of N interacting quantum particles, either fermions or bosons, is a complicated business. In this chapter we will present the simplest approach to such a problem, the Hartree-Fock (HF) theory. We will see Hartree-Fock at work in closed shell atoms, specifically He, where, as we will show, it performs very well. We will understand the reason for this good performance, analyzing briefly a scheme that goes beyond HF, the so-called *Configuration Interaction* technique, popular among quantum chemists. Finally, we will appreciate the pitfalls of HF, induced by quasi-degeneracy of single-particle eigenvalues, in an extremely simple molecule like H_2 . Before we embark with HF, however, it is essential to learn the basic properties of the many-particle states which are physically allowed. We will review these basic properties and introduce the formalism of second quantization in the next two sections.

2.1 Many-particle basis states for fermions and bosons.

Suppose we have a system of N identical particles. Consider an appropriate basis set of *single-particle states* $|\alpha\rangle$. Generally speaking, each one particle state can be expressed in terms of real-space spin dependent wavefunctions, henceforth named spin orbitals, by taking the scalar product with the position-spin eigenstates $|r\rangle = |\mathbf{r}\rangle_o|\sigma\rangle_s$,¹

$$\psi_\alpha(r) \stackrel{def}{=} \langle r|\alpha\rangle \quad (2.1)$$

Often the spin and the orbital dependence in the spin orbital is factored in an orbital part $\phi_\alpha(\mathbf{r})$ and a spin part $\chi_\alpha(\sigma)$:

$$\psi_\alpha(r) = \phi_\alpha(\mathbf{r}) \times \chi_\alpha(\sigma) . \quad (2.2)$$

¹We will often use the symbol r to mean the combination of \mathbf{r} , the position of a particle, and σ , its spin projection along the z-axis.

where the spin dependent function χ_α is usually a Kronecker δ , selecting a given value of the spin component $\sigma_\alpha = \pm\frac{1}{2}$, namely $\chi_\alpha(\sigma) = \delta_{\sigma_\alpha, \sigma}$ ²

Examples of such single particle spin-orbitals might be the *plane waves*, $\alpha = (\mathbf{k}, \sigma_\alpha)$ and $\phi_\alpha(\mathbf{r}) = e^{i\mathbf{k}\cdot\mathbf{r}}$, the *hydrogenoid atomic orbitals*, $\alpha = (nlm, \sigma_\alpha)$ and $\phi_{nlm}(\mathbf{r}) = R_n(r)Y_{lm}(\hat{\Omega})$, the Bloch or the Wannier states of a crystalline solid, etc. whichever is more appropriate to describe the system under consideration.

A state for N identical particles may be written down as product of N single particle states

$$|\alpha_1, \alpha_2, \dots, \alpha_N\rangle = |\alpha_1\rangle \cdot |\alpha_2\rangle \cdots |\alpha_N\rangle, \quad (2.3)$$

Product
states

or, in terms of wavefunctions,

$$(r_1\sigma_1, r_2, \sigma_2 \cdots, r_N\sigma_N | \alpha_1, \alpha_2, \dots, \alpha_N) = \psi_{\alpha_1}(\mathbf{r}_1, \sigma_1) \psi_{\alpha_2}(\mathbf{r}_2, \sigma_2) \cdots \psi_{\alpha_N}(\mathbf{r}_N, \sigma_N). \quad (2.4)$$

However, such product wavefunctions are *not allowed* for systems of identical particles. The allowed states depend on the *statistics* of the particles under consideration, and must be *totally antisymmetric* under permutations of the particle labels, for fermions, or *totally symmetric* for bosons (see below). This permutation symmetry, however, is easy to enforce by applying, essentially, a projection operator to the product states. Consider a permutation $P : (1, \dots, N) \rightarrow (P_1, \dots, P_N)$, and define a permutation operator \mathbf{P} to act on product states in the following way:

$$\mathbf{P} |\alpha_1, \alpha_2, \dots, \alpha_N\rangle \stackrel{def}{=} |\alpha_{P_1}, \alpha_{P_2}, \dots, \alpha_{P_N}\rangle. \quad (2.5)$$

Define now $(-1)^P$ to be the parity of the permutation P . This will appear shortly in constructing the antisymmetric states for fermions. In order to have a notation common to both fermion and boson cases, we introduce the symbol $\xi = -1$ for fermions and $\xi = +1$ for bosons, and form the correctly *symmetrized states*³

Symmetrized
states

$$|\alpha_1, \alpha_2, \dots, \alpha_N\rangle \stackrel{def}{=} \frac{1}{\sqrt{N!}} \sum_P \xi^P \mathbf{P} |\alpha_1, \alpha_2, \dots, \alpha_N\rangle = \frac{1}{\sqrt{N!}} \sum_P \xi^P |\alpha_{P_1}, \alpha_{P_2}, \dots, \alpha_{P_N}\rangle, \quad (2.6)$$

where the sum is performed over the $N!$ possible permutations of the labels. Indeed, it is very simple to verify that

Exercise 2.1 *The symmetrized states $|\alpha_1, \alpha_2, \dots, \alpha_N\rangle$ satisfy the relationship*

$$\mathbf{P} |\alpha_1, \alpha_2, \dots, \alpha_N\rangle = |\alpha_{P_1}, \alpha_{P_2}, \dots, \alpha_{P_N}\rangle = \xi^P |\alpha_1, \alpha_2, \dots, \alpha_N\rangle. \quad (2.7)$$

This is the precise formulation of what one means in saying that a state is totally antisymmetric (for fermions, $\xi = -1$) or totally symmetric (for bosons, $\xi = 1$).

²The requirement of orthonormality might be relaxed, if necessary, at the price of introducing the so-called overlap matrix.

³We will consistently use the symbol $|\dots\rangle$, with round parenthesis, for the product states, and the ket notation $|\dots\rangle$ for symmetrized states.

Perhaps a more familiar expression is obtained by writing down the corresponding real-space wavefunctions: ⁴

$$\begin{aligned}\psi_{\alpha_1, \alpha_2, \dots, \alpha_N}(r_1, r_2, \dots, r_N) &\stackrel{def}{=} (r_1, r_2, \dots, r_N | \alpha_1, \alpha_2, \dots, \alpha_N) \\ &= \frac{1}{\sqrt{N!}} \sum_P \xi^P \psi_{\alpha_{P_1}}(r_1) \psi_{\alpha_{P_2}}(r_2) \cdots \psi_{\alpha_{P_N}}(r_N).\end{aligned}\quad (2.8)$$

For the case of fermions, this is the so-called *Slater determinant*

Slater
determinant

$$\begin{aligned}\psi_{\alpha_1, \alpha_2, \dots, \alpha_N}(r_1, r_2, \dots, r_N) &= \frac{1}{\sqrt{N!}} \sum_P (-1)^P \psi_{\alpha_{P_1}}(r_1) \psi_{\alpha_{P_2}}(r_2) \cdots \psi_{\alpha_{P_N}}(r_N) \\ &= \frac{1}{\sqrt{N!}} \det \begin{bmatrix} \psi_{\alpha_1}(r_1) & \psi_{\alpha_2}(r_1) & \cdots & \psi_{\alpha_N}(r_1) \\ \psi_{\alpha_1}(r_2) & \psi_{\alpha_2}(r_2) & \cdots & \psi_{\alpha_N}(r_2) \\ \vdots & \cdots & \ddots & \vdots \\ \psi_{\alpha_1}(r_N) & \psi_{\alpha_2}(r_N) & \cdots & \psi_{\alpha_N}(r_N) \end{bmatrix}.\end{aligned}\quad (2.9)$$

The corresponding expression for Bosons is called a *permanent*, but it is much less nicer than the determinant, computationally.

For Fermions, it is very simple to show that the *same label cannot appear twice in the state*, an expression of the *Pauli principle*. Indeed, suppose $\alpha_1 = \alpha_2$, for instance. Then, by applying the permutation $P : (1, 2, 3, \dots, N) \rightarrow (2, 1, 3, \dots, N)$ which transposes 1 and 2, we have, on one hand, no effect whatsoever on the labels Pauli principle

$$\mathbf{P}|\alpha_1, \alpha_1, \alpha_3, \dots, \alpha_N\rangle = |\alpha_{P_1}, \alpha_{P_2}, \alpha_{P_3}, \dots, \alpha_{P_N}\rangle = |\alpha_1, \alpha_1, \alpha_3, \dots, \alpha_N\rangle,$$

but, on the other hand, the action of \mathbf{P} must result in a minus sign because the state is totally antisymmetric

$$\mathbf{P}|\alpha_1, \alpha_1, \alpha_3, \dots, \alpha_N\rangle = (-1)^P |\alpha_1, \alpha_1, \alpha_3, \dots, \alpha_N\rangle = -|\alpha_1, \alpha_1, \alpha_3, \dots, \alpha_N\rangle,$$

and a state equal to minus itself is evidently *zero*. Perhaps more directly, we can see the result from the expression of the corresponding Slater determinant, which has the first two columns which are identical, and therefore vanishes, by a known properties of determinants. So, if we define

$$n_\alpha = \text{number of times the label } \alpha \text{ appears in } (\alpha_1, \dots, \alpha_N), \quad (2.10)$$

then Pauli principle requires $n_\alpha \leq 1$. For Bosons, on the contrary, there is no limit to n_α .

A few examples should clarify the notation. Consider two particles occupying, in the plane-wave basis, $\alpha_1 = \mathbf{k}_1, \uparrow$, and $\alpha_2 = \mathbf{k}_2, \downarrow$ or $\alpha_2 = \mathbf{k}_2, \uparrow$ (we will do both spin calculations in one shot). The correctly symmetrized states are: Examples

$$(r_1, r_2 | \mathbf{k}_1 \uparrow, \mathbf{k}_2 \downarrow (\uparrow)) = \frac{1}{\sqrt{2}} [\phi_{\mathbf{k}_1}(\mathbf{r}_1) \phi_{\mathbf{k}_2}(\mathbf{r}_2) \chi_{\uparrow}(\sigma_1) \chi_{\downarrow(\uparrow)}(\sigma_2) \mp \phi_{\mathbf{k}_2}(\mathbf{r}_1) \phi_{\mathbf{k}_1}(\mathbf{r}_2) \chi_{\downarrow(\uparrow)}(\sigma_1) \chi_{\uparrow}(\sigma_2)], \quad (2.11)$$

⁴Observe that we take the scalar product with the *product state* $|r_1, \dots, r_N\rangle$.

where the upper sign refers to fermions, and $\phi_{\mathbf{k}}(\mathbf{r}) = e^{i\mathbf{k}\cdot\mathbf{r}}$. Notice that, in general, such a state is not an eigenvector of the total spin. Exceptions are: i) when both spins are \uparrow , in which case you obtain a maximally polarized triplet state:

$$(r_1, r_2 | \mathbf{k}_1 \uparrow, \mathbf{k}_2 \uparrow) = \frac{1}{\sqrt{2}} [\phi_{\mathbf{k}_1}(\mathbf{r}_1)\phi_{\mathbf{k}_2}(\mathbf{r}_2) \mp \phi_{\mathbf{k}_2}(\mathbf{r}_1)\phi_{\mathbf{k}_1}(\mathbf{r}_2)] \chi_{\uparrow}(\sigma_1)\chi_{\uparrow}(\sigma_2), \quad (2.12)$$

or when the two orbital labels coincide. In general, good eigenstates of the total spin are obtained only by linear combination of more than one symmetrized state. For the example above, for instance, it is simple to show that

$$\frac{1}{\sqrt{2}} [(r_1, r_2 | \mathbf{k}_1 \uparrow, \mathbf{k}_2 \downarrow) \pm (r_1, r_2 | \mathbf{k}_1 \downarrow, \mathbf{k}_2 \uparrow)] \quad (2.13)$$

is a triplet (upper sign) or a singlet (lower sign).

Normaliza-
tion

The normalization, or more generally the scalar product, of symmetrized states involves a bit of permutation algebra.

Exercise 2.2 Show that the scalar product between two correctly-symmetrized states $|\alpha_1, \alpha_2, \dots, \alpha_N\rangle$ and $|\alpha'_1, \alpha'_2, \dots, \alpha'_N\rangle$ is non-zero only if the set of labels $(\alpha'_1, \alpha'_2, \dots, \alpha'_N)$ is a permutation of $(\alpha_1, \alpha_2, \dots, \alpha_N)$. Verify then that:

$$\langle \alpha'_1, \alpha'_2, \dots, \alpha'_N | \alpha_1, \alpha_2, \dots, \alpha_N \rangle = \xi^P \prod_{\alpha} n_{\alpha}!$$

where P is a permutation that makes the labels to coincide, and n_{α} is the number of times a certain label α appears.

As a consequence, fermionic symmetrized states (Slater determinants) are normalized to 1, since $n_{\alpha} \leq 1$, while bosonic ones not necessarily. One can easily normalize bosonic states by defining

$$|\{n_{\alpha}\}\rangle = \frac{1}{\sqrt{\prod_{\alpha} n_{\alpha}!}} |\alpha_1, \dots, \alpha_N\rangle \quad (2.14)$$

where we simply label the normalized states by the occupation number n_{α} of each label, since the order in which the labels appear does not matter for Bosons.

Expansion of
general $|\Psi\rangle$

We conclude by stressing the fact that the symmetrized states constructed are simply a *basis set* for the many-particle Hilbert space, in terms of which one can expand any N -particle state $|\Psi\rangle$

$$|\Psi\rangle = \sum_{\alpha_1, \alpha_2, \dots, \alpha_N} C_{\alpha_1, \alpha_2, \dots, \alpha_N} |\alpha_1, \alpha_2, \dots, \alpha_N\rangle, \quad (2.15)$$

with appropriate coefficients $C_{\alpha_1, \alpha_2, \dots, \alpha_N}$. The whole difficulty of interacting many-body systems is that the relevant low-lying excited states of the systems often involve a large (in principle infinite) number of symmetrized states in the expansion.

2.2 Second quantization: brief outline.

It is quite evident that the only important information contained in the symmetrized states $|\alpha_1, \alpha_2, \dots, \alpha_N\rangle$ is how many times every label α is present, which we will indicate by n_{α} ; the

rest is automatic permutation algebra. The introduction of creation operators a_α^\dagger is a device by which we take care of the labels present in a state and of the permutation algebra in a direct way.

Given any single-particle orthonormal basis set $\{|\alpha\rangle\}$ we define operators a_α^\dagger which satisfy the following rule: ⁵ Creation operators

$$\boxed{\begin{aligned} a_\alpha^\dagger|0\rangle &\stackrel{def}{=} |\alpha\rangle \\ a_\alpha^\dagger|\alpha_1, \alpha_2, \dots, \alpha_N\rangle &\stackrel{def}{=} |\alpha, \alpha_1, \alpha_2, \dots, \alpha_N\rangle \end{aligned}} \quad (2.16)$$

The first is also the definition of a new state $|0\rangle$, called *vacuum* or state with no particles, which should not be confused with the zero of a Hilbert space: infact, we postulate $\langle 0|0\rangle = 1$. It is formally required in order to be able to obtain the original single-particle states $|\alpha\rangle$ by applying an operator that creates a particle with the label α to *something*: that “something” has no particles, and obviously no labels whatsoever. The second equation defines the action of the creation operator a_α^\dagger on a generic correctly-symmetrized state. Notice immediately that, as defined, a_α^\dagger does two things in one shot: 1) it creates a new label α in the state, 2) it performs the appropriate permutation algebra in such a way that the resulting state is a correctly-symmetrized state. Iterating the creation rule starting from the vacuum $|0\rangle$, it is immediate to show that The vacuum

$$\boxed{a_{\alpha_1}^\dagger a_{\alpha_2}^\dagger \dots a_{\alpha_N}^\dagger |0\rangle = |\alpha_1, \alpha_2, \dots, \alpha_N\rangle} \quad (2.17)$$

We can now ask ourselves what commutation properties must the operators a_α^\dagger satisfy in order to enforce the correct permutation properties of the resulting states. This is very simple. Since

$$|\alpha_2, \alpha_1, \dots, \alpha_N\rangle = \xi|\alpha_1, \alpha_2, \dots, \alpha_N\rangle$$

for every possible state and for every possible choice of α_1 and α_2 , it must follow that

$$a_{\alpha_2}^\dagger a_{\alpha_1}^\dagger = \xi a_{\alpha_1}^\dagger a_{\alpha_2}^\dagger, \quad (2.18)$$

i.e., creation operators *anticommute* for Fermions, *commute* for Bosons. Explicitly:

$$\{a_{\alpha_1}^\dagger, a_{\alpha_2}^\dagger\} = 0 \quad \text{for Fermions} \quad (2.19)$$

$$[a_{\alpha_1}^\dagger, a_{\alpha_2}^\dagger] = 0 \quad \text{for Bosons}, \quad (2.20)$$

with $\{A, B\} = AB + BA$ (the anticommutator) and $[A, B] = AB - BA$ (the commutator).

The rules for a_α^\dagger clearly fix completely the rules of action of its *adjoint* $a_\alpha = (a_\alpha^\dagger)^\dagger$, since it must satisfy the obvious relationship Destruction operators

$$\langle \Psi_2 | a_\alpha \Psi_1 \rangle = \langle a_\alpha^\dagger \Psi_2 | \Psi_1 \rangle \quad \forall \Psi_1, \Psi_2, \quad (2.21)$$

where Ψ_1, Ψ_2 are correctly-symmetrized many-particle basis states. First of all, by taking the adjoint of the Eqs. (2.19), it follows that

$$\{a_{\alpha_1}, a_{\alpha_2}\} = 0 \quad \text{for Fermions} \quad (2.22)$$

$$[a_{\alpha_1}, a_{\alpha_2}] = 0 \quad \text{for Bosons}. \quad (2.23)$$

⁵It might seem strange that one defines directly the *adjoint* of an operator, instead of defining the operator a_α itself. The reason is that the action of a_α^\dagger is simpler to write.

There are a few simple properties of a_α that one can show by using the rules given so far. For instance,

$$\boxed{a_\alpha|0\rangle = 0 \quad \forall \alpha,} \quad (2.24)$$

since $\langle \Psi_2 | a_\alpha | 0 \rangle = \langle a_\alpha^\dagger \Psi_2 | 0 \rangle = 0, \forall \Psi_2$, because of the mismatch in the number of particles.⁶ More generally, it is simple to prove that that an attempt at destroying label α , by application of a_α , gives zero if α is not present in the state labels,

$$\boxed{a_\alpha |\alpha_1, \alpha_2, \dots, \alpha_N\rangle = 0 \quad \text{if } \alpha \notin (\alpha_1, \alpha_2, \dots, \alpha_N).} \quad (2.25)$$

Consider now the case $\alpha \in (\alpha_1, \dots, \alpha_N)$. Let us start with Fermions. Suppose α is just in first position, $\alpha = \alpha_1$. Then, it is simple to show that

$$a_{\alpha_1} |\alpha_1, \alpha_2, \dots, \alpha_N\rangle = |\hat{\alpha}_1, \alpha_2, \dots, \alpha_N\rangle = |\alpha_2, \dots, \alpha_N\rangle, \quad (2.26)$$

where by $\hat{\alpha}_1$ we simply mean a state with the label α_1 missing (clearly, it is a $N - 1$ particle state). To convince yourself that this is the correct result, simply take the scalar product of both sides of Eq. (2.26) with a generic $N - 1$ particle state $|\alpha'_2, \dots, \alpha'_N\rangle$, and use the adjoint rule. The left hand side gives:

$$\langle \alpha'_2, \dots, \alpha'_N | a_{\alpha_1} |\alpha_1, \alpha_2, \dots, \alpha_N\rangle = \langle \alpha_1, \alpha'_2, \dots, \alpha'_N | \alpha_1, \alpha_2, \dots, \alpha_N\rangle,$$

which is equal to $(-1)^P$ when P is a permutation bringing $(\alpha_2, \dots, \alpha_N)$ into $(\alpha'_2, \dots, \alpha'_N)$, and 0 otherwise. The right hand side gives

$$\langle \alpha'_2, \dots, \alpha'_N | \alpha_2, \dots, \alpha_N\rangle,$$

and coincides evidently with the result just stated for the left hand side. If α is not in first position, say $\alpha = \alpha_i$, then you need to first apply a permutation to the state that brings α_i in first position, and proceed with the result just derived. The permutation brings an extra factor $(-1)^{i-1}$, since you need $i - 1$ transpositions. As a result:

$$\boxed{a_{\alpha_i} |\alpha_1, \alpha_2, \dots, \alpha_N\rangle = (-1)^{i-1} |\alpha_1, \alpha_2, \dots, \hat{\alpha}_i, \dots, \alpha_N\rangle.} \quad (2.27)$$

The bosonic case needs a bit of extra care for the fact that the label α might be present *more than once*.

Exercise 2.3 Show that for the bosonic case the action of the destruction operator is

$$\boxed{a_{\alpha_i} |\alpha_1, \alpha_2, \dots, \alpha_N\rangle = n_{\alpha_i} |\alpha_1, \alpha_2, \dots, \hat{\alpha}_i, \dots, \alpha_N\rangle.} \quad (2.28)$$

Armed with these results we can finally prove the most difficult commutation relations, those involving a a_α with a $a_{\alpha'}^\dagger$. Consider first the case $\alpha \neq \alpha'$ and do the following.

Exercise 2.4 Evaluating the action of $a_\alpha a_{\alpha'}^\dagger$ and of $a_{\alpha'}^\dagger a_\alpha$ on a generic state $|\alpha_1, \dots, \alpha_N\rangle$, show that

$$\{a_\alpha, a_{\alpha'}^\dagger\} = 0 \quad \text{for Fermions} \quad (2.29)$$

$$[a_\alpha, a_{\alpha'}^\dagger] = 0 \quad \text{for Bosons.} \quad (2.30)$$

⁶A state which has vanishing scalar product with any state of a Hilbert space, must be the zero.

Next, let us consider the case $\alpha = \alpha'$. For fermions, if $\alpha \notin (\alpha_1, \dots, \alpha_N)$ then

$$a_\alpha a_\alpha^\dagger |\alpha_1, \dots, \alpha_N\rangle = a_\alpha |\alpha, \alpha_1, \dots, \alpha_N\rangle = |\alpha_1, \dots, \alpha_N\rangle,$$

while

$$a_\alpha^\dagger a_\alpha |\alpha_1, \dots, \alpha_N\rangle = 0.$$

If, on the other hand, $\alpha \in (\alpha_1, \dots, \alpha_N)$, say $\alpha = \alpha_i$, then

$$a_{\alpha_i} a_{\alpha_i}^\dagger |\alpha_1, \dots, \alpha_N\rangle = 0,$$

because Pauli principle forbids occupying twice the same label, while

$$a_{\alpha_i}^\dagger a_{\alpha_i} |\alpha_1, \dots, \alpha_N\rangle = a_{\alpha_i}^\dagger (-1)^{i-1} |\alpha_1, \dots, \hat{\alpha}_i, \dots, \alpha_N\rangle = |\alpha_1, \dots, \alpha_N\rangle,$$

because the $(-1)^{i-1}$ is reabsorbed in bringing the created particle to the original position. Summarizing, we see that for Fermions, in all possible cases

$$a_\alpha a_\alpha^\dagger + a_\alpha^\dagger a_\alpha = 1 \tag{2.31}$$

Exercise 2.5 Repeat the algebra for the Bosonic case to show that

$$a_\alpha a_\alpha^\dagger - a_\alpha^\dagger a_\alpha = 1 \tag{2.32}$$

We can finally summarize all the commutation relations derived, often referred to as the *canonical commutation relations*.

	$\{a_{\alpha_1}^\dagger, a_{\alpha_2}^\dagger\} = 0$ $\{a_{\alpha_1}, a_{\alpha_2}\} = 0$ $\{a_{\alpha_1}, a_{\alpha_2}^\dagger\} = \delta_{\alpha_1, \alpha_2}$	Fermions \implies	$[a_{\alpha_1}^\dagger, a_{\alpha_2}^\dagger] = 0$ $[a_{\alpha_1}, a_{\alpha_2}] = 0$ $[a_{\alpha_1}, a_{\alpha_2}^\dagger] = \delta_{\alpha_1, \alpha_2}$	Bosons \implies	\cdot (2.33)	Canonical commutation relations
--	--	---------------------	--	-------------------	---	---------------------------------------

Before leaving the section, it is worth pointing out the special role played by the operator Number
operator

$$\hat{n}_\alpha \stackrel{def}{=} a_\alpha^\dagger a_\alpha \tag{2.34}$$

often called the *number operator*, because it simply counts how many times a label α is present in a state.

Exercise 2.6 Verify that

$$\hat{n}_\alpha |\alpha_1, \dots, \alpha_N\rangle = n_\alpha |\alpha_1, \dots, \alpha_N\rangle; \tag{2.35}$$

where n_α is the number of times the label α is present in $(\alpha_1, \dots, \alpha_N)$.

Clearly, one can write an operator \hat{N} that counts the *total number of particles* in a state by

$$\hat{N} \stackrel{def}{=} \sum_\alpha \hat{n}_\alpha = \sum_\alpha a_\alpha^\dagger a_\alpha. \tag{2.36}$$

2.2.1 Changing the basis set.

Suppose we want to switch from $|\alpha\rangle$ to some other basis set $|i\rangle$, still orthonormal. Clearly there is a unitary transformation between the two single-particle basis sets:

$$|i\rangle = \sum_{\alpha} |\alpha\rangle \langle \alpha|i\rangle = \sum_{\alpha} |\alpha\rangle U_{\alpha,i}, \quad (2.37)$$

where $U_{\alpha,i} = \langle \alpha|i\rangle$ is the unitary matrix of the transformation. The question is: How is a_i^\dagger determined in terms of the original a_α^\dagger ? The answer is easy. Since, by definition, $|i\rangle = a_i^\dagger|0\rangle$ and $|\alpha\rangle = a_\alpha^\dagger|0\rangle$, it immediately follows that

$$a_i^\dagger|0\rangle = \sum_{\alpha} a_\alpha^\dagger|0\rangle U_{\alpha,i}. \quad (2.38)$$

By linearity, one can easily show that this equation has to hold not only when applied to the vacuum, but also as an *operator identity*, i.e.,

$$\boxed{\begin{array}{l} a_i^\dagger = \sum_{\alpha} a_\alpha^\dagger U_{\alpha,i} \\ a_i = \sum_{\alpha} a_\alpha U_{\alpha,i}^* \end{array}}, \quad (2.39)$$

the second equation being simply the adjoint of the first. The previous argument is a convenient mnemonic rule for rederiving, when needed, the correct relations.

2.2.2 The field operators.

The construction of the field operators can be seen as a special case of Eqs. (2.39), when we take as new basis the coordinate and spin eigenstates $|i\rangle = |\mathbf{r}, \sigma\rangle$. By definition, the field operator $\Psi^\dagger(\mathbf{r}, \sigma)$ is the creation operator of the state $|\mathbf{r}, \sigma\rangle$, i.e.,

$$\Psi^\dagger(\mathbf{r}, \sigma)|0\rangle = |\mathbf{r}, \sigma\rangle. \quad (2.40)$$

Then, the analog of Eq. (2.37) reads:

$$|\mathbf{r}, \sigma\rangle = \sum_{\alpha} |\alpha\rangle \langle \alpha|\mathbf{r}, \sigma\rangle = \sum_{\alpha} |\alpha\rangle \phi_\alpha^*(\mathbf{r}, \sigma), \quad (2.41)$$

where we have identified the real-space wavefunction of orbital α as $\phi_\alpha(\mathbf{r}) = \langle \mathbf{r}|\alpha\rangle$, and used the fact that $\langle \sigma_\alpha|\sigma\rangle = \delta_{\sigma,\sigma_\alpha}$. The analog of Eqs. (2.39) reads, then,

$$\begin{aligned} \Psi^\dagger(\mathbf{r}, \sigma) &= \sum_{\alpha} \phi_\alpha^*(\mathbf{r}, \sigma) a_\alpha^\dagger \\ \Psi(\mathbf{r}, \sigma) &= \sum_{\alpha} \phi_\alpha(\mathbf{r}, \sigma) a_\alpha. \end{aligned} \quad (2.42)$$

These relationships can be easily inverted to give:

$$\begin{aligned} a_\alpha^\dagger &= \sum_{\sigma} \int d\mathbf{r} \phi_\alpha(\mathbf{r}, \sigma) \Psi^\dagger(\mathbf{r}, \sigma) \\ a_\alpha &= \sum_{\sigma} \int d\mathbf{r} \phi_\alpha^*(\mathbf{r}, \sigma) \Psi(\mathbf{r}, \sigma). \end{aligned} \quad (2.43)$$

2.2.3 Operators in second quantization.

We would like to be able to calculate matrix elements of a Hamiltonian like, for instance, that of N interacting electrons in some external potential $v(\mathbf{r})$,

$$H = \sum_{i=1}^N \left(\frac{\mathbf{p}_i^2}{2m} + v(\mathbf{r}_i) \right) + \frac{1}{2} \sum_{i \neq j} \frac{e^2}{|\mathbf{r}_i - \mathbf{r}_j|}. \quad (2.44)$$

In order to do so, we need to express the operators appearing in H in terms of the creation and destruction operators a_α^\dagger and a_α of the selected basis, i.e., as operators in the so-called Fock space.

Observe that there are two possible types of operators of interest to us:

1) *one-body operators*, like the total kinetic energy $\sum_i \mathbf{p}_i^2/2m$ or the external potential $\sum_i v(\mathbf{r}_i)$, which act on one-particle at a time, and their effect is then summed over all particles in a totally symmetric way, generally One-body operators

$$U_N^{1\text{-body}} = \sum_{i=1}^N U(i); \quad (2.45)$$

2) *two-body operators*, like the Coulomb interaction between electrons $(1/2) \sum_{i \neq j} e^2/|\mathbf{r}_i - \mathbf{r}_j|$, which involve two-particle at a time, and are summed over all pairs of particles in a totally symmetric way, Two-body operators

$$V_N^{2\text{-body}} = \frac{1}{2} \sum_{i \neq j} V(i, j). \quad (2.46)$$

The Fock (second quantized) versions of these operators are very simple to state. For a one-body operator:

$$\boxed{U_N^{1\text{-body}} \implies U_{\text{Fock}} = \sum_{\alpha, \alpha'} \langle \alpha' | U | \alpha \rangle a_{\alpha'}^\dagger a_\alpha}, \quad (2.47)$$

where $\langle \alpha' | U | \alpha \rangle$ is simply the single-particle matrix element of the individual operator $U(i)$, for instance, in the examples above,

$$\begin{aligned} \langle \alpha' | \mathbf{p}^2/2m | \alpha \rangle &= \delta_{\sigma_\alpha, \sigma_{\alpha'}} \int d\mathbf{r} \phi_{\alpha'}^*(\mathbf{r}) \left(-\frac{\hbar^2 \nabla^2}{2m} \right) \phi_\alpha(\mathbf{r}) \\ \langle \alpha' | v(\mathbf{r}) | \alpha \rangle &= \delta_{\sigma_\alpha, \sigma_{\alpha'}} \int d\mathbf{r} \phi_{\alpha'}^*(\mathbf{r}) v(\mathbf{r}) \phi_\alpha(\mathbf{r}). \end{aligned} \quad (2.48)$$

For a two-body operator:

$$\boxed{V_N^{2\text{-body}} \implies V_{\text{Fock}} = \frac{1}{2} \sum_{\alpha_1, \alpha_2, \alpha'_1, \alpha'_2} (\alpha'_2 \alpha'_1 | V | \alpha_1 \alpha_2) a_{\alpha'_2}^\dagger a_{\alpha'_1}^\dagger a_{\alpha_1} a_{\alpha_2}}, \quad (2.49)$$

where the matrix element needed is, for a general spin-independent interaction potential $V(\mathbf{r}_1, \mathbf{r}_2)$,

$$(\alpha'_2 \alpha'_1 | V | \alpha_1 \alpha_2) = \delta_{\sigma_{\alpha_1}, \sigma_{\alpha'_1}} \delta_{\sigma_{\alpha_2}, \sigma_{\alpha'_2}} \int d\mathbf{r}_1 d\mathbf{r}_2 \phi_{\alpha'_2}^*(\mathbf{r}_2) \phi_{\alpha'_1}^*(\mathbf{r}_1) V(\mathbf{r}_1, \mathbf{r}_2) \phi_{\alpha_1}(\mathbf{r}_1) \phi_{\alpha_2}(\mathbf{r}_2). \quad (2.50)$$

We observe that the order of the operators is extremely important (for fermions).

The proofs are not very difficult but a bit long and tedious. We will briefly sketch that for the one-body case. Michele Fabrizio will give full details in the Many-Body course.

2.3 Why a quadratic hamiltonian is easy.

Before we consider the Hartree-Fock problem, let us pause for a moment and consider the reason why one-body problems are considered simple in a many-body framework. If the Hamiltonian is simply a sum of one-body terms $H = \sum_{i=1}^N h(i)$, for instance $h(i) = \mathbf{p}_i^2/2m + v(\mathbf{r}_i)$, we know that in second quantization it reads

$$H = \sum_{\alpha, \alpha'} h_{\alpha', \alpha} a_{\alpha'}^\dagger a_{\alpha} , \quad (2.51)$$

where the matrix elements are

$$h_{\alpha', \alpha} = \langle \alpha' | h | \alpha \rangle = \delta_{\sigma_{\alpha}, \sigma_{\alpha'}} \int d\mathbf{r} \phi_{\alpha'}^*(\mathbf{r}) \left(-\frac{\hbar^2 \nabla^2}{2m} + v(\mathbf{r}) \right) \phi_{\alpha}(\mathbf{r}) . \quad (2.52)$$

So, H is purely *quadratic* in the operators. The crucial point is now that any quadratic problem can be diagonalized completely, by switching to a new basis $|i\rangle$ made of solutions of the one-particle Schrödinger equation ⁷

$$h|i\rangle = \epsilon_i|i\rangle \quad \Longrightarrow \quad \left(-\frac{\hbar^2 \nabla^2}{2m} + v(\mathbf{r}) \right) \phi_i(\mathbf{r}) = \epsilon_i \phi_i(\mathbf{r}) . \quad (2.53)$$

Working with this diagonalizing basis, and the corresponding a_i^\dagger , the Hamiltonian simply reads:

$$H = \sum_i \epsilon_i a_i^\dagger a_i = \sum_i \epsilon_i \hat{n}_i , \quad (2.54)$$

where we assume having ordered the energies as $\epsilon_1 \leq \epsilon_2 \leq \dots$. With H written in this way, we can immediately write down all possible many-body exact eigenstates as single Slater determinants (for Fermions) and the corresponding eigenvalues as sums of ϵ_i 's,

$$\begin{aligned} |\Psi_{i_1, \dots, i_N}\rangle &= a_{i_1}^\dagger \cdots a_{i_N}^\dagger |0\rangle \\ E_{i_1, \dots, i_N} &= \epsilon_{i_1} + \dots + \epsilon_{i_N} . \end{aligned} \quad (2.55)$$

So, the full solution of the many-body problem comes automatically from the solution of the corresponding one-body problem, and the exact many-particle states are simply single Slater determinants.

2.4 The Hartree-Fock equations.

We state now the Hartree-Fock problem for the ground state (T=0).

Hartree-Fock
problem

Ground State Hartree-Fock problem. Find the best possible single particle states $|\alpha\rangle$ in such a way that the total energy of a single Slater determinant made out of the selected orbitals, $\langle \alpha_1, \dots, \alpha_N | H | \alpha_1, \dots, \alpha_N \rangle$, is minimal.

⁷Being simple does not mean that solving such a one-body problem is trivial. Indeed it can be technically quite involved. Band theory is devoted exactly to this problem.

Quite clearly, it is a problem based on the *variational principle*, where the restriction made on the states $|\Psi\rangle$ which one considers is that they are *single Slater determinants*. We stress the fact that, although any state can be expanded in terms of Slater determinants, the ground state of a genuinely interacting problem is not, in general, a *single* Slater determinant.

As a simple exercise in second quantization, let us evaluate the average energy of a single Slater determinant $|\alpha_1, \dots, \alpha_N\rangle = a_{\alpha_1}^\dagger \dots a_{\alpha_N}^\dagger |0\rangle$. The $\{\alpha\}$ here specify a generic orthonormal basis set, which we are asked to optimize, in the end. So, we plan to calculate

$$\langle \alpha_1, \dots, \alpha_N | H | \alpha_1, \dots, \alpha_N \rangle = \langle \alpha_1, \dots, \alpha_N | \hat{h} | \alpha_1, \dots, \alpha_N \rangle + \langle \alpha_1, \dots, \alpha_N | \hat{V} | \alpha_1, \dots, \alpha_N \rangle. \quad (2.56)$$

Let us start from the one-body part of H , $\langle \hat{h} \rangle$. Its contribution is simply:

$$\langle \hat{h} \rangle = \sum_{\alpha', \alpha} h_{\alpha', \alpha} \langle \alpha_1, \dots, \alpha_N | a_{\alpha'}^\dagger a_\alpha | \alpha_1, \dots, \alpha_N \rangle.$$

Clearly, in the sum we must have $\alpha \in (\alpha_1, \dots, \alpha_N)$, otherwise the destruction operator makes the result to vanish. Moreover, if the particle created has a label $\alpha' \neq \alpha$ (the particle just destroyed) the resulting state is different from the starting state and the diagonal matrix element we are looking for is again zero. So, we must have $\alpha' = \alpha = \alpha_i$, and eventually

$$\langle \hat{h} \rangle = \sum_{\alpha', \alpha} h_{\alpha', \alpha} \delta_{\alpha', \alpha} \sum_i \delta_{\alpha, \alpha_i} = \sum_{i=1}^N h_{\alpha_i, \alpha_i}. \quad (2.57)$$

Let us consider now the interaction potential part,

$$\langle \alpha_1, \dots, \alpha_N | \hat{V} | \alpha_1, \dots, \alpha_N \rangle = \frac{1}{2} \sum_{\alpha, \beta, \alpha', \beta'} (\beta' \alpha' | V | \alpha \beta) \langle \alpha_1, \dots, \alpha_N | a_{\beta'}^\dagger a_{\alpha'}^\dagger a_\alpha a_\beta | \alpha_1, \dots, \alpha_N \rangle \quad (2.58)$$

One again, both α and β must be in the set $(\alpha_1 \dots \alpha_N)$. Let $\alpha = \alpha_i$ and $\beta = \alpha_k$, with $i \neq k$. There are now *two* possibilities for the creation operator labels α' and β' , in order to go back to the starting state: a) the *direct term*, for $\alpha' = \alpha = \alpha_i$ and $\beta' = \beta = \alpha_k$, or b) the *exchange term*, for $\alpha' = \beta = \alpha_k$ and $\beta' = \alpha = \alpha_i$. In the direct term the order of the operators is such that no minus sign is involved:

$$\langle \alpha_1, \dots, \alpha_N | a_{\alpha_k}^\dagger a_{\alpha_i}^\dagger a_{\alpha_i} a_{\alpha_k} | \alpha_1, \dots, \alpha_N \rangle = \langle \alpha_1, \dots, \alpha_N | \hat{n}_{\alpha_k} \hat{n}_{\alpha_i} | \alpha_1, \dots, \alpha_N \rangle = 1,$$

because $\hat{n}_{\alpha_i} a_{\alpha_k} = a_{\alpha_k} \hat{n}_{\alpha_i}$. In the exchange term, on the contrary, we must pay an extra *minus sign* in anticommuting the operators,

$$\langle \alpha_1, \dots, \alpha_N | a_{\alpha_i}^\dagger a_{\alpha_k}^\dagger a_{\alpha_i} a_{\alpha_k} | \alpha_1, \dots, \alpha_N \rangle = - \langle \alpha_1, \dots, \alpha_N | \hat{n}_{\alpha_k} \hat{n}_{\alpha_i} | \alpha_1, \dots, \alpha_N \rangle = -1.$$

Summing up, we get:

$$\langle \alpha_1, \dots, \alpha_N | \hat{V} | \alpha_1, \dots, \alpha_N \rangle = \frac{1}{2} \sum_{i \neq k}^N [(\alpha_k \alpha_i | V | \alpha_i \alpha_k) - (\alpha_i \alpha_k | V | \alpha_i \alpha_k)]. \quad (2.59)$$

Finally, summing one-body and two-body terms we get:

$$\langle \alpha_1, \dots, \alpha_N | H | \alpha_1, \dots, \alpha_N \rangle = \sum_{i=1}^N h_{\alpha_i, \alpha_i} + \frac{1}{2} \sum_{i \neq k}^N [(\alpha_k \alpha_i | V | \alpha_i \alpha_k) - (\alpha_i \alpha_k | V | \alpha_i \alpha_k)]. \quad (2.60)$$

One can appreciate the relative simplicity of this calculation, as opposed to the traditional one where one decomposes the Slater determinant into product states, and goes through all the permutation algebra. In a sense, we have done that algebra once and for all in deriving the second quantized expression of states and operators!

The Hartree-Fock equations for the orbitals $|\alpha\rangle$ come out of the requirement that the average $\langle \alpha_1, \dots, \alpha_N | H | \alpha_1, \dots, \alpha_N \rangle$ we just calculated is minimal. We do not go into a detailed derivation of them.⁸ We simply state the result, guided by intuition. If it were just for the one-body term

$$\sum_{i=1}^N h_{\alpha_i, \alpha_i} = \sum_{i=1}^N \int d\mathbf{r} \phi_{\alpha_i}^*(\mathbf{r}) \left(-\frac{\hbar^2 \nabla^2}{2m} + v(\mathbf{r}) \right) \phi_{\alpha_i}(\mathbf{r}), \quad (2.61)$$

we would immediately write that the correct orbitals must satisfy

$$\left(-\frac{\hbar^2 \nabla^2}{2m} + v(\mathbf{r}) \right) \phi_{\alpha_i}(\mathbf{r}) = \epsilon_i \phi_{\alpha_i}(\mathbf{r}), \quad (2.62)$$

and the Ground State (GS) is obtained by occupying the lowest ϵ_i respecting the Pauli principle. Consider now the direct term:

$$\begin{aligned} \langle \hat{V} \rangle_{\text{dir}} &= \frac{1}{2} \sum_{i \neq k}^N (\alpha_k \alpha_i | V | \alpha_i \alpha_k) \\ &= \frac{1}{2} \sum_{i \neq k}^N \int d\mathbf{r}_1 d\mathbf{r}_2 \phi_{\alpha_k}^*(\mathbf{r}_2) \phi_{\alpha_i}^*(\mathbf{r}_1) V(\mathbf{r}_1, \mathbf{r}_2) \phi_{\alpha_i}(\mathbf{r}_1) \phi_{\alpha_k}(\mathbf{r}_2). \end{aligned} \quad (2.63)$$

Quite clearly, you can rewrite it as:

$$\langle \hat{V} \rangle_{\text{dir}} = \frac{1}{2} \sum_{i=1}^N \int d\mathbf{r}_1 \phi_{\alpha_i}^*(\mathbf{r}_1) V_{\text{dir}}^{(i)}(\mathbf{r}_1) \phi_{\alpha_i}(\mathbf{r}_1),$$

where

$$V_{\text{dir}}^{(i)}(\mathbf{r}_1) = \sum_{k \neq i}^N \int d\mathbf{r}_2 V(\mathbf{r}_1, \mathbf{r}_2) |\phi_{\alpha_k}(\mathbf{r}_2)|^2, \quad (2.64)$$

is simply the average potential felt by the electron in state α_i due to all the other electrons occupying the orbitals $\alpha_k \neq \alpha_i$. Not surprisingly, if I were to carry the minimization procedure by including this term only, the resulting equations for the orbitals would look very much like Eq. (2.62)

Hartree
equations

$$\boxed{\left(-\frac{\hbar^2 \nabla^2}{2m} + v(\mathbf{r}) + V_{\text{dir}}^{(i)}(\mathbf{r}) \right) \phi_{\alpha_i}(\mathbf{r}) = \epsilon_i \phi_{\alpha_i}(\mathbf{r}),} \quad (2.65)$$

with $V_{\text{dir}}^{(i)}(\mathbf{r})$ adding up to the external potential. These equations are known as *Hartree equations*, and the only tricky point to mention is that the factor 1/2 present in $\langle \hat{V} \rangle_{\text{dir}}$ is cancelled out by a factor 2 due to the quartic nature of the interaction term. Finally, consider the exchange term:

$$\begin{aligned} \langle \hat{V} \rangle_{\text{exc}} &= -\frac{1}{2} \sum_{i \neq k}^N (\alpha_i \alpha_k | V | \alpha_i \alpha_k) \\ &= -\frac{1}{2} \sum_{i \neq k}^N \delta_{\sigma_{\alpha_k}, \sigma_{\alpha_i}} \int d\mathbf{r}_1 d\mathbf{r}_2 \phi_{\alpha_i}^*(\mathbf{r}_2) \phi_{\alpha_k}^*(\mathbf{r}_1) V(\mathbf{r}_1, \mathbf{r}_2) \phi_{\alpha_i}(\mathbf{r}_1) \phi_{\alpha_k}(\mathbf{r}_2). \end{aligned} \quad (2.66)$$

⁸At least two different derivations will be given in the Many-Body course.

Notice the $\delta_{\sigma_{\alpha_k}, \sigma_{\alpha_i}}$ coming from the exchange matrix element. This term cannot be rewritten as a local potential term, but only as a *non-local potential* of the form

$$\langle \hat{V} \rangle_{\text{exc}} = \frac{1}{2} \sum_{i=1}^N \int d\mathbf{r}_1 d\mathbf{r}_2 \phi_{\alpha_i}^*(\mathbf{r}_2) V_{\text{exc}}^{(i)}(\mathbf{r}_2, \mathbf{r}_1) \phi_{\alpha_i}(\mathbf{r}_1),$$

where

$$V_{\text{exc}}^{(i)}(\mathbf{r}_2, \mathbf{r}_1) = - \sum_{k \neq i}^N \delta_{\sigma_{\alpha_k}, \sigma_{\alpha_i}} \phi_{\alpha_k}^*(\mathbf{r}_1) V(\mathbf{r}_1, \mathbf{r}_2) \phi_{\alpha_k}(\mathbf{r}_2). \quad (2.67)$$

Notice the *minus sign* in front of the exchange potential $V_{\text{exc}}^{(i)}$, and the fact that exchange acts only between electrons with the *same spin*, as enforced by the $\delta_{\sigma_{\alpha_k}, \sigma_{\alpha_i}}$. Upon minimization one would obtain, finally,

$$\left(-\frac{\hbar^2 \nabla^2}{2m} + v(\mathbf{r}) + V_{\text{dir}}^{(i)}(\mathbf{r}) \right) \phi_{\alpha_i}(\mathbf{r}) + \int d\mathbf{r}' V_{\text{exc}}^{(i)}(\mathbf{r}, \mathbf{r}') \phi_{\alpha_i}(\mathbf{r}') = \epsilon_i \phi_{\alpha_i}(\mathbf{r}), \quad (2.68)$$

where, once again, the factor 1/2 has cancelled out, and the non-local nature of the exchange potential appears clearly. These are the *Hartree-Fock equations*. Their full solution is not trivial at all, in general. They are coupled, non-local Schrödinger equations which must be solved *self-consistently*, because the potentials themselves depend on the orbitals we are looking for. The self-consistent nature of the HF equations is dealt with an *iterative procedure*: one starts assuming some approximate form for the orbitals $|\alpha\rangle$, calculated $V_{\text{dir}}^{(i)}$ and $V_{\text{exc}}^{(i)}$, solve the Schrödinger equations for the new orbitals, recalculated the potentials, and so on until self-consistency is reached. Notice that the restriction $k \neq i$ is actually redundant in the HF equations (but not in the Hartree exchange potentials. As a consequence, we can also write the direct and exchange potentials in a form where the $k \neq i$ restriction no longer appears:

$$\begin{aligned} V_{\text{dir}}(\mathbf{r}_1) &= \sum_k^{\text{occ}} \int d\mathbf{r}_2 V(\mathbf{r}_1, \mathbf{r}_2) |\phi_{\alpha_k}(\mathbf{r}_2)|^2 \\ V_{\text{exc}}^{(\sigma_{\alpha_i})}(\mathbf{r}_1, \mathbf{r}_2) &= - \sum_k^{\text{occ}} \delta_{\sigma_{\alpha_k}, \sigma_{\alpha_i}} \phi_{\alpha_k}^*(\mathbf{r}_1) V(\mathbf{r}_1, \mathbf{r}_2) \phi_{\alpha_k}(\mathbf{r}_2). \end{aligned} \quad (2.69)$$

The HF equations could easily have more than one solution, and the ultimate minimal solution is often not known. Even in simple cases, like homogeneous systems, where the external potential $v(\mathbf{r}) = 0$ and a solution in terms of plane-waves is simple to find, the ultimate solutions might break some of the symmetries of the problem, like translation invariance (Overhauser's Charge Density Wave solutions do so).

Notice that, as discussed until now, the HF equations are equations for the occupied orbitals $\alpha_1 \cdots \alpha_N$. However, once a self-consistent solution for the occupied orbitals has been found, one can fix the direct and exchange potential to their self-consistent values, and solve the HF equations for all the orbitals and eigenvalues, including the *unoccupied* ones.

A totally equivalent form of the HF equations is obtained by multiplying both sides of Eq. (2.68) by $\phi_{\alpha_j}^*(\mathbf{r})$ and integrating over \mathbf{r} , which leads to the matrix form of the HF equations:

$$h_{\alpha_j, \alpha_i} + \sum_k^{\text{occ}} [(\alpha_k \alpha_j | V | \alpha_i \alpha_k) - (\alpha_j \alpha_k | V | \alpha_i \alpha_k)] = \epsilon_i \delta_{i,j}. \quad (2.70)$$

Hartree-Fock
equations

Self
interaction
cancellation

A few words about the *eigenvalues* ϵ_i of the HF equations. One would naively expect that the final HF energy, i.e., the average value of H on the optimal Slater determinant, is simply given by the sum of the lowest N values of ϵ_i , but this is not true. Recall that the correct definition of E_{HF} is simply:

$$\begin{aligned} E_{HF} &= \langle \alpha_1, \dots, \alpha_N | H | \alpha_1, \dots, \alpha_N \rangle \\ &= \sum_i^{\text{occ}} h_{\alpha_i, \alpha_i} + \frac{1}{2} \sum_{i,k}^{\text{occ}} [(\alpha_k \alpha_i | V | \alpha_i \alpha_k) - (\alpha_i \alpha_k | V | \alpha_i \alpha_k)] , \end{aligned} \quad (2.71)$$

where the $\{\alpha_i\}$ are now assumed to label the final optimal orbitals we found by solving the HF equations. Notice the important factor $1/2$ in front of the interaction contributions, which is missing from the HF equations (compare, for instance, with the matrix form Eq. (2.70)). Indeed, upon taking the diagonal elements $j = i$ in Eq. (2.70) and summing over the occupied α_i we easily get:

$$\sum_i^{\text{occ}} h_{\alpha_i, \alpha_i} + \sum_{i,k}^{\text{occ}} [(\alpha_k \alpha_i | V | \alpha_i \alpha_k) - (\alpha_i \alpha_k | V | \alpha_i \alpha_k)] = \sum_i^{\text{occ}} \epsilon_i . \quad (2.72)$$

So, the sum of the occupied HF eigenvalues *overcounts* the interaction contributions by a factor two. There is nothing wrong with that. Just remember to subtract back this overcounting, by writing

$$E_{HF} = \sum_i^{\text{occ}} \epsilon_i - \frac{1}{2} \sum_{i,k}^{\text{occ}} [(\alpha_k \alpha_i | V | \alpha_i \alpha_k) - (\alpha_i \alpha_k | V | \alpha_i \alpha_k)] . \quad (2.73)$$

2.5 Hartree-Fock in closed shell atoms: the example of Helium.

Suppose we would like to solve the He atom problem within HF. More generally, we can address a two-electron ion like Li^+ , Be^{2+} , etc. with a generic nuclear charge $Z \geq 2$. The Hamiltonian for an atom with N electrons is evidently:

$$H = \sum_{i=1}^N \left(\frac{\mathbf{p}_i^2}{2m} - \frac{Ze^2}{r_i} \right) + \frac{1}{2} \sum_{i \neq j} \frac{e^2}{|\mathbf{r}_i - \mathbf{r}_j|} , \quad (2.74)$$

where we have assumed the N interacting electrons to be in the Coulomb field of a nucleus of charge Ze , which we imagine fixed at $\mathbf{R} = 0$. We have neglected spin-orbit effects and other relativistic corrections. We plan to do the case $N = 2$ here. Evidently, a good starting basis set of single-particle functions is that of hydrogenoid orbitals which are solutions of the one-body Hamiltonian $\hat{h} = \mathbf{p}^2/2m - Ze^2/r$. We know that such functions are labelled by orbital quantum numbers (nlm) , and that

$$\left(\frac{\mathbf{p}^2}{2m} - \frac{Ze^2}{r} \right) \phi_{nlm}(\mathbf{r}) = \epsilon_n \phi_{nlm}(\mathbf{r}) . \quad (2.75)$$

The eigenvalues ϵ_n are those of the Coulomb potential, and therefore independent of the angular momentum quantum numbers lm :

$$\epsilon_n = -\frac{Z^2 e^2}{2 a_B n^2} , \quad (2.76)$$

where $a_B = \hbar^2/(me^2) \approx 0.529$ rA is the Bohr radius and $e^2/a_B = 1$ Hartree ≈ 27.2 eV. The wavefunctions $\phi_{nlm}(\mathbf{r})$ are well known: for instance, for the $1s$ orbital ($n = 1, l = 0, m = 0$) one has

$$\phi_{1s}(r) = \frac{1}{\sqrt{\pi}} \left(\frac{Z}{a_B} \right)^{3/2} e^{-Zr/a_B} .$$

It is very convenient here to adopt *atomic units*, where lengths are measured in units of the Bohr length a_B , and energies in units of the Hartree, e^2/a_B .

We write H in second quantization in the basis chosen. It reads

$$H = \sum_{nlm\sigma} \epsilon_n a_{nlm\sigma}^\dagger a_{nlm\sigma} + \frac{1}{2} \sum_{\alpha_1, \alpha_2, \alpha'_1, \alpha'_2} (\alpha'_2 \alpha'_1 | V | \alpha_1 \alpha_2) a_{\alpha'_2}^\dagger a_{\alpha'_1}^\dagger a_{\alpha_1} a_{\alpha_2} , \quad (2.77)$$

where we have adopted the shorthand notation $\alpha_1 = n_1 l_1 m_1 \sigma_1$, etc. in the interaction term. If we start ignoring the Coulomb potential, we would put our $N = 2$ electrons in the lowest two orbitals available, i.e., $1s \uparrow$ and $1s \downarrow$, forming the Slater determinant

$$|1s \uparrow, 1s \downarrow\rangle = a_{1s\uparrow}^\dagger a_{1s\downarrow}^\dagger |0\rangle . \quad (2.78)$$

The real-space wavefunction of this Slater determinant is simply:

$$\Psi_{1s\uparrow, 1s\downarrow}(r_1, r_2) = \phi_{1s}(\mathbf{r}_1) \phi_{1s}(\mathbf{r}_2) \frac{1}{\sqrt{2}} [\chi_\uparrow(\sigma_1) \chi_\downarrow(\sigma_2) - \chi_\downarrow(\sigma_1) \chi_\uparrow(\sigma_2)] ,$$

i.e., the product of a symmetric orbital times a spin singlet state. The one-body part of the Hamiltonian contributes an energy

$$E^{(\text{one-body})} = \langle 1s \uparrow, 1s \downarrow | \hat{h} | 1s \uparrow, 1s \downarrow \rangle = 2\epsilon_{1s} = -Z^2 \text{ a.u.} . \quad (2.79)$$

For He, where $Z = 2$, this is -4 a.u. a severe underestimate of the total energy, which is known to be $E^{(\text{exact, He})} \approx -2.904$ a.u.. This can be immediately cured by including the average of the Coulomb potential part, which is simply the *direct Coulomb integral* $K_{1s, 1s}$ of the $1s$ orbital, often indicated by U_{1s} in the strongly correlated community,

$$\langle 1s \uparrow, 1s \downarrow | \hat{V} | 1s \uparrow, 1s \downarrow \rangle = \int d\mathbf{r}_1 d\mathbf{r}_2 |\phi_{1s}(\mathbf{r}_2)|^2 \frac{e^2}{|\mathbf{r}_1 - \mathbf{r}_2|} |\phi_{1s}(\mathbf{r}_1)|^2 \stackrel{\text{def}}{=} K_{1s, 1s} = U_{1s} . \quad (2.80)$$

direct
Coulomb
integral

The calculation of Coulomb integrals can be performed analytically by exploiting rotational invariance. We simply state here the result:

$$U_{1s} = \frac{5}{8} Z \text{ a.u.} . \quad (2.81)$$

Summing up, we obtain the average energy of our Slater determinant as

$$E_{1s\uparrow, 1s\downarrow} = \left(-Z^2 + \frac{5}{8} Z \right) \text{ a.u.} = -2.75 \text{ a.u.} , \quad (2.82)$$

where the last number applies to He ($Z = 2$). What we should do to perform a HF calculation, is the optimization of the orbitals used. Let us look more closely to our problem. Having a closed shell atom it is reasonable to aim at a *restricted Hartree-Fock* calculation, which imposes the same orbital wave-function for the two opposite spin states

Restricted
HF

$$\psi_{\alpha_o \uparrow}(r) = \phi_{\alpha_o}(\mathbf{r}) \chi_\uparrow(\sigma) \quad \Longrightarrow \quad \psi_{\alpha_o \downarrow}(r) = \phi_{\alpha_o}(\mathbf{r}) \chi_\downarrow(\sigma) . \quad (2.83)$$

We stress the fact that a more general HF approach, so-called *unrestricted HF* exploits the extra variational freedom of choosing different orbital wavefunctions for the two opposite spin states, which clearly breaks spin rotational symmetry.⁹ Going back to our He exercise, we will put two electrons, one with \uparrow spin, the other with \downarrow spin, in the lowest orbital solution of the HF equations

$$\left(-\frac{\hbar^2 \nabla^2}{2m} - \frac{Ze^2}{r} + V_{\text{dir}}(\mathbf{r}) \right) \phi_{1s}(\mathbf{r}) = \epsilon_{1s} \phi_{1s}(\mathbf{r}), \quad (2.84)$$

where now the $1s$ label denotes the orbital quantum numbers of the lowest energy solution of a rotationally invariant potential, and we have dropped the exchange term which does not enter in the calculation of the *occupied orbitals*, since the two orbitals are associated to *different spins*. The form of the direct (Hartree) potential $V_{\text{dir}}(\mathbf{r})$ is

$$V_{\text{dir}}(\mathbf{r}) = \int d\mathbf{r}' \frac{e^2}{|\mathbf{r} - \mathbf{r}'|} |\phi_{1s}(\mathbf{r}')|^2, \quad (2.85)$$

because the electron in ϕ_{1s} feels the repulsion of the other electron in the same orbital. We immediately understand that the Hartree potential partially screens at large distances the nuclear charge $+Ze$. Indeed, for $r \rightarrow \infty$ we can easily see that

$$V_{\text{dir}}(\mathbf{r}) \sim \frac{e^2}{r} \int d\mathbf{r}' |\phi_{1s}(\mathbf{r}')|^2 = \frac{e^2}{r}, \quad (2.86)$$

so that the total effective charge seen by the electron at large distances is just $(Z-1)e$, and not Ze . This is intuitively obvious. The fact that we chose our original ϕ_{1s} orbital as solution of the hydrogenoid problem with nuclear charge Ze gives to that orbital a wrong tail at large distances. This is, primarily, what a self-consistent HF calculation needs to adjust to get a better form of ϕ_{1s} . Indeed, there is a simple variational scheme that we can follow instead of solving Eq. (2.84). Simply consider the hydrogenoid orbital $\phi_{1s}^{(Z_{eff})}$ which is solution of the Coulomb potential with an effective nuclear charge $Z_{eff}e$ (with Z_{eff} a real number),

$$\left(\frac{\mathbf{p}^2}{2m} - \frac{Z_{eff}e^2}{r} \right) \phi_{1s}^{(Z_{eff})}(\mathbf{r}) = \epsilon_{1s} \phi_{1s}^{(Z_{eff})}(\mathbf{r}), \quad (2.87)$$

and form the Slater determinant $|1s \uparrow, 1s \downarrow; Z_{eff}\rangle$ occupying twice $\phi_{1s}^{(Z_{eff})}$, with Z_{eff} used as a single *variational parameter*. The calculation of the average energy $E_{1s\uparrow,1s\downarrow}(Z_{eff})$ is quite straightforward,¹⁰ and gives:

$$E_{1s\uparrow,1s\downarrow}(Z_{eff}) = \langle 1s \uparrow, 1s \downarrow; Z_{eff} | \hat{H} | 1s \uparrow, 1s \downarrow; Z_{eff} \rangle = Z_{eff}^2 - 2ZZ_{eff} + \frac{5}{8}Z_{eff}. \quad (2.88)$$

Minimizing with respect to Z_{eff} this quadratic expression we find $Z_{eff}^{opt} = Z - 5/16 = 1.6875$ and

$$E_{1s\uparrow,1s\downarrow}(Z_{eff}^{opt}) = -(Z - 5/16)^2 \text{ a.u.} \approx -2.848 \text{ a.u.},$$

⁹This fact of gaining variational energy by appropriately breaking symmetries is a pretty common feature of an unrestricted HF calculation. As a matter of fact, it can be shown that, under quite general circumstances, it brings to the fact that “there are no unfilled shells in unrestricted HF”, i.e., there is always a gap between the last occupied orbital and the lowest unoccupied one. See Bach, Lieb, Loss, and Solovej, Phys. Rev. Lett. **72**, 2981 (1994).

¹⁰You simply need to calculate the average of $\mathbf{p}^2/2m$ and of $1/r$ over $\phi_{1s}^{(Z_{eff})}$.

where the numbers are appropriate to Helium. This value of the energy is not too far from the exact HF solution, which would give

$$E_{HF} \approx -2.862 \text{ a.u.} \quad (\text{for Helium}).$$

In turn, the full HF solution differs very little from the exact non-relativistic energy of Helium, calculated by Configuration Interaction (see below). A quantity that measures how far HF differs from the exact answer is the so-called *correlation energy*, defined simply as:

$$E_{\text{corr}} \stackrel{\text{def}}{=} E^{\text{exact}} - E_{HF}, \quad (2.89)$$

which, for Helium amounts to $E_{\text{corr}} \approx -0.042 \text{ a.u.}$, a bit more than 1% of the total energy.

2.5.1 Beyond Hartree-Fock: Configuration Interaction.

The next step will be rationalizing the finding that HF works very well for He. Suppose we have fully solved the HF equations, finding out *both occupied and unoccupied orbitals*, with corresponding eigenvalues ϵ_i . From such a complete HF solution, we can set up a new single-particle basis set made of the HF orbitals. Call once again $\{\alpha\}$ such a basis. Obviously, *full Hamiltonian* H is expressed in such a basis in the usual way. Imagine now applying the Hamiltonian to the HF Slater determinant for the Ground State, which we denote by $|HF\rangle = |\alpha_1, \dots, \alpha_N\rangle$:

$$H|HF\rangle = \sum_{\alpha', \alpha} h_{\alpha', \alpha} a_{\alpha'}^\dagger a_\alpha |HF\rangle + \frac{1}{2} \sum_{\alpha, \beta, \alpha', \beta'} (\beta' \alpha' | V | \alpha \beta) a_{\beta'}^\dagger a_{\alpha'}^\dagger a_\alpha a_\beta |HF\rangle. \quad (2.90)$$

Among all the terms which enter in $H|HF\rangle$, we notice three classes of terms: 1) the fully diagonal ones, which give back the state $|HF\rangle$ (those are the terms we computed in Sec. 2.4) 2) terms in which a *single particle-hole excitation is created* on $|HF\rangle$, i.e., a particle is removed from an occupied orbital and put in one of the unoccupied orbitals; 3) terms in which *two particle-hole excitations are created*. By carefully considering these three classes, one can show that:

Exercise 2.7 *The application of the full Hamiltonian H to the HF Ground State Slater determinant $|HF\rangle$ produces the following*

$$H|HF\rangle = E_{HF}|HF\rangle + \frac{1}{2} \sum_{\alpha, \beta}^{\text{occ}} \sum_{\alpha', \beta'}^{\text{unocc}} (\beta' \alpha' | V | \alpha \beta) a_{\beta'}^\dagger a_{\alpha'}^\dagger a_\alpha a_\beta |HF\rangle, \quad (2.91)$$

where the first piece is due to terms of type 1) above, the second piece is due to terms of type 3) above, while terms of type 2) make no contribution due to the fact that the orbitals are chosen to obey the HF equations.

So, in essence, having solved the HF equations automatically optimizes the state with respect to states which differ by a single particle promoted onto an excited state. In the example of Helium we were considering, the application of H to our HF ground state $|1s \uparrow, 1s \downarrow\rangle$ generates Slater determinants in which both particles are put into higher unoccupied HF orbitals like, for instance,

the $2s \uparrow, 2s \downarrow$. Indeed, any two-electron Slater determinant which has the same quantum numbers as $|HF\rangle$, i.e., total angular momentum $L = 0$ and total spin $S = 0$, is coupled directly to $|HF\rangle$ by the Hamiltonian. Then, we could imagine of improving *variationally* the wavefunction for the Ground State, by using more than just one Slater determinant, writing

$$|\Psi\rangle = \lambda_0|HF\rangle + \lambda_1|2s \uparrow, 2s \downarrow\rangle + \lambda_2|(2p - 2p)_{L=0, S=0}\rangle + \lambda_3|3s \uparrow, 3s \downarrow\rangle + \dots, \quad (2.92)$$

with the λ_i used as variational parameters. Here $|(2p - 2p)_{L=0, S=0}\rangle$ denotes the state made by two p-electrons having total $L = 0$ and total $S = 0$, which is, in itself, a sum of several Slater determinants. In general, the sum might go on and on, and is truncated when further terms make a negligible contribution or when your computer power is exhausted.¹¹ This scheme is called *Configuration Interaction* by the quantum chemists. Let us try to understand why the corrections should be small for He. Suppose we truncate our corrections to the first one, i.e., including $|2s \uparrow, 2s \downarrow\rangle$. The expected contribution to the ground state energy due to this state, in second order perturbation theory, is simply given by

Configuration
Interaction

$$\Delta E^{(2)}(2s, 2s) = \frac{|(2s, 2s|V|1s, 1s)|^2}{\Delta_{2s-1s}}, \quad (2.93)$$

where Δ_{2s-1s} is the difference between the diagonal energy of the state $|2s \uparrow, 2s \downarrow\rangle$ and the corresponding diagonal energy of $|1s \uparrow, 1s \downarrow\rangle$ (the latter being simply E_{HF}). $\Delta E^{(2)}(2s, 2s)$ turns out to be small, compared to E_{HF} for two reasons: i) the Coulomb matrix element involved in the numerator,

$$(2s, 2s|V|1s, 1s) = \int d\mathbf{r}_1 d\mathbf{r}_2 \phi_{2s}^*(\mathbf{r}_2) \phi_{2s}^*(\mathbf{r}_1) \frac{e^2}{|\mathbf{r}_1 - \mathbf{r}_2|} \phi_{1s}(\mathbf{r}_1) \phi_{1s}(\mathbf{r}_2), \quad (2.94)$$

is much smaller than the ones entering E_{HF} , i.e, $U_{1s} = (1s, 1s|V|1s, 1s)$;¹² the denominator involves *large gaps* due to the excitations of two particles to the next shell. (As an exercise, get the expression for Δ_{2s-1s} in terms of HF eigenvalues and Coulomb matrix elements.) Both effects conspire to make the result for the energy correction rather small. The argument can be repeated, *a fortiori*, for all the higher two particle-hole excitations.

2.6 Hartree-Fock fails: the H_2 molecule.

Consider now what appears, at first sight, only a slightly modification of two-electron problem we have done for Helium: the H_2 molecule. The electronic Hamiltonian can be written as

$$H_{\text{elec}} = \sum_{i=1}^2 \left(\frac{\mathbf{p}_i^2}{2m} + v(\mathbf{r}_i) \right) + \frac{e^2}{|\mathbf{r}_1 - \mathbf{r}_2|}, \quad (2.95)$$

¹¹In principle, for more than $N = 2$ electrons, the sum should include also terms with more than two particle-hole excitations, since each excited states appearing in $H|HF\rangle$, when acted upon by H generated further particle-hole excitations, in an infinite cascade.

¹²The integral would vanish, for orthogonality, if it were not for the Coulomb potential $e^2/|\mathbf{r}_1 - \mathbf{r}_2|$. The result is in any case much smaller than any *direct* Coulomb term.

i.e., differs from that of the Helium atom only in the fact that the external potential $v(\mathbf{r})$ is no longer $-2e^2/r$ but

$$v(\mathbf{r}) = -\frac{e^2}{|\mathbf{r} - \mathbf{R}_a|} - \frac{e^2}{|\mathbf{r} - \mathbf{R}_b|}, \quad (2.96)$$

being due to the two protons which are located at \mathbf{R}_a and at \mathbf{R}_b , with $\mathbf{R}_b - \mathbf{R}_a = \mathbf{R}$. In the limit $\mathbf{R} \rightarrow 0$ we recover the Helium atom, obviously. The fact that we talk here about *electronic Hamiltonian* is due to the fact that, in studying a molecule, we should include the Coulomb repulsion of the two nuclei, e^2/R , as well as the kinetic energy of the two nuclei. In the spirit of the *Born-Oppenheimer approximation*, however, we first solve for the electronic ground state energy for fixed nuclear position, $E_{GS}(\mathbf{R})$, and then obtain the effective potential governing the motion of the nuclei as

$$V_{\text{ion-ion}}(R) = \frac{e^2}{R} + E_{GS}(R). \quad (2.97)$$

Important quantities characterizing $V_{\text{ion-ion}}(R)$ are the equilibrium distance between the two

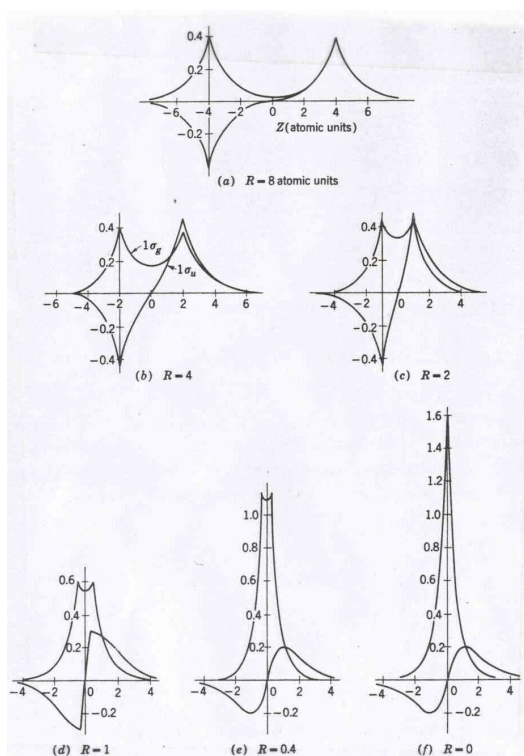


Figure 2.1: Lowest two wavefunctions of the H_2^+ problem as a function of the internuclear distance R . Taken from Slater.

nuclei, given by the position of the minimum R_{min} of the potential, and the *dissociation energy*, given by the difference between the potential at infinity, $V_{\text{ion-ion}}(R = \infty)$, and the potential at the minimum $V_{\text{ion-ion}}(R_{min})$. The gross qualitative features of $V_{\text{ion-ion}}(R)$ are easy to guess from the qualitative behaviour of $E_{GS}(R)$. $E_{GS}(R)$ must smoothly interpolate between the ground state of Helium, obtained for $R = 0$, and the ground state of two non-interacting Hydrogen atoms (-1 a.u.), obtained for $R = \infty$. The corresponding curve for $V_{\text{ion-ion}}(R)$ is easy to sketch, with a large distance van der Waals tail approaching -1 a.u., a minimum at some finite R_{min} , and a e^2/R

divergence at small R . One could ask how this picture is reproduced by HF. In principle, what we should perform is a calculation of

$$\left(-\frac{\hbar^2 \nabla^2}{2m} - \frac{e^2}{|\mathbf{r} - \mathbf{R}_a|} - \frac{e^2}{|\mathbf{r} - \mathbf{R}_b|} + V_{\text{dir}}(\mathbf{r}) \right) \phi_{e(o)}(\mathbf{r}) = \epsilon_{e(o)} \phi_{e(o)}(\mathbf{r}), \quad (2.98)$$

where $e(o)$ label solutions which are even (odd) with respect to the origin, which we imagine located midway between the two nuclei, and $V_{\text{dir}}(\mathbf{r})$ denotes the usual Hartree self-consistent potential. Rotational invariance is no longer applicable, and the calculation, which can use only *parity* as a good quantum number in a *restricted HF scheme*, is technically much more involved than the He atom counterpart. It turns out that the *even wavefunction* $\phi_e(\mathbf{r})$ is always the lowest solution,¹³ so that the self-consistent HF ground state is obtained by occupying twice, with an \uparrow and a \downarrow electron, the state $\phi_e(\mathbf{r})$. In order to get a feeling for the form of such a HF ground state, imagine calculating $\phi_{e(o)}$ by simply *dropping* the Hartree term $V_{\text{dir}}(\mathbf{r})$, solving therefore the one-electron problem relevant to H_2^+ , the ionized Hydrogen molecule:

$$\left(-\frac{\hbar^2 \nabla^2}{2m} - \frac{e^2}{|\mathbf{r} - \mathbf{R}_a|} - \frac{e^2}{|\mathbf{r} - \mathbf{R}_b|} \right) \phi_{e(o)}(\mathbf{r}) = \epsilon_{e(o)} \phi_{e(o)}(\mathbf{r}). \quad (2.99)$$

Fig. 2.1 here shows the two lowest wavefunctions ϕ_e and ϕ_o of the H_2^+ problem, as a function of the internuclear distance R . Notice how such wavefunctions start from the $1s$ and $2p$ states of He^+ , for $R = 0$, and smoothly evolve, as R increases, towards the *bonding and antibonding* combinations of $1s$ orbitals centered at the two nuclei.

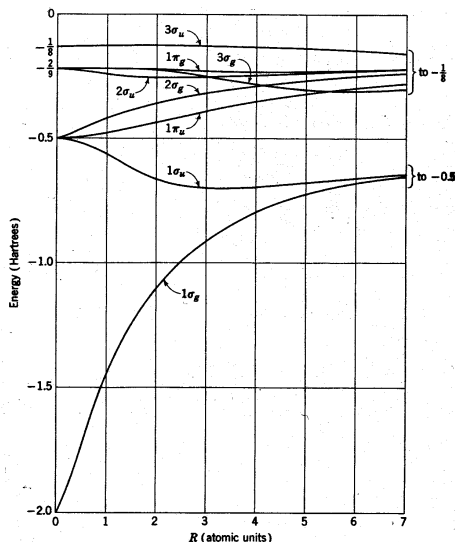


Figure 2.2: Lowest eigenvalues of the H_2^+ problem as a function of the internuclear distance R . Taken from Slater. wavefunction for the Slater determinant with ϕ_e doubly occupied is simply:

$$\Psi_{e\uparrow,e\downarrow}(r_1, r_2) = \phi_e(\mathbf{r}_1)\phi_e(\mathbf{r}_2) \frac{1}{\sqrt{2}} [\chi_\uparrow(\sigma_1)\chi_\downarrow(\sigma_2) - \chi_\downarrow(\sigma_1)\chi_\uparrow(\sigma_2)], \quad (2.101)$$

¹³Indeed, it has no nodes.

¹⁴For a full treatment of the problem see J.Slater, *Quantum Theory of Matter*, McGraw-Hill. It is shown there that the approximation in Eq. (2.100) is actually quite good down to distances of the order of $R = 2$ a.u..

Fig. 2.2 here shows the lowest eigenvalues of the H_2^+ problem as a function of the internuclear distance R . Once again, notice how ϵ_e and ϵ_o , the two lowest eigenvalues, evolve from, respectively, the $1s$ and $2p$ eigenvalues of He^+ , and smoothly evolve, as R increases towards two *very close eigenvalues* split by $2t$, where t is the *overlap matrix element* between too far apart $1s$ orbitals, as usual in the tight-binding theory.

So, for large R , it is fair to think of $\phi_{e(o)}(\mathbf{r})$ as bonding and antibonding combinations of $1s$ orbitals centered at the two nuclei:

$$\phi_{e(o)}(\mathbf{r}) = \frac{1}{\sqrt{2}} [\phi_{1s}(\mathbf{r} - \mathbf{R}_a) \pm \phi_{1s}(\mathbf{r} - \mathbf{R}_b)], \quad (2.100)$$

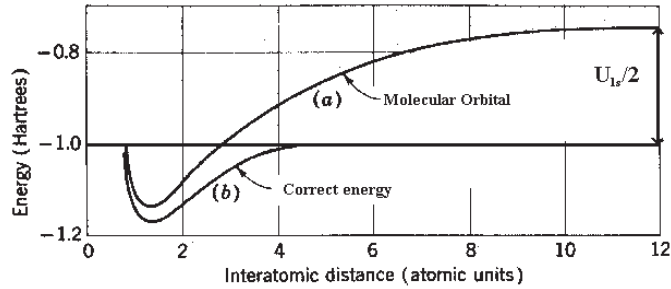
where we have neglected the small non-orthogonality between the two ϕ_{1s} .¹⁴ As a consequence, the

where the orbital part of the wavefunction can be expanded as follows:

$$\begin{aligned} \phi_e(\mathbf{r}_1)\phi_e(\mathbf{r}_2) = & \frac{1}{2}[\phi_{1s}(\mathbf{r}_1 - \mathbf{R}_a)\phi_{1s}(\mathbf{r}_2 - \mathbf{R}_b) + \phi_{1s}(\mathbf{r}_1 - \mathbf{R}_b)\phi_{1s}(\mathbf{r}_2 - \mathbf{R}_a) + \\ & \phi_{1s}(\mathbf{r}_1 - \mathbf{R}_a)\phi_{1s}(\mathbf{r}_2 - \mathbf{R}_a) + \phi_{1s}(\mathbf{r}_1 - \mathbf{R}_b)\phi_{1s}(\mathbf{r}_2 - \mathbf{R}_b)] . \end{aligned} \quad (2.102)$$

Notice that half of the wavefunction, precisely the two final terms, consists of configurations which are totally unphysical for large R , i.e., those in which both electrons occupy the ϕ_{1s} located on the *same atom*, which correspond to *ionized configurations* of the type H^-H^+ . Quite clearly, such configurations suffer from the large direct Coulomb integral U_{1s} .

It is therefore not surprising that the total energy of this wavefunction is so much higher than that of two Hydrogen atoms at $R = \infty$. Fig. 2.3 here shows two curves for $V_{ion-ion}(R)$ as a function of the internuclear distance R . The curve labelled “Correct energy” represents the exact result, whereas the one labelled “Molecular Orbital” represents the result of the calculation we have just sketched,



known as Molecular Orbital theory: essentially a one-electron tight-binding calculation for the molecule. Quite clearly, although the region close to the minimum is fairly well reproduced by the Molecular Orbital theory, the dissociation energy is completely off, wrong by a quantity which one can readily estimate to be roughly given by

$$U_{1s}/2 = 5/16 \text{ a.u.} \approx 8.5\text{eV}.$$

We would like to stress that this is not due to our having neglected the Hartree-term in performing our molecular orbital calculation, i.e., having used (2.99) instead of (2.98): it is a pitfall of HF with its requiring the wavefunction to be represented by a *single Slater determinant!*¹⁵ Quite clearly, allowing already *two* Slater determinants,

$$\frac{1}{\sqrt{2}}[\Psi_{e\uparrow,e\downarrow}(r_1, r_2) - \Psi_{o\uparrow,o\downarrow}(r_1, r_2)] , \quad (2.103)$$

including the one in which we occupy with two electrons the close in energy ϕ_o orbital, would cancel the unwanted part describing ionized configurations. The scheme that does so goes under the name of Heitler-London theory.¹⁶

The important message we learn from these simple examples is that correlation effects tend to be very important whenever there are small single-particle energy scales in the problem, like in solids with narrow electronic bands. Indeed, there are situations where the massive degeneracy of the single-particle levels makes the correlation terms completely dominating the physics, like in

¹⁵Combined with the requirements of a restricted HF approach, where parity and spin are taken as good quantum numbers.

¹⁶For a good discussion of this story, and the implications on magnetism, see the book by P. Fazekas, *Lecture Notes on Correlation and Magnetism*, World Scientific.

the Fractional Quantum Hall Effect: when there is a huge number of possible Slater determinants to choose from, all with the same average energy, it would be meaningless to pick up just one, forgetting all the others.

Chapter 3

Exact diagonalization and Lanczos algorithm

In this Chapter, we describe and discuss the Lanczos algorithm, which is an *exact* method for describing the low-energy spectrum of a *finite-size* system. The main idea is to express the ground state and the low-lying energy states in terms of a small set of orthonormal wave functions, that are built up iteratively. In this way, one is able to diagonalize the Hamiltonian in the low-energy sector, extracting properties like the energy of the ground-state and of a few low-lying excited states, and correlation functions.

Before describing the Lanczos algorithm, it is useful to introduce the Hubbard model, which is the simplest microscopic model for strongly correlated systems, and to consider a very simple case with only two sites, where we can perform analytically all the calculations.

3.1 Hubbard model

We consider a D-dimensional hypercubic lattice where at each site there is only one orbital (for simplicity we can consider an *s* orbital). Therefore, on each site *i*, at position R_i , we have only four possible states, that is the Hilbert space of the single site problem has dimension four:

$$\begin{aligned} 0 \text{ electrons} &\Rightarrow |0\rangle_i, \\ 1 \text{ up electron} &\Rightarrow |\uparrow\rangle_i = c_{i,\uparrow}^\dagger |0\rangle_i, \\ 1 \text{ down electron} &\Rightarrow |\downarrow\rangle_i = c_{i,\downarrow}^\dagger |0\rangle_i, \\ 2 \text{ electrons} &\Rightarrow |\uparrow\downarrow\rangle_i = c_{i,\uparrow}^\dagger c_{i,\downarrow}^\dagger |0\rangle_i. \end{aligned}$$

Here $c_{i,\sigma}^\dagger$ creates an electron in the Wannier orbital centered around the site R_i , corresponding to the wavefunction $\phi_\sigma(r - R_i)$. The total Hilbert space of the entire lattice is the direct product of the Hilbert spaces of each site.

The main approximation of the Hubbard model resides in considering that only the *on-site* Coulomb repulsion is different from zero. This is a very crude approximation for the Coulomb repulsion (a true long-range potential) and we can think that this is the result of a screening effect, which is very effective in metallic systems. We indicate by U the on-site Coulomb repulsion:

$$U = \int d\mathbf{r}_1 d\mathbf{r}_2 |\phi_\uparrow(\mathbf{r}_2)|^2 \frac{e^2}{|\mathbf{r}_1 - \mathbf{r}_2|} |\phi_\downarrow(\mathbf{r}_1)|^2, \quad (3.1)$$

in complete analogy with the direct Coulomb integral encountered in the previous Chapter. Then, the electrons can hop from a site i to a site j with an amplitude t_{ij} :

$$-t_{ij} = \int dr \phi_\sigma^*(r - R_i) h_{\text{one-body}} \phi_\sigma(r - R_j). \quad (3.2)$$

For simplicity, we can consider the case where $t_{ij} \neq 0$ for nearest-neighbor sites only. In the following we will indicate by t the nearest-neighbor hopping. This term corresponds to the usual kinetic energy of the electrons on the lattice. Finally, the ions are considered to be fixed at their equilibrium positions and, therefore, there is no lattice dynamics nor electron-phonon interaction.

Hubbard
model

Having done all these assumptions, we arrive at the *Hubbard model*:

$$H = -t \sum_{\langle i,j \rangle, \sigma} (c_{i\sigma}^\dagger c_{j\sigma} + H.c.) + U \sum_i n_{i\uparrow} n_{i\downarrow}, \quad (3.3)$$

where the symbol $\langle i, j \rangle$ stands for nearest-neighbor sites, $c_{i\sigma}^\dagger$ ($c_{i\sigma}$) creates (destroys) an electron of spin σ on site i , and $n_{i\sigma} = c_{i\sigma}^\dagger c_{i\sigma}$ is the electron density at the site i . In general, because the total number of electron is conserved (i.e., the total number of electron commutes with the Hubbard Hamiltonian), we will study the case of n electrons on a N -site hypercubic lattice.

Although the Hubbard Hamiltonian looks very simple, an exact solution for $U \neq 0$ is known only in one-dimensional systems (by using the so-called *Bethe ansatz*), and even the ground-state properties are unknown in all the most interesting cases (one exception is the case with $U = \infty$ and $n = N - 1$, where the ground state is totally polarized, i.e., it is ferromagnetic).

Notice that for $U = 0$ the Hubbard model is trivial because it describes free tight-binding electrons moving in an hypercubic lattice, and the Hamiltonian can be easily diagonalized by a Fourier transformation to Bloch waves $c_{\mathbf{k}\sigma}$:

$$c_{j\sigma} = \frac{1}{\sqrt{N}} \sum_{\mathbf{k}}^{BZ} e^{i\mathbf{k} \cdot \mathbf{R}_j} c_{\mathbf{k}\sigma}. \quad (3.4)$$

where the sum over \mathbf{k} is restricted to a Brillouin Zone (BZ). After this transformation, the Hamiltonian reads:

$$H = \sum_{\mathbf{k}, \sigma}^{BZ} \epsilon_{\mathbf{k}} c_{\mathbf{k}\sigma}^\dagger c_{\mathbf{k}\sigma}, \quad (3.5)$$

where the energy band $\epsilon_{\mathbf{k}}$ is

$$\epsilon_{\mathbf{k}} = -2t \sum_{\mu=1}^D \cos k_\mu, \quad (3.6)$$

with the lattice spacing taken to be one, $a = 1$. More explicitly, we have that

$$\begin{aligned} \text{1D :} \quad \epsilon_{\mathbf{k}} &= -2t \cos k \\ \text{2D :} \quad \epsilon_{\mathbf{k}} &= -2t(\cos k_x + \cos k_y) \\ \text{3D :} \quad \epsilon_{\mathbf{k}} &= -2t(\cos k_x + \cos k_y + \cos k_z). \end{aligned}$$

In this case the complete spectrum is known, and the eigenstates are

$$|\Psi\rangle = \prod_{\mathbf{k}}^{occ} c_{\mathbf{k}\uparrow}^\dagger \prod_{\mathbf{q}}^{occ} c_{\mathbf{q}\downarrow}^\dagger |0\rangle, \quad (3.7)$$

with energy

$$E = \sum_{\mathbf{k}, \sigma}^{occ} n_{\mathbf{k}\sigma} \epsilon_{\mathbf{k}}, \quad (3.8)$$

where $n_{\mathbf{k}\sigma} = 1$ (or 0) if the state \mathbf{k} is occupied (unoccupied) by an electron $i\sigma$. Thus, having fixed the number of up and down electrons, the ground state consists in occupying the lowest k states in accordance with the Pauli principle.

When U is finite, in two spatial dimensions, the phase diagram (number of electrons n versus U) is unknown and represents one of the most debated issues of the modern theory of strongly correlated systems. The main problem is that when U is large, compared to the bare bandwidth $4Dt$, it is no longer possible to use an independent electron picture, or a mean-field approach, where, for instance, the ground state is found by filling the lowest-energy levels of given bands. Indeed, in strongly correlated systems, the energy levels crucially depend on the Coulomb repulsion and the electron density. When the electron correlation is strong enough, the assumption that the free electronic state is adiabatically connected with the interacting state (the criterion on which the Landau theory of Fermi liquids is based) is no longer true and the elementary excitations are not simply connected to the ones of the non-interacting system. As an example, we consider the case of $n = N$, which is called half-filling, and an equal amount of up and down spins, $n_\uparrow = n_\downarrow = n/2$. For $U = 0$ the ground state is a metal, all the states with $\epsilon_k < \epsilon_F = 0$ are occupied by two electrons with opposite spins. The states with $\epsilon_k > 0$ are unoccupied, therefore, low-energy charge excitations are possible, simply by moving one electron from ϵ_F to a state with energy $\epsilon_F + \delta\epsilon$. In the opposite limit, $U \gg t$, the ground state is an insulator: all the sites are singly occupied and the charge excitations, that correspond to promote one electron on top to an other one (respecting the Pauli principle), have very high energy gap, $\Delta E \sim U$, two electrons being on the same site. In the extreme limit of $t = 0$, all the states with one electron per site are degenerate (with energy $E = 0$), independently on the actual spin configuration, this huge degeneracy is removed when a very small hopping term is allowed. Therefore, from this simple argument, it turn out that at half-filling there must be a metal-insulator transition by increasing the Coulomb interaction U . Actually, it is possible to show that, in the presence of nearest-neighbor hopping only, the ground state is an insulator, with long-range antiferromagnetic order, for any finite U .

3.2 Two-site Hubbard problem: a toy model.

It is very instructive to consider the case of two sites only:

$$H = -t \sum_{\sigma} (c_{1\sigma}^{\dagger} c_{2\sigma} + c_{2\sigma}^{\dagger} c_{1\sigma}) + U(n_{1\uparrow} n_{1\downarrow} + n_{2\uparrow} n_{2\downarrow}), \quad (3.9)$$

which we consider at half-filling, $n = N$, that is with $n = 2$ electrons. This exercise is also instructive as a simple toy model of the H_2 molecule at large enough R , discussed in the previous Chapter.

It is easy to verify that the Hamiltonian commutes with the total spin component in the z direction, S^z , $[H, S^z] = 0$, and, therefore, it is possible to diagonalize H separately on each subspace of given S^z . In the subspace of $S^z = 1$, we have only one state

$$c_{1\uparrow}^{\dagger} c_{2\uparrow}^{\dagger} |0\rangle, \quad (3.10)$$

and this state has $E = 0$. In a similar way, there is only one state in the subspace $S^z = -1$

$$c_{1\downarrow}^{\dagger} c_{2\downarrow}^{\dagger} |0\rangle, \quad (3.11)$$

again with $E = 0$. On the contrary, in the $S^z = 0$ subspace we have four states:

$$|1\rangle = c_{1\uparrow}^{\dagger} c_{2\downarrow}^{\dagger} |0\rangle, \quad (3.12)$$

$$|2\rangle = c_{1\downarrow}^{\dagger} c_{2\uparrow}^{\dagger} |0\rangle, \quad (3.13)$$

$$|3\rangle = c_{1\uparrow}^{\dagger} c_{1\downarrow}^{\dagger} |0\rangle, \quad (3.14)$$

$$|4\rangle = c_{2\uparrow}^{\dagger} c_{2\downarrow}^{\dagger} |0\rangle, \quad (3.15)$$

and the action of H is simply calculated to be:

$$H|1\rangle = -t|3\rangle - t|4\rangle, \quad (3.16)$$

$$H|2\rangle = +t|3\rangle + t|4\rangle, \quad (3.17)$$

$$H|3\rangle = -t|1\rangle + t|2\rangle + U|3\rangle, \quad (3.18)$$

$$H|4\rangle = -t|1\rangle + t|2\rangle + U|4\rangle. \quad (3.19)$$

Therefore, in principle, in order to diagonalize the Hamiltonian in the $S^z = 0$ subspace, we have to diagonalize a 4×4 matrix. However, we can also notice that:

$$H(|1\rangle + |2\rangle) = .0 \quad (3.20)$$

Indeed, the (normalized) state $1/\sqrt{2}(|1\rangle + |2\rangle)$ corresponds to the $S^z = 0$ state of the triplet. It is quite easy to show that the Hubbard Hamiltonian commutes not only with the z component of the total spin, but also with the total spin S^2 : in other words, the Hubbard Hamiltonian is $SU(2)$ invariant, and, therefore, the total spin is a good quantum number. It follows that all the triplet states with different S^z must be degenerate.

Moreover, we can also define the following states:

$$|1 - 2\rangle = \frac{1}{\sqrt{2}}(|1\rangle - |2\rangle), \quad (3.21)$$

$$|3 + 4\rangle = \frac{1}{\sqrt{2}}(|3\rangle + |4\rangle), \quad (3.22)$$

$$|3 - 4\rangle = \frac{1}{\sqrt{2}}(|3\rangle - |4\rangle), \quad (3.23)$$

obtaining

$$H|1 - 2\rangle = -2t|3 + 4\rangle, \quad (3.24)$$

$$H|3 + 4\rangle = -2t|1 - 2\rangle + U|3 + 4\rangle, \quad (3.25)$$

$$H|3 - 4\rangle = U|3 - 4\rangle. \quad (3.26)$$

Therefore, the (normalized) single state $1/\sqrt{2}|3 - 4\rangle$ is an eigenstate with eigenvalue U , and in order to find the remaining two singlet eigenstates we have to diagonalize a 2×2 matrix:

$$H = \begin{pmatrix} 0 & -2t \\ -2t & U \end{pmatrix}.$$

The two eigenvalues are given by:

$$\lambda_{\pm} = \frac{U \pm \sqrt{U^2 + 16t^2}}{2}, \quad (3.27)$$

and the two eigenstates are:

$$|\Psi_{-}\rangle = a_{-}|1 - 2\rangle + b_{-}|3 + 4\rangle, \quad (3.28)$$

$$|\Psi_{+}\rangle = a_{+}|1 - 2\rangle + b_{+}|3 + 4\rangle, \quad (3.29)$$

where a_{\pm} and b_{\pm} satisfy:

$$\frac{-U \mp \sqrt{U^2 + 16t^2}}{2} a_{\pm} - 2tb_{\pm} = 0 \quad (3.30)$$

$$(a_{\pm})^2 + (b_{\pm})^2 = 1. \quad (3.31)$$

After some simple algebra, we find:

$$a_{+} = \sqrt{\frac{1}{2} \left[1 - \frac{U}{\sqrt{U^2 + 16t^2}} \right]}, \quad (3.32)$$

$$a_{-} = \sqrt{\frac{1}{2} \left[1 + \frac{U}{\sqrt{U^2 + 16t^2}} \right]}, \quad (3.33)$$

$$b_{+} = -\sqrt{\frac{1}{2} \left[1 + \frac{U}{\sqrt{U^2 + 16t^2}} \right]}, \quad (3.34)$$

$$b_{-} = \sqrt{\frac{1}{2} \left[1 - \frac{U}{\sqrt{U^2 + 16t^2}} \right]}. \quad (3.35)$$

Notice that, because λ_{-} is always negative, the actual ground state is the singlet $|\Psi_{-}\rangle$.

It is very instructive to consider the limit of $U \gg t$, in this case the two eigenvalues are

$$\lambda_- \sim -\frac{4t^2}{U}, \quad (3.36)$$

$$\lambda_+ \sim U + \frac{4t^2}{U}, \quad (3.37)$$

and the two eigenstates are

$$|\Psi_-\rangle \sim |1-2\rangle, \quad (3.38)$$

$$|\Psi_+\rangle \sim |3+4\rangle. \quad (3.39)$$

$$(3.40)$$

This result should be contrasted with the Molecular Orbital theory of the H_2 molecule discussed in the previous Chapter, where the candidate ground state is taken to be, when expressed in terms of the previous states,

$$|\Psi_{e\uparrow, e\downarrow}\rangle = \frac{1}{\sqrt{2}}[|3+4\rangle + |1-2\rangle].$$

Thus, in the strong-coupling regime, the low-energy state almost consists of a state with no doubly occupied sites (i.e., $b_- \ll a_-$), and, most importantly, the two electrons have *opposite* spins. The gain in having antiparallel spins, with respect to the case of two parallel spins (with energy $E = 0$, independent on U), is $\lambda_- \sim -\frac{4t^2}{U}$.

The fact that in the strong coupling limit there is a tendency to have antiparallel spins comes out from a very general result, which is valid for the Hubbard model on any lattice: in the strong coupling limit $U \gg t$, it is indeed possible to show, by using perturbation theory, that the Hubbard model maps onto the antiferromagnetic Heisenberg model:

$$H_{heis} = J \sum_{\langle i,j \rangle} \vec{S}_i \cdot \vec{S}_j + \text{const}, \quad (3.41)$$

where $J = 4t^2/U$ is an *antiferromagnetic* coupling, favoring antiparallel spins, and $\vec{S}_i = (S_i^x, S_i^y, S_i^z)$ is the spin operator at the site i reading, in the fermionic representation, as

$$S_i^\alpha = \frac{1}{2} \sum_{\mu\nu} c_{i\mu}^\dagger (\sigma^\alpha)_{\mu\nu} c_{i\nu}, \quad (3.42)$$

with σ^α the Pauli matrices.

3.3 Lanczos algorithm

In the previous Section we have considered the case of the Hubbard model on two sites and we have found analytically all the spectrum and the eigenstates. By increasing the number of lattice sites, it becomes almost impossible to tackle the problem by using simple analytical tools. An alternative approach is to calculate the matrix that describe the Hamiltonian in a given basis $|\psi_k\rangle$ ($k = 1, \dots, \mathcal{N}_H$) (in the previous example we have chosen the basis of localized electron with a given spin in the z direction)

$$H_{k,k'} = \langle \psi_k | H | \psi_{k'} \rangle, \quad (3.43)$$

which is a $\mathcal{N}_H \times \mathcal{N}_H$ matrix, and diagonalize it by using standard diagonalization routines (e.g., the LAPACK routines). Unfortunately, this approach works only if the Hilbert space \mathcal{N}_H is not too large (a few thousands). Indeed, the disk space to keep in memory the matrix increases like \mathcal{N}_H^2 and the CPU-time like \mathcal{N}_H^3 .

In general the Hilbert space grows exponentially by increasing the number of sites, indeed by fixing the number of sites N , and the number of up and down electrons, n_\uparrow and n_\downarrow , respectively, the Hilbert space (for the Hubbard model) is

$$\mathcal{N}_H = \frac{N!}{n_\uparrow!(N-n_\uparrow)!} \times \frac{N!}{n_\downarrow!(N-n_\downarrow)!}, \quad (3.44)$$

for instance, for $N = 16$ and $n_\uparrow = n_\downarrow = 8$, $\mathcal{N}_H = (12870)^2 = 165636900$, which means that we should diagonalize a $165636900 \times 165636900$ matrix, which is impossible to tackle with a standard diagonalization routine.

The main ideas of the Lanczos method rely on the following points:

- The matrix $H_{k,k'}$ is a *sparse* matrix, i.e., most of its $\mathcal{N}_H \times \mathcal{N}_H$ elements are zero.
- In general we are interested in the properties of the ground state and of few excited states, and *not* in the full spectrum.

The Lanczos method uses a convenient basis set to diagonalize the Hamiltonian: starting from a trial state $|\Psi_{trial}\rangle$, which is assumed not to be orthogonal to the actual ground state, we construct iteratively an orthonormal basis, generated from $H^m|\Psi_{trial}\rangle$. The core part of the Lanczos algorithm is the calculation of $H|\Psi\rangle$, which, of course, must use the sparseness of H . The convergence of the method is very fast for the low-energy eigenstates. Fig. (3.1 shows the convergence of the lowest eigenvalues found by the Lanczos method (see below) as a function of the Lanczos iteration number n_L , for a $N = 16$ sites spin-1/2 Heisenberg chain with periodic boundary conditions. Notice the quick convergence of the ground state energy and of the first few excited states.

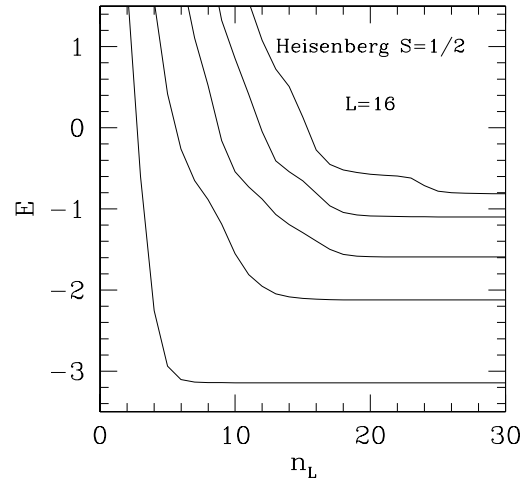


Figure 3.1: Convergence of the lowest eigenvalues of the Lanczos tridiagonal matrix as a function of the Lanczos iteration number n_L .

In the following, we will describe in some detail the Lanczos algorithm. We will proceed constructing a basis $|\Psi_k\rangle$ for the many-body system, in terms of which every state can be written as:

$$|\Psi\rangle = \sum_{k=1}^{\mathcal{N}_H} a_k |\Psi_k\rangle. \quad (3.45)$$

The starting point is a normalized trial wave function $|\Psi_{trial}\rangle$, that, in the following, will be denoted by $|\Psi_1\rangle$. From $|\Psi_1\rangle$, we can construct a second normalized state $|\Psi_2\rangle$, which is orthogonal to the previous one:

$$\beta_2|\Psi_2\rangle = H|\Psi_1\rangle - \alpha_1|\Psi_1\rangle. \quad (3.46)$$

To make $|\Psi_2\rangle$ orthogonal to $|\Psi_1\rangle$ we impose that

$$\langle\Psi_1|\Psi_2\rangle = \langle\Psi_1|H|\Psi_1\rangle - \alpha_1\langle\Psi_1|\Psi_1\rangle = 0, \quad (3.47)$$

and because $|\Psi_1\rangle$ is normalized, we obtain

$$\alpha_1 = \langle\Psi_1|H|\Psi_1\rangle, \quad (3.48)$$

that is α_1 is the average energy of $|\Psi_1\rangle$. In addition, β_2 can be found by taking the scalar product of Eq. (3.46) with $\langle\Psi_2|$

$$\beta_2 = \langle\Psi_2|H|\Psi_1\rangle. \quad (3.49)$$

Notice that, by using Eq. (3.46), we also have that

$$\beta_2^2 = \langle\Psi_1|(H - \alpha_1)(H - \alpha_1)|\Psi_1\rangle = \langle\Psi_1|H^2|\Psi_1\rangle - \alpha_1^2, \quad (3.50)$$

that is β_2 is the mean square energy deviation of $|\Psi_1\rangle$.

Let us go on with the application of H and define the third normalized vector, in such a way that it is orthogonal both to $|\Psi_1\rangle$ and to $|\Psi_2\rangle$

$$\beta_3|\Psi_3\rangle = H|\Psi_2\rangle - \alpha_2|\Psi_2\rangle - A|\Psi_1\rangle. \quad (3.51)$$

The conditions of orthogonality are

$$\langle\Psi_2|\Psi_3\rangle \Leftrightarrow \alpha_2 = \langle\Psi_2|H|\Psi_2\rangle, \quad (3.52)$$

$$\langle\Psi_1|\Psi_3\rangle \Leftrightarrow \langle\Psi_1|H|\Psi_2\rangle - A = 0 \Leftrightarrow A = \beta_2, \quad (3.53)$$

and finally, the fact that $|\Psi_3\rangle$ is normalized leads to

$$\beta_3 = \langle\Psi_3|H|\Psi_2\rangle. \quad (3.54)$$

A further step is needed in order to show a very important point of the Lanczos procedure. Therefore, let us go on and define the fourth normalized vector

$$\beta_4|\Psi_4\rangle = H|\Psi_3\rangle - \alpha_3|\Psi_3\rangle - A_2|\Psi_2\rangle - A_1|\Psi_1\rangle. \quad (3.55)$$

The conditions of orthogonality are

$$\langle\Psi_3|\Psi_4\rangle \Leftrightarrow \alpha_3 = \langle\Psi_3|H|\Psi_3\rangle, \quad (3.56)$$

$$\langle\Psi_2|\Psi_4\rangle \Leftrightarrow \langle\Psi_2|H|\Psi_3\rangle - A_2 = 0 \Leftrightarrow A_2 = \beta_3, \quad (3.57)$$

$$\langle\Psi_1|\Psi_4\rangle \Leftrightarrow A_1 = \langle\Psi_1|H|\Psi_3\rangle = 0, \quad (3.58)$$

the last result can be verified by using the fact that $H|\Psi_1\rangle = \beta_2|\Psi_2\rangle + \alpha_1|\Psi_1\rangle$, and thus

$$A_1 = \langle\Psi_1|H|\Psi_3\rangle = \beta_2\langle\Psi_2|\Psi_3\rangle + \alpha_1\langle\Psi_1|\Psi_3\rangle = 0. \quad (3.59)$$

Therefore, it comes out that $|\Psi_4\rangle$, once orthogonalized to $|\Psi_2\rangle$ and $|\Psi_3\rangle$, is *automatically* orthogonal to $|\Psi_1\rangle$. The fact that, in this procedure, at a given step, it is sufficient to orthogonalize only to the previous two vectors is a general feature, that makes the Lanczos algorithm very efficient. Indeed, suppose we have constructed the Lanczos vector up to $|\Psi_{m-1}\rangle$

$$\beta_{m-1}|\Psi_{m-1}\rangle = H|\Psi_{m-2}\rangle - \alpha_{m-2}|\Psi_{m-2}\rangle - \beta_{m-2}|\Psi_{m-3}\rangle, \quad (3.60)$$

with

$$\alpha_{m-2} = \langle \Psi_{m-2} | H | \Psi_{m-2} \rangle, \quad (3.61)$$

$$\beta_{m-2} = \langle \Psi_{m-2} | H | \Psi_{m-3} \rangle, \quad (3.62)$$

$$\beta_{m-1} = \langle \Psi_{m-1} | H | \Psi_{m-2} \rangle, \quad (3.63)$$

orthogonal to all $|\Psi_k\rangle$ with $k \leq m-2$. Then we define

$$\beta_m |\Psi_m\rangle = H|\Psi_{m-1}\rangle - \alpha_{m-1}|\Psi_{m-1}\rangle - \tilde{\beta}|\Psi_{m-2}\rangle - \sum_{j=1}^{m-3} A_j |\Psi_j\rangle. \quad (3.64)$$

The conditions of orthogonality reads as

$$\langle \Psi_{m-1} | \Psi_m \rangle \Leftrightarrow \alpha_{m-1} = \langle \Psi_{m-1} | H | \Psi_{m-1} \rangle, \quad (3.65)$$

$$\langle \Psi_{m-2} | \Psi_m \rangle \Leftrightarrow \tilde{\beta} = \langle \Psi_{m-2} | H | \Psi_{m-1} \rangle = \beta_{m-1}, \quad (3.66)$$

$$A_j = \langle \Psi_j | H | \Psi_{m-1} \rangle, \quad (3.67)$$

but, because we have (here we suppose, of course that for $j > 1$)

$$H|\Psi_j\rangle = \beta_{j+1}|\Psi_{j+1}\rangle + \alpha_j|\Psi_j\rangle + \beta_j|\Psi_{j-1}\rangle, \quad (3.68)$$

and $j+1 \leq m-2$, we obtain that

$$A_j = 0. \quad (3.69)$$

Then, $|\Psi_m\rangle$, once orthogonalized to $|\Psi_{m-1}\rangle$ and $|\Psi_{m-2}\rangle$, it is automatically orthogonal to all the previous vectors.

Thus, the very important outcome is that, at each Lanczos step, we have to orthogonalize the vector only to the previous two vectors, and the orthogonality with the previous ones is automatic. Of course, when this procedure is done *numerically*, there is some rounding error due to the machine precision, and the vectors can have a very small component parallel to the previous ones.

In the Lanczos algorithm, the only constants that are needed are the α_m 's and the β_m 's, in term of which, if we truncate the calculation to $n_L \leq \mathcal{N}_H$, we have

$$H = \begin{pmatrix} \alpha_1 & \beta_2 & 0 & 0 & \dots \\ \beta_2 & \alpha_2 & \beta_3 & 0 & \dots \\ 0 & \beta_3 & \alpha_3 & \beta_4 & \dots \\ 0 & 0 & \beta_4 & \alpha_4 & \dots \\ \dots & \dots & \dots & \dots & \dots \end{pmatrix}.$$

that is, in the Lanczos basis, the Hamiltonian is a tridiagonal symmetric matrix, with α_m on the diagonal and β_m below the diagonal. The key point is that, in order to obtain the low-energy spectrum, we need

$$n_L \ll \mathcal{N}_H. \quad (3.70)$$

In practice, it is sufficient to perform $n_L \sim 10^2$ Lanczos steps to get a very accurately the ground-state vector.

The memory requirements are quite limited compared to \mathcal{N}_H^2 . Indeed, we need only two or three vectors of dimension \mathcal{N}_H (two vectors are enough for making the Lanczos procedure), then, generally, the Hamiltonian is kept as a compact matrix of dimension $\approx N \times \mathcal{N}_H$. When we are interested in having the ground-state vector, and not only the eigenvalues, three vectors are useful to avoid a lot of writing and reading from the hard disk. Finally, as far as the CPU-time is concerned, the Lanczos algorithm scales like $\text{const} \times \mathcal{N}_H$, instead of \mathcal{N}_H^3 as in the standard diagonalization.

Part II

Monte Carlo methods

Chapter 4

Probability theory

4.1 Introduction

We have seen that one of the important advantages of the Hartree-Fock theory (apart from providing a simple choice for the unknown many-body wavefunction, in the form of a single Slater determinant) is to reduce a $3N$ -dimensional integral, corresponding to the calculation of the total energy of N electrons, to a much simpler one, containing only one- and two-body matrix elements, and involving at most 6-dimensional integrals. This is an enormous simplification, as for a conventional $3N$ -dimensional integration, the effort in evaluating the integrand grows exponentially with N , limiting N to very small values.

In general, when the wavefunction is not simply a *single Slater determinant*, this simplification is not possible, and even a slight modification of the Slater determinant, including some simple form of correlations between electrons, through a prefactor of the determinant (Jastrow factor), restores immediately the problem of the integration over $3N$ variables. In the configuration interaction approach, this problem is solved by expanding a correlated wavefunction in terms of a certain number of Slater determinants. However, within this approach, the number of terms has to increase very quickly with N (e.g., for a lattice model, the Hilbert space grows exponentially, and similarly also the number of Slater determinants required for convergence has to increase).

In the following, we will introduce a statistical method to solve the problem of large multidimensional integrals, by means of the so-called Monte Carlo approach. The name Monte Carlo originates, according to some, from a game played in Monte Carlo by the young children. They used to throw paper balls in a circular region limited by a square perimeter. Then, after many trials, they used to sum all the balls inside the circular region in order to determine the winner. Probably, they did not know that the ratio of the number of balls inside the region divided by the ones inside the whole square perimeter should give the area of the circle divided by the surrounding square, namely the number $\pi/4$. This story about the origin of the name “Monte Carlo” is probably not historically true, but it is amusing to imagine that the most powerful technique for

multidimensional integrals was originated by a game.

Before describing this powerful technique, we need to introduce the concept of probability, and some basic standard definitions such as random variables, mean value, variance, etc. A clear and comprehensive treatment of the theory of probability, including its axiomatic foundations, is given in the book by B. Gnedenko, *The theory of probability*, MIR.

4.2 A bit of probability theory

In principle, by using classical physics laws, we can make *exact* predictions of events by knowing exactly the initial conditions. In practice, there are several events that are unpredictable, essentially because it is impossible to have the exact knowledge of the initial conditions, and a very small error in those conditions will grow exponentially in time, invalidating any attempt to follow the exact equations of motion: The weather forecast and the rolling of a die are examples of such unpredictable phenomena. We will see that, though it is essentially impossible to predict exactly what number will show up after rolling a die, it is perfectly defined to ask ourselves what is the probability that a given number will come out.

In the definition of probability, it is important to *assume* that there exist reproducible experiments, that, under very similar initial conditions (e.g., rolling of a die using always the same die and similar speed and direction), produce different events (denoted here by E_i): For a die the event number i , E_i , maybe defined “successful” when the die shows up the number i , for $i = 1, \dots, 6$. For weather forecast, the event “it is raining” or “it is cloudy” maybe analogously defined “successful” or “unsuccessful”. It is therefore natural to introduce the probability of the event E_i as:

Probability

$$P(E_i) = p_i = \frac{\text{Number of successful events}}{\text{Total number of experiments}}. \quad (4.1)$$

In the following, we will see that the number p_i , i.e., the probability of the event E_i , is consistently defined in the limit of a large number of experiments. For instance, we can easily imagine that, after rolling the die several times, the number of times any given number has appeared will be approximately 1/6 of the total number of trials.

4.2.1 Events and probability

We describe in the following some simple properties of events.

Two events E_i and E_j are said to be *mutually exclusive events* if and only if the occurrence of E_i implies that E_j does not occur and vice versa. If E_i and E_j are mutually exclusive,

$$\begin{aligned} P(E_i \text{ and } E_j) &= 0 \\ P(E_i \text{ or } E_j) &= p_i + p_j \end{aligned} \quad (4.2)$$

A whole class of events can be mutually exclusive for all i and j . When the class is exhaus-

tive, that is *all* possible events have been enumerated, being M the number of exclusive events characterizing the experiment, then, by using (4.2) clearly:

$$P(\text{some } E_i) = \sum_{i=1}^M p_i = 1. \quad (4.3)$$

In order to characterize all possible exclusive events one can define *composite* events.¹ For instance, rolling two dice is an experiment that can be characterized by E_i^1 and E_j^2 , where E_j^1 (E_j^2) refers to the possible outcomes of the first (second) die. For composite events, the probability is labeled by more than one index, in particular the *joint probability* $p_{i,j}$ is defined as:

$$p_{i,j} = P(E_i^1 \text{ and } E_j^2). \quad (4.4)$$

Suppose E_i^1 and E_j^2 define a composite event of an exhaustive class of events, as for instance the event "it is cloudy" and the one "it is raining", then the joint probability can be written:

$$p_{i,j} = \sum_k p_{i,k} \left[\frac{p_{i,j}}{\sum_k p_{i,k}} \right] = p(i) \left[\frac{p_{i,j}}{\sum_k p_{i,k}} \right] = p(i) p(j|i), \quad (4.5)$$

Marginal and
conditional
probability

where

$$p(i) = \sum_k p_{i,k} \quad (4.6)$$

defines the so-called *marginal probability* that the event E_i^1 (e.g. it is cloudy) occurs, whatever the second event may be (does not matter whether it is raining or not). The second factor in Eq. (4.5) is the so-called *conditional probability*:

$$p(j|i) = \frac{p_{i,j}}{\sum_k p_{i,k}}, \quad (4.7)$$

that is the probability for the occurrence of the event E_j^2 (e.g. it is raining), given that the event E_i^1 (it is cloudy) has occurred. The conditional probability is normalized to 1, $\sum_j p(j|i) = 1$, as it should be for representing a probability. Finally, Eq. (4.5) shows that any joint probability can be factorized into a marginal probability times a conditional probability. Analogously one can define the marginal probability of the second event $p(j) = \sum_k p_{k,j}$ and the conditional probability of the first event given that the second E_j^2 has a given value j ; $p(i|j) = \frac{p_{i,j}}{\sum_k p_{k,j}}$ so that the basic relation (4.5) can be easily extended to:

$$p_{i,j} = p(j) p(i|j) \quad (4.8)$$

$$p_{i,j} = p(i) p(j|i) \quad (4.9)$$

Whenever the conditional probability $p(j|i)$ ($p(i|j)$) of the second (first) event does not depend on the first (second) event, namely the conditional probability depends only on the left index, then the event E_i^1 (E_j^2) is said to be independent of the event E_j^2 (E_i^1), because the occurrence of

¹In a more formal approach, originally due to Kolmogorov, one defines, starting from a set of elementary events E_i , the set of all possible combinations of events under the operations of 'union', 'intersection', and 'negation', forming what is sometimes called a σ -algebra of events, or a *Borel field of events*. We will not pursue this formal approach. The interested reader can consult the book by Gnedenko.

the first (second) event does not depend on the second (first) one. In this case it is simple to show, using (4.8), that (i) reciprocity: if the first event is independent of the second one also the second is independent of the first. Indeed given that by assumption $p(i|j)$ does not depend on j , using (4.5) we can evaluate $p(j|i)$ in (4.7) and show that also this one does not depend on i , namely $p(j|i) = \frac{p(j)p(i|j)}{\sum_k p(k)p(i|k)} = p(j)$ as $\sum_k p(k) = 1$. (ii) if two composite events are independent than the joint probability $p(i, j)$ factorizes into a product of the two corresponding marginal probabilities:

$$p_{i,j} = p(i)p(j) = P(E_i^1)P(E_j^2) \quad (4.10)$$

We finally remark that we can define as composite events the ones obtained by two or more realizations of the *same experiment*. By definition, we assume that different realizations of the same experiment are always independent, otherwise there should exist some particular external condition (e.g., the speed of rolling the die) that has a clear influence on the experiment and has not been correctly taken into account to classify exhaustively the events of the experiment. In principle, the joint probability of N realizations of the same experiment can always be written as:

$$p_{i_1, i_2, \dots, i_N} = P(E_{i_1}^1 \text{ and } E_{i_2}^2 \cdots \text{ and } E_{i_N}^N) = P(E_{i_1}^1)P(E_{i_2}^2) \cdots P(E_{i_N}^N), \quad (4.11)$$

where $E_{i_1}^1, E_{i_2}^2 \cdots E_{i_N}^N$ indicate the N events of the same experiment repeated N times.

4.2.2 Random variables, mean value and variance

Random
variable

Once for a given experiment E all the possible *exclusive* events E_j are classified, for each realization of the experiment there is only one integer i such that E_i is verified. Therefore we can define a *random variable* $i \rightarrow x_i$, as a real-valued function associated to any possible successful event E_i .² The simplest random variable is the *characteristic* random variable $x^{[j]}$:

$$x_i^{[j]} = \begin{cases} 1 & \text{if } E_j \text{ is satisfied} \\ 0 & \text{otherwise} \end{cases},$$

i.e., in words, $x_i^{[j]} = \delta_{i,j}$ and is non zero only if the event E_j is successful. As another example, when rolling a die, a random variable could be the actual outcome of the experiment, i.e., the number that shows up:

$$x_i = i \text{ if } E_i \text{ is satisfied} \quad \text{for } i = 1, \dots, 6,$$

Mean value

For any random variable x , we can define its *mean value* $\langle x \rangle$, i.e., the expected average value after repeating several times the same experiment. According to the basic definition of probability, Eq. (4.1), this quantity is simply related to the probability p_i of the experiment that satisfies the event E_i with random variable x_i :

$$\langle x \rangle = \sum_i x_i p_i. \quad (4.12)$$

²Notice that, as a function defined on the space of the events, x_i is a perfectly deterministic function. It is unpredictable only the *value* the random variable x_i attains due to the unpredictability to determine what particular event E_i is satisfied in the given experiment E .

Notice that for the characteristic random variable $x^{[j]}$ of the event E_j , we simply have $\langle x^{[j]} \rangle = p_j$.

In general, the n^{th} moment of a random variable x_i is defined as the expectation values of the n^{th} power of x_i :

$$\langle x^n \rangle = \sum_i x_i^n p_i, \quad (4.13)$$

where obviously x_i^n stands for $(x(E_i))^n$. The second moment allows us to define a particularly important quantity, which is the *variance* of the variable x , defined as:

Variance

$$\text{var}(x) \stackrel{\text{def}}{=} \langle x^2 \rangle - \langle x \rangle^2 = \sum_i (x_i - \langle x \rangle)^2 p_i. \quad (4.14)$$

The variance is a positive quantity, as shown explicitly by the last equality, which is very simple to prove. The variance can be zero only when all the events having a non-vanishing probability give the same value for the variable x , i.e., $x_i = \langle x \rangle$ for all i 's for which $p_i \neq 0$. In other words, whenever the variance is zero, the random character of the variable is completely lost and the experiment “what value will the variable x assume” becomes predictable. In general, the square root of the variance is a measure of the dispersion of the random variable, and is called the *standard deviation* $\sigma = \sqrt{\text{var}(x)}$.

4.2.3 The Chebyshev's inequality

Whenever the variance is very small, the random variable x becomes close to being predictable, in the sense that its value x_i for each event E_i with a non-negligible probability is close to the mean value $\langle x \rangle$, the uncertainty in the value being determined by a small standard deviation $\sigma = \sqrt{\text{var}(x)}$. In order to be more precise in the above statement, we will prove in the following a very simple and powerful inequality, known as the Chebyshev's inequality.

Chebyshev's inequality

Let us consider the probability \bar{P} that the value attained by a random variable x will depart from its mean $\langle x \rangle$ by a given amount $\sqrt{\frac{\text{var}(x)}{\delta}}$ larger than the standard deviation ($\delta < 1$):

$$\bar{P} = P \left[(x - \langle x \rangle)^2 \geq \frac{\text{var}(x)}{\delta} \right] = \sum_{(x_i - \langle x \rangle)^2 \geq \frac{\text{var}(x)}{\delta}} p_i. \quad (4.15)$$

Then, one can show that the probability for the occurrence of such an event is bounded by δ itself, namely:

$$\bar{P} \leq \delta. \quad (4.16)$$

Indeed, by the definition of the variance given in Eq. (4.14), we have:

$$\begin{aligned} \text{var}(x) &= \sum_i (x_i - \langle x \rangle)^2 p_i \\ &\geq \sum_{(x_i - \langle x \rangle)^2 \geq \frac{\text{var}(x)}{\delta}} (x_i - \langle x \rangle)^2 p_i \geq \frac{\text{var}(x)}{\delta} \bar{P}, \end{aligned} \quad (4.17)$$

where the last inequality is simply obtained by replacing $(x_i - \langle x \rangle)^2$ with its lower bound $\frac{\text{var}(x)}{\delta}$, and then using the definition of \bar{P} in Eq. (4.15). Inverting the last inequality, we finally obtain the desired upper-bound $\bar{P} \leq \delta$.

4.2.4 The law of large numbers: consistency of the definition of probability

A simple way to reduce the uncertainty of a given measurement is to repeat the experiment several times, taking the average of the individual outcomes of the desired observable. Let us consider the random variable \bar{x} obtained by averaging a large number N of independent realizations of the same experiment, each providing a value x_i for some given observable:

$$\bar{x} = \frac{1}{N} \sum_i x_i . \quad (4.18)$$

Since all experiments are identical and independent from each other, the joint-probability of all the N events is known and given by the expression in Eq. (4.11), the probability of each single event being $P(E_i)$. Therefore, it is easy to compute the mean value of the average value \bar{x} in Eq. (4.18). All the N terms in the sum give an identical contribution, equal to $\langle x \rangle$, thus resulting in:

$$\langle \bar{x} \rangle = \langle x \rangle , \quad (4.19)$$

namely, the mean value of the average \bar{x} coincides exactly with the mean value of the single experiment, as it is rather obvious to expect.

In order to compute the variance of \bar{x} , we simply notice that, by averaging \bar{x}^2 over the distribution (4.11), we get:

$$\langle \bar{x}^2 \rangle = \frac{1}{N^2} \sum_{i,j} \langle x_i x_j \rangle = \frac{1}{N^2} [N \langle x^2 \rangle + N(N-1) \langle x \rangle^2] . \quad (4.20)$$

There are two contributions in the latter equation, the first one coming from the terms $i = j$ in the expansion of the square, and giving simply N times $\langle x_i^2 \rangle$ (that do not depend on i), the second being originated by the $N(N-1)$ terms obtained for $i \neq j$, and giving simply products of independent simple means, $\langle x_i \rangle \langle x_j \rangle = \langle x \rangle^2$. Using the relationship in Eq. (4.20), and the definition of variance, we finally obtain:

$$\text{var}(\bar{x}) \stackrel{def}{=} \langle \bar{x}^2 \rangle - \langle \bar{x} \rangle^2 = \frac{1}{N} \text{var}(x) . \quad (4.21)$$

Therefore, for large N , the random variable \bar{x} , corresponding to averaging a large number of realizations of the same experiment, is determined with much less uncertainty than the single-experiment mean, as from the Chebyshev's inequality (4.16) used for $\delta = \frac{1}{\sqrt{N}}$. almost all possible average measurements (each of them characterized by N different realizations of the same experiment) gives a value for \bar{x} close to the theoretical mean value $\langle x \rangle + O(\frac{1}{\sqrt{N}})$.

Suppose now that the random variable x_i is just the characteristic random variable of a given event E_j , $x^{[j]}$. For this random variable we have already noticed that the mean value is the probability of the event E_j . namely $\langle x^{[j]} \rangle = p_j$. Then, in view of the discussion of the present section, the mean of the random variable \bar{x} obtained by averaging N independent realizations of the same experiment gives an estimate of p_j , with a standard deviation $\sigma = \sqrt{\text{var}(\bar{x})}$ which decreases like $1/\sqrt{N}$, by Eq. (4.21). This uncertainty can be made arbitrarily small, by increasing N , so that the probability p_j of the event E_j is a well defined quantity in the limit of $N \rightarrow \infty$. In conclusion,

we have consistently justified the definition (4.1), which is the basis of the classical approach to probability. In this scheme the concept of probability is strongly related to the reproducibility of the experiments, which is the basis of the physical method.

4.2.5 Extension to continuous random variables and central limit theorem

The generalization of the above analysis holds obviously also for random variables defined on the continuum. In order to go from discrete to continuous variables, we will have to replace summations with integrals, with rather obvious generalizations. For instance, whenever the set of events is not countable but is a *continuum* in the Chebyshev's inequality (4.16), we have to appropriately generalize what we mean by E_i and p_i .

Let us consider the event that a continuous random variable x is smaller than y , where y is a given fixed real number. The probability $P\{x \leq y\}$ of such an event is a well defined function $F(y)$,

$$F(y) = P\{x \leq y\} , \quad (4.22)$$

which is called the *cumulative probability* of the random variable x . Clearly $F(\infty) = 1$, and $F(y)$ is a monotonically increasing function. The latter property derives from the definition of probability, Eq. (4.1), as the events which are successful for a given y_1 , $x \leq y_1$, are *a fortiori* also successful for a larger $y_2 \geq y_1$, since $x \leq y_1 \leq y_2$, implying that $F(y_1) \leq F(y_2)$.

Given the above properties we can define a *positive definite* function called the *probability density* $\rho(y)$, which represents the analog of the p_i used for discrete random variables: Probability density

$$\rho(y) = \frac{dF(y)}{dy} . \quad (4.23)$$

Obviously $\rho(y) \geq 0$, being F monotonically increasing. The above derivative can be defined also in the sense of *distributions*, so that it represents a very general definition; in particular, whenever the number of possible events E_i is discrete, $\rho(y)$ is just a sum of δ -functions, $\rho(y) = \sum_i p_i \delta(y - x(E_i))$. The mean value and the variance of continuous random variables are then obtained by replacing p_i with the corresponding probability density ρ , and substituting sums with integrals, as follows:

$$\langle x \rangle = \int_{-\infty}^{\infty} dx \rho(x) x , \quad (4.24)$$

$$\text{var}(x) = \int_{-\infty}^{\infty} dx \rho(x) (x - \langle x \rangle)^2 , \quad (4.25)$$

where obviously the normalization condition $\int_{-\infty}^{\infty} \rho(x) = F(\infty) = 1$ holds for the probability density. Notice that the *existence* of the variance, and of higher moments as well, is not a priori guaranteed in the continuous case: The probability density $\rho(x)$ has to decrease sufficiently fast at $x \rightarrow \pm\infty$ in order for the corresponding integrals to exist. For instance, if $\rho(x)$ has a Lorentzian form, $\rho(x) = \gamma/(\pi(x^2 + \gamma^2))$, then the variance and all the higher moments are not defined.

An important quantity related to the probability density $\rho(x)$ is the characteristic function $\hat{\rho}_x(t)$, which is basically the Fourier transform of the probability density, defined as:

$$\hat{\rho}_x(t) = \int_{-\infty}^{\infty} dx \rho(x) e^{i(x-\langle x \rangle)t} . \quad (4.26)$$

For small t , if the variance $\sigma^2 = \text{var}(x)$ is finite, one can expand the exponential up to second order in t , yielding,

$$\hat{\rho}_x(t) = 1 - \sigma^2 t^2 / 2 + \dots . \quad (4.27)$$

Analogously to the discrete case, the probability density of independent random variables x and y is the product of the corresponding probability densities. It is then very simple to show that the characteristic function of a *sum* of two independent random variables $z = x + y$ is just the *product* of the two, namely:

$$\hat{\rho}_z(t) = \hat{\rho}_x(t) \hat{\rho}_y(t) . \quad (4.28)$$

Using the above properties, and the expansion in Eq. (4.27), it is readily obtained the so-called *central limit theorem*, which provides the asymptotic probability distribution of average quantities over several realizations of a given experiment. We will see that this allows a much better estimate of the uncertainty of these average quantities compared with the Chebyshev's inequality estimate (4.16). Going back to the discussion of Sec. 4.2.4, let us consider the probability distribution of the average $\bar{x} = (1/N) \sum_i x_i$ of N independent measurements of the *same* quantity. We already know that the mean of the average \bar{x} coincides with $\langle x \rangle$, the single-experiment mean, but we would like to understand better the fluctuations of \bar{x} around this mean value. To this end, let us consider the following continuous random variable Y directly related to $\bar{x} - \langle x \rangle$:

$$Y = \frac{\sum_{i=1}^N (x_i - \langle x \rangle)}{\sqrt{N}} = \sqrt{N}(\bar{x} - \langle x \rangle) , \quad (4.29)$$

whose mean value is $\langle Y \rangle = 0$. By using iteratively Eq. (4.28), we can simply derive that

$$\hat{\rho}_Y(t) = \left[\hat{\rho}_x\left(\frac{t}{\sqrt{N}}\right) \right]^N . \quad (4.30)$$

For large enough N , at fixed t , it is legitimate to substitute the expansion (4.27) for ρ_x in the above equation, obtaining a well defined limit for $\hat{\rho}_Y(t)$, independent of most of the details of the probability density $\rho(x)$:

$$\rho_Y(t) \rightarrow \exp(-t^2 \sigma^2 / 2) \quad \text{for } N \rightarrow \infty . \quad (4.31)$$

Central limit theorem This means that the distribution function ρ_Y of the random variable Y in the limit $N \rightarrow \infty$ becomes a Gaussian, centered at $\langle Y \rangle = 0$, with variance σ^2 . This statement goes under the name of *central limit theorem*.

Going back to our average \bar{x} , we arrive at the conclusion that \bar{x} is Gaussian distributed, for large N , according to the probability density:

$$\rho(\bar{x}) = \frac{1}{\sqrt{2\pi\sigma^2/N}} \exp \left[-\frac{(\bar{x} - \langle x \rangle)^2}{2\sigma^2/N} \right] . \quad (4.32)$$

k	Chebyshev	Gaussian
1	1	0.31731
2	1/4	0.0455
3	1/9	0.0027
4	1/16	6.33-e5
5	1/25	5.77e-7
6	1/36	1.97e-9
7	1/49	2.55e-12
8	1/64	1.22e-15

Table 4.1: Probability \bar{P} that a random variable has a fluctuation away from its mean value larger than k standard deviations. The Chebyshev's bound holds for generic distributions, whereas the rightmost column holds for the Gaussian distribution.

The standard deviation $\bar{\sigma} = \frac{\sigma}{\sqrt{N}}$ of the random variable \bar{x} is decreasing with N , and its distribution is approaching, for large N , the Gaussian one. Therefore, as shown in Table (4.1), the central limit allows us to reduce substantially the uncertainty on the mean value, as it is clear that, for large N , this statistical uncertainty can be pushed down to arbitrarily small values. This is essentially the rationale behind the scheme for computing integrals with Monte Carlo, in principle with arbitrarily small accuracy. Remember, however, that the possibility of having fluctuations from the mean value of more than one error bar is the norm in Monte Carlo (see Table 4.1). Only results within at least 3 error bars have a sufficient degree of reliability: the probability that a fluctuation of more than 3 error bars will occur is less than 3/1000. It happens, in several papers, that strong statements are made that can be invalidated in presence of fluctuations of two error bars. In general, before starting to use the Monte Carlo technique, it is a good idea to familiarize with Table 4.1.

Exercise 4.1 What is the variance σ_z^2 of the difference $z = x - y$ of two independent random variables x and y , with corresponding variance σ_x and σ_y ?

Exercise 4.2 Consider a continuous random variable $0 \leq x < 1$ distributed according to the uniform distribution $\rho(x) = 1$ of a "random number generators",

- Compute the mean average $\langle x \rangle$ and its variance $\text{var}\langle x \rangle$.
- What should be the autocorrelation time

$$C(\tau) = \langle x_{n+\tau} x_n \rangle - \langle x_{n+\tau} \rangle \langle x_n \rangle \quad (4.33)$$

as a function of the integer τ , for a perfect random number generator that generates for any trial n an independent random number (namely the variables x_n and $x_{n+\tau}$ are independent) ?

- Is it a sufficient condition for a perfect random number generator? hint: Consider the probability density $\rho(x, y) = N((xy)^2 + b(x + y) + c)$, for the two variables x, y defined in the

interval $0 \leq x, y < 1$ where $N = 1/(b + c + 1/9)$ is the normalization constant, and b and c are such that $\rho(x, y) \geq 0$. Show that the function $\rho(x, y)$ represents a probability density when:

$$\begin{aligned} I & \quad b > 0 & \quad c > 0 \\ II & \quad -2 \leq b < 0 & \quad c > \frac{b^2}{4} - b \\ III & \quad b \leq -2 & \quad c > -(1 + 2b) \end{aligned}$$

Show that the correlation $C = \langle xy \rangle - \langle x \rangle \langle y \rangle = \frac{b}{432} + \frac{(c-b^2)}{144}$ may vanish even when $c \neq 0$ or $b \neq 0$, namely when the two random variables x and y are not independent.

Exercise 4.3 Consider a continuous random variable x distributed according to the Lorentzian probability density $\rho(x) = 1/\pi(1 + x^2)$, determine the distribution of the mean average of the variable \bar{x} over several independent samples of the same Lorentzian random variable:

$$\bar{x} = \frac{1}{N} \sum_i x_i \quad (4.34)$$

- Compute the probability density of the random variable \bar{x} . Hint: the Fourier transform of the Lorentzian is $\exp(-|t|)$.
- Does the central limit theorem hold for the random variable \bar{x} ? If not explain why.

Exercise 4.4 Consider the N independent realization $x_i, i = 1, \dots, N$ of the same random variable x , distributed according to a given probability density $\rho(x)$ with finite mean x_M and variance σ . In order to estimate the variance σ from the given set $\{x_i\}$, one can consider the random variable:

$$y = \frac{(\sum_i x_i^2)}{N} - \left(\frac{\sum_i x_i}{N}\right)^2 \quad (4.35)$$

- Show that $\langle y \rangle = (N-1)/N\sigma$, thus a better estimate of the variance is given by $yN/(N-1)$, as well known.
- What is the estimate of the variance of the mean average:

$$\bar{x} = \frac{1}{N} \sum_i x_i \quad (4.36)$$

in terms of y ,

- and the variance of this estimate? hint: assume for simplicity $x_M = 0$, and N large.

Chapter 5

Quantum Monte Carlo: The variational approach

5.1 Introduction: importance of correlated wavefunctions

The simplest Hamiltonian in which electron-electron correlations play an important role is the one-dimensional Hubbard model:

$$H = -t \sum_{\langle i,j \rangle} \sum_{\sigma} (c_{i\sigma}^{\dagger} c_{j\sigma} + H.c.) + U \sum_i n_{i\uparrow} n_{i\downarrow}, \quad (5.1)$$

where $c_{i\sigma}^{\dagger}$ ($c_{i\sigma}$) creates (destroys) an electron with spin σ on the site i , $n_{i,\sigma} = c_{i\sigma}^{\dagger} c_{i\sigma}$ is the electron number operator (for spin σ) at site i , and the symbol $\langle i, j \rangle$ indicates nearest-neighbor sites. Finally, the system is assumed to be finite, with L sites, and with periodic boundary conditions (alternatively, you can think of having a *ring* of L sites).

A particularly important case is when the number N of electrons is equal to the number of sites L , a condition that is usually called *half filling*. In this case, the non-interacting system has a metallic ground state: For $U = 0$, the electronic band is half filled and, therefore, it is possible to have low-energy charge excitations near the Fermi surface. In the opposite limit, for $t = 0$, the ground state consists in having one electron (with spin up or down) on each site, the total energy being zero. Of course, because the total energy does not depend on the spin direction of each spin, the ground state is highly degenerate (its degeneracy is exactly equal to 2^N). The charge excitations are gapped – the lowest one corresponding to creating an empty and a doubly occupied site, with an energy cost of U – and, therefore, the ground state is insulating. This insulator state, obtained in the limit of large values of U/t , is called *Mott insulator*. In this case, the insulating behavior is due to the strong electron correlations, since, according to band theory, one should obtain a metal (we have an odd number of electrons per unit cell). Because of the different behavior of the ground state in the two limiting cases, $U = 0$ and $t = 0$, a metal-insulator transition is expected to appear for intermediate values of U/t . Actually, in one dimension, the

Hubbard model is exactly solvable by using the so-called *Bethe Ansatz*, and the ground state is found to be an insulator for all $U/t > 0$, but, in general, one expects that the insulating state appears only for (U/t) above some positive critical value $(U/t)_c$.

Hereafter, we define an electron configuration $|x\rangle$ as a state where all the electron *positions* and *spins* along the z -axis are defined. In the one-dimensional Hubbard model, an electron configuration can be written as:

$$|x\rangle = |\uparrow, \uparrow\downarrow, 0, 0, \downarrow, \dots\rangle = c_{1,\uparrow}^\dagger c_{2,\uparrow}^\dagger c_{2,\downarrow}^\dagger c_{5,\downarrow}^\dagger \dots |0\rangle, \quad (5.2)$$

namely, on each site we can have no particle (0), a singly occupied site (\uparrow or \downarrow) or a doubly occupied site ($\uparrow\downarrow$). Notice that on each configuration the number of doubly occupied sites $D = \sum_i n_{i,\uparrow} n_{i,\downarrow}$ is a well defined number. The state $|x\rangle$ we have written is nothing but a Slater determinant in position-spin space.

The $U = 0$ exact ground state solution of the Hubbard model, $|\Psi_0\rangle$, can be expanded in terms of the complete set of configurations $|x\rangle$:

$$|\Psi_0\rangle = \prod_{k \leq k_F, \sigma} c_{k,\sigma}^\dagger |0\rangle = \sum_x |x\rangle \langle x | \Psi_0\rangle. \quad (5.3)$$

In the case of $U/t \gg 1$, this very simple wavefunction is not a good variational state, and the reason is that the configurations with doubly occupied states have too much weight (verify that the average density of doubly occupied sites is 1/4 for the state $|\Psi_0\rangle$). Indeed, by increasing U/t , all the configurations with one or more doubly occupied sites will be “projected out” from the exact ground state, simply because they have a very large (of order of U/t) average energy. A simple correlated wavefunction that is able to describe, at least qualitatively, the physics of the Mott insulator is the so-called *Gutzwiller wavefunction*. In this wavefunction the uncorrelated weights $\langle x | \Psi_0\rangle$ are modified according to the number of doubly occupied sites in the configuration $|x\rangle$:

$$|\Psi_g\rangle = e^{-gD} |\Psi_0\rangle = \sum_x |x\rangle e^{-g\langle x | D | x\rangle} \langle x | \Psi_0\rangle \quad (5.4)$$

For $g = \infty$, only those configurations $|x\rangle$ without doubly occupied sites remain in the wavefunction, and the state is correctly an insulator with zero energy expectation value.

The importance of electronic correlation in the Gutzwiller wavefunction is clear: In order to satisfy the strong local constraint of having no doubly occupied sites, one has to expand the wavefunction in terms of a huge number of Slater determinants (in position-spin space), each satisfying the constraint. This is the opposite of what happens in a weakly correlated system, where one, or at most a few, Slater determinants (with appropriate orbitals selected) can describe qualitatively well, and also quantitatively, the ground state.

5.2 Expectation value of the energy

Once a correlated wavefunction is defined, as in Eq. (5.4), the problem of computing the expectation value of the Hamiltonian (the variational energy) is very involved, because each configuration $|x\rangle$

in the expansion of the wavefunction will contribute in a different way, due to the Gutzwiller weight $\exp(-g\langle x|D|x\rangle)$. In order to solve this problem numerically, we can use a Monte Carlo sampling of the huge Hilbert space containing 4^L different configurations. To this purpose, using the completeness of the basis, $\mathbf{1} = \sum_x |x\rangle\langle x|$, we can write the expectation value of the energy in the following way:

$$E(g) = \frac{\langle \Psi_g | H | \Psi_g \rangle}{\langle \Psi_g | \Psi_g \rangle} = \frac{\sum_x e_L(x) \psi_g^2(x)}{\sum_x \psi_g^2(x)}, \quad (5.5)$$

where $\psi_g(x) = \langle x | \Psi_g \rangle$ and $e_L(x)$ is the so-called *local energy* :

Local energy

$$e_L(x) = \frac{\langle x | H | \Psi_g \rangle}{\langle x | \Psi_g \rangle}. \quad (5.6)$$

Therefore, we can recast the calculation of $E(g)$ as the average of a random variable $e_L(x)$ over a probability distribution p_x given by:

$$p_x = \frac{\psi_g^2(x)}{\sum_x \psi_g^2(x)}. \quad (5.7)$$

As we will show in the following, it is possible to define a stochastic algorithm (Markov chain), which is able of generating a sequence of configurations $\{|x_n\rangle\}$ distributed according to the desired probability p_x . Then, since the local energy can be easily computed for any given configuration, with at most L^3 operations, we can evaluate the expectation value of the energy as the mean of the random variable $e_L(x)$ over the visited configurations:

$$E(g) = \frac{1}{N} \sum_{n=1}^N e_L(x_n). \quad (5.8)$$

Notice that the probability itself, p_{x_n} , of a given configuration x_n does not appear in Eq. (5.8). This might seem surprising at a first glance. The important point to notice, however, is that we have assumed that the configurations x_n are already distributed according to the desired probability p_x , so that configurations x with larger probability p_x will automatically be generated more often than those with a smaller probability. The factor p_x is therefore automatically accounted for, and would be incorrect to include it in Eq. (5.8).¹ This approach is very general and can be extended (with essentially the same definitions) to continuous systems (replace summations with multidimensional integrals), and to general Hermitian operators \hat{O} (for instance the doubly occupied site number D), the corresponding local estimator, replacing $e_L(x)$ in Eq. (5.8), being analogously defined:

$$O_L(x) = \frac{\langle x | \hat{O} | \Psi_g \rangle}{\langle x | \Psi_g \rangle}. \quad (5.9)$$

5.3 Zero variance property

An important feature of the variational approach is the so-called *zero variance property*. Suppose that the variational state $|\Psi_g\rangle$ coincides with an exact eigenstate of H (not necessarily the ground

¹It is worth noticing here that p_x is generally easy to calculate up to a normalization constant, which is instead very complicated, virtually impossible, to calculate. In the present case, for instance, $\psi_g^2(x)$ is assumed to be simple, but $\sum_x \psi_g^2(x)$ involves a sum over the huge Hilbert space of the system, and is therefore numerically inaccessible in most cases.

state), namely $H|\Psi_g\rangle = E(g)|\Psi_g\rangle$. Then, it follows that the local energy $e_L(x)$ is constant:

$$e_L(x) = \frac{\langle x|H|\Psi_g\rangle}{\langle x|\Psi_g\rangle} = E(g) \frac{\langle x|\Psi_g\rangle}{\langle x|\Psi_g\rangle} = E(g). \quad (5.10)$$

Therefore, the random variable $e_L(x)$ is independent on $|x\rangle$, which immediately implies that its variance is zero, and its mean value $E(g)$ coincides with the exact eigenvalue. Clearly the closer is the variational state $|\Psi_g\rangle$ to an exact eigenstate, the smaller the variance of $e_L(x)$ will be, and this is very important to reduce the statistical fluctuations and improve the numerical efficiency.

Notice that the average square of the local energy $\langle e_L^2(x) \rangle$ corresponds to the exact quantum average of the Hamiltonian squared. Indeed:

$$\frac{\langle \Psi_g | H^2 | \Psi_g \rangle}{\langle \Psi_g | \Psi_g \rangle} = \frac{\sum_x \langle \Psi_g | H | x \rangle \langle x | H | \Psi_g \rangle}{\sum_x \langle \Psi_g | x \rangle \langle x | \Psi_g \rangle} = \frac{\sum_x e_L^2(x) \psi_g^2(x)}{\sum_x \psi_g^2(x)} = \langle e_L^2 \rangle. \quad (5.11)$$

Thus, the variance of the random variable $e_L(x)$ is exactly equal to the quantum variance of the Hamiltonian on the variational state $|\Psi_g\rangle$:

$$\sigma^2 = \frac{\langle \Psi_g | (H - E_g)^2 | \Psi_g \rangle}{\langle \Psi_g | \Psi_g \rangle} = \text{var}(e_L). \quad (5.12)$$

It is therefore clear that the smaller the variance is, the closer the variational state to the exact eigenstate will be.

Instead of minimizing the energy, it is sometime convenient to *minimize the variance* (e.g., as a function of the parameter g). From the variational principle, the smaller the energy is the better the variational state will be, but, without an exact solution, it is hard to judge how accurate the variational approximation is. On the contrary, the variance is very useful, because the smallest possible variance, equal to zero, is known *a priori*, and in this case the variational state represent an exact eigenstate of the hamiltonian.

5.4 Markov chains: stochastic walks in configuration space

A Markov chain is a non deterministic dynamics, for which a random variable, denoted by x_n , evolves as a function of a discrete iteration time n , according to a stochastic dynamics given by:

$$x_{n+1} = F(x_n, \xi_n). \quad (5.13)$$

Here F is a known given function, independent of n , and the stochastic nature of the dynamics is due to the ξ_n , which are random variables (quite generally, ξ_n can be a vector whose coordinates are independent random variables), distributed according to a given probability density $\chi(\xi_n)$, independent on n . The random variables ξ_n at different iteration times are independent (they are independent realizations of the same experiment), so that, e.g., $\chi(\xi_n, \xi_{n+1}) = \chi(\xi_n)\chi(\xi_{n+1})$. In the following, for simplicity of notation, we will indicate x_n and ξ_n as simple random variables, even though they can generally represent multidimensional random vectors. Furthermore, we will also consider that the random variables x_n assume a discrete set of values,² as opposed to continuous

²For instance $\{x_n\}$ defines the discrete Hilbert space of the variational wavefunction in a finite lattice Hamiltonian

ones, so that multidimensional integrals may be replaced by simple summations. Generalizations to multidimensional continuous cases are rather obvious.

It is simple to simulate a Markov chain on a computer, by using the so-called *pseudo-random number generator* for obtaining the random variables ξ_n , and this is the reason why Markov chains are particularly important for Monte Carlo calculations. Indeed, we will see that, using Markov chains, we can easily define random variables x_n that, after the so called "equilibration time", namely for n large enough, will be distributed according to any given probability density $\bar{\rho}(x_n)$ (in particular, for instance, the one which is required for the variational calculation in Eq. (5.7)).

The most important property of a Markov chain is that the random variable x_{n+1} depends only on the previous one, x_n , and on ξ_n , but not on quantities at time $n - 1$ or before. Though ξ_{n+1} and ξ_n are independent random variables, the random variables x_n and x_{n+1} are *not independent*; therefore we have to consider the generic joint probability distribution $f_n(x_{n+1}, x_n)$, and decompose it, according to Eq. (4.5), into the product of the marginal probability $\rho_n(x_n)$ of the random variable x_n , times the conditional probability $K(x_{n+1}|x_n)$:

$$f_n(x_{n+1}, x_n) = K(x_{n+1}|x_n) \rho_n(x_n). \quad (5.14)$$

Notice that the conditional probability K does not depend on n , as a consequence of the Markovian nature of Eq. (5.13), namely that the function F and the probability density χ of the random variable ξ_n do not depend on n .

We are now in the position of deriving the so-called *Master equation* associated to a Markov chain. Indeed, from Eq. (4.6), the marginal probability of the variable x_{n+1} is given by $\rho_{n+1}(x_{n+1}) = \sum_{x_n} f(x_{n+1}, x_n)$, so that, using Eq. (5.14), we get:

$$\rho_{n+1}(x_{n+1}) = \sum_{x_n} K(x_{n+1}|x_n) \rho_n(x_n). \quad (5.15)$$

The Master equation allows us to calculate the evolution of the marginal probability ρ_n as a function of n , since the conditional probability $K(x'|x)$ is univocally determined by the stochastic dynamics in Eq. (5.13). More precisely, though the actual value of the random variable x_n at the iteration n is not known deterministically, the probability distribution of the random variable x_n is instead known *exactly*, in principle, at each iteration n , once an initial condition is given, for instance at iteration $n = 0$, through a $\rho_0(x_0)$. The solution for $\rho_n(x_n)$ is then obtained iteratively by solving the Master equation, starting from the given initial condition up to the desired value of n .

5.5 Detailed balance

A quite natural question to pose concerns the existence of a limiting distribution reached by $\rho_n(x)$, for sufficiently large n , upon iterating the Master equation: Does $\rho_n(x)$ converge to some limiting distribution $\bar{\rho}(x)$ as n gets large enough? The question is actually twofold: i) Does it exist a stationary distribution $\bar{\rho}(x)$, i.e., a distribution which satisfies the Master equation (5.15) when

plugged in both the right-hand and the left-hand side? ii) Starting from a given arbitrary initial condition $\rho_0(x)$, under what conditions it is guaranteed that $\rho_n(x)$ will converge to $\bar{\rho}(x)$ as n increases? The first question (i) requires:

$$\bar{\rho}(x_{n+1}) = \sum_{x_n} K(x_{n+1}|x_n) \bar{\rho}(x_n). \quad (5.16)$$

In order to satisfy this stationarity requirement, it is sufficient (but not necessary) to satisfy the so-called *detailed balance* condition:

$$K(x'|x) \bar{\rho}(x) = K(x|x') \bar{\rho}(x'). \quad (5.17)$$

This relationship indicates that the number of processes undergoing a transition $x \rightarrow x'$ has to be exactly compensated, to maintain a stable stationary condition, by the same amount of reverse processes $x' \rightarrow x$; the similarity with the Einstein's relation for the problem of radiation absorption/emission in atoms is worth to be remembered.

It is very simple to show that the detailed balance condition allows a stationary solution of the Master equation. Indeed, if for some n we have that $\rho_n(x_n) = \bar{\rho}(x_n)$, then:

$$\rho_{n+1}(x_{n+1}) = \sum_{x_n} K(x_{n+1}|x_n) \bar{\rho}(x_n) = \bar{\rho}(x_{n+1}) \sum_{x_n} K(x_n|x_{n+1}) = \bar{\rho}(x_{n+1}), \quad (5.18)$$

where we used the detailed balance condition (5.17) for the variables $x' = x_{n+1}$ and $x = x_n$, and the normalization condition for the conditional probability $\sum_{x_n} K(x_n|x_{n+1}) = 1$.

The answer to question (ii) is quite more complicated in general. In this context it is an important simplification to consider that the conditional probability function $K(x'|x)$, satisfying the detailed balance condition (5.17), can be written in terms of a symmetric function $\bar{H}_{x',x} = \bar{H}_{x,x'}$ apart for a similarity transformation:

$$K(x'|x) = -\bar{H}_{x',x} g(x') / g(x) \quad (5.19)$$

where $\bar{H}_{x',x} < 0$ and $g(x) = \sqrt{\bar{\rho}(x)}$ is a positive function which is non zero for all configurations x , and is normalized $\sum_x g^2(x) = 1$. Though the restriction to satisfy the detailed balance condition is not general, it basically holds in many applications of the Monte Carlo technique, as we will see in the following.

The function $\bar{H}_{x',x}$, being symmetric, can be thought as the matrix elements of an Hamiltonian with non positive off diagonal matrix elements. The ground state of this fictitious hamiltonian will be bosonic (i.e. non negative for each element x) for well known properties of quantum mechanics that we will briefly remind here. This "bosonic" property of the ground state will be very useful to prove the convergence properties of a Markov chain described by (5.19). Indeed due to the normalization condition $\sum_{x'} K(x',x) = 1$, the positive function $g(x)$ is just the bosonic ground state of \bar{H} with eigenvalue $\lambda_0 = -1$.

It is then simple to show that no other eigenvalue λ_i of \bar{H} can be larger than 1 in modulus, namely $|\lambda_i| \leq 1$. Indeed suppose it exists an eigenvector $\psi_i(x)$ of H with maximum modulus

eigenvalue $|\lambda_i| > 1$, then:

$$|\lambda_i| = \left| \sum_{x,x'} \psi_i(x) (-\bar{H}(x,x')) \psi_i(x') \right| \leq \sum_{x,x'} |\psi_i(x)| (-\bar{H}(x,x')) |\psi_i(x')| \quad (5.20)$$

Thus $|\psi_i(x)|$ may be considered a trial state with expectation value of the energy larger or equal than $|\lambda_i|$ in modulus. Since the matrix \bar{H} is symmetric, by the well known properties of the minimum/maximum expectation value, this is possible only if the state $\psi_{Max}(x) = |\psi_i(x)|$ with all non negative elements is also an eigenstate with maximum eigenvalue $|\lambda_i|$. By assumption we know that $g(x)$ is also an eigenstate with all positive elements and therefore the assumption of $|\lambda_i| > 1$ cannot be fulfilled as the overlap between eigenvectors corresponding to different eigenvalues has to be zero and instead $\sum_x g(x) \psi_{Max}(x) > 0$. The only possibility is that $|\lambda_i| \leq 1$ for all eigenvalues, and $g(x)$ is a bosonic ground state of \bar{H} as we have anticipated.

A further assumption needed to show that the equilibrium density distribution $\bar{\rho}(x)$ can be reached for large n , is that the Markov chain is *ergodic*, i.e., any configuration x' can be reached, in a sufficiently large number of Markov iterations, starting from any initial configuration x . This implies that $g(x)$ is the *unique* ground state of \bar{H} with maximum modulus eigenvalue, a theorem known as the Perron-Frobenius. To prove this theorem, suppose that there exists another ground state $\psi_0(x)$ of \bar{H} different from $g(x)$. Then, by linearity and for any constant λ , also $g(x) + \lambda \psi_0(x)$ is a ground state of \bar{H} , so that by the previous discussion also the bosonic state $\bar{\psi}(x) = |g(x) + \lambda \psi_0(x)|$ is a ground state of \bar{H} , and the constant λ can be chosen to have $\bar{\psi}(x) = 0$ for a particular configuration $x = x_0$. By using that $\bar{\psi}$ is an eigenstate of \bar{H} , we have:

$$\sum_{x(\neq x_0)} \bar{H}_{x_0,x} \bar{\psi}(x) = \lambda_0 \bar{\psi}(x_0) = 0$$

so that, in order to fulfill the previous condition, $\bar{\psi}(x) = 0$ for all configurations connected to x_0 by \bar{H} , since $\bar{\psi}(x)$ is non negative and $-\bar{H}_{x_0,x}$ is strictly positive. By applying iteratively the previous condition to the new configurations connected with x_0 , we can continue, by using ergodicity, to have that

$$\bar{\psi}(x) = 0$$

for *all* configurations. This would imply that $g(x)$ and $\psi_0(x)$ differ at most by an overall constant $-\lambda$ and therefore $g(x)$ is the unique ground state of \bar{H} .

We have finally derived that if ergodicity and detailed balance hold, the ground state of the fictitious hamiltonian \bar{H} (5.19) is unique and equal to $g(x)$ with eigenvalue $\lambda_0 = -1$. This implies, as readily shown later on, that any initial $\rho_0(x)$ will converge in the end towards the limiting stationary distribution $\bar{\rho}(x) = g(x)^2$. In fact:

$$\rho_n(x') = \sum_x g(x') [-\bar{H}]_{x',x}^n / g(x) \rho_0(x) \quad (5.21)$$

where the n^{th} power of the matrix \bar{H} can be expanded in terms of its eigenvectors:

$$[-\bar{H}]_{x',x}^n = \sum_i (-\lambda_i)^n \psi_i(x') \psi_i(x) \quad (5.22)$$

Since $\psi_0(x) = g(x)$ is the unique eigenvector with eigenvalue $\lambda_0 = -1$, by replacing the expansion (5.22) in (5.21) we obtain:

$$\rho_n(x) = g(x) \sum_i \psi_i(x) (-\lambda_i)^n \left[\sum_{x'} \psi_i(x') \rho_0(x') / g(x') \right] \quad (5.23)$$

Thus for large n only the $i = 0$ term remains in the above summation and all the other ones decay exponentially as $|\lambda_i| < 1$ for $i \neq 0$. It is simple then to realize that for large n

$$\rho_n(x) = g^2(x) \quad (5.24)$$

as the initial distribution is normalized and:

$$\left[\sum_{x'} \psi_0(x') \rho_0(x') / g(x') \right] = \sum_{x'} \rho_0(x') = 1$$

Summarizing, if a Markov chain satisfies detailed balance and is ergodic, then the equilibrium distribution $\bar{\rho}(x)$ will be always reached, for large enough n , independently of the initial condition at $n = 0$. The convergence is always exponential and indeed the dynamic has a well defined finite correlation time equal to the inverse gap to the first excited state of the hamiltonian matrix $\bar{H}_{x',x}$

5.6 The Metropolis algorithm

Suppose we want to generate a Markov chain such that, for large n , the configurations x_n are distributed according to a given probability distribution $\bar{\rho}(x)$. We want to construct, accordingly, a conditional probability $K(x'|x)$ satisfying the detailed balance condition Eq. (5.17) with the desired $\bar{\rho}(x)$. How do we do that, in practice? In order to do that, Metropolis and collaborators introduced a very simple scheme. They started considering a transition probability $T(x'|x)$, defining the probability of going to x' given x , which can be chosen with great freedom, as long as ergodicity is ensured, without any requirement of detailed balance. In order to define a Markov chain satisfying the detailed balance condition, the new configuration x' generated by the chosen transition probability $T(x'|x)$ is then accepted only with a probability:

$$A(x'|x) = \text{Min} \left\{ 1, \frac{\bar{\rho}(x') T(x|x')}{\bar{\rho}(x) T(x'|x)} \right\}, \quad (5.25)$$

so that the resulting conditional probability $K(x',x)$ is given by:

$$K(x'|x) = A(x'|x) T(x'|x) \quad \text{for } x' \neq x. \quad (5.26)$$

The value of $K(x'|x)$ for $x' = x$ is determined by the normalization condition $\sum_{x'} K(x'|x) = 1$. The proof that detailed balance is satisfied by the $K(x'|x)$ so constructed is quite elementary, and is left as an exercise for the reader. It is also simple to show that the conditional probability $K(x'|x)$ defined above can be casted in the form (5.19), for which, in the previous section, we have proved that the equilibrium distribution can be always reached after many iterations. In particular:

$$g(x) = \sqrt{\bar{\rho}(x)} \quad (5.27)$$

$$\bar{H}(x',x) = -A(x'|x) T(x'|x) g(x) / g(x') \quad (5.28)$$

In fact from the definition of the acceptance probability (5.25), it is simple to verify that \bar{H} in (5.27) is symmetric and that the results of the previous section obviously hold also in this case.

Summarizing, if x_n is the configuration at time n , the Markov chain iteration is defined in two steps:

1. A *move* is proposed by generating a configuration x' according to the transition probability $T(x'|x_n)$;
2. The move is *accepted*, and the new configuration x_{n+1} is taken to be equal to x' , if a random number ξ_n (uniformly distributed in the interval $(0, 1]$) is such that $\xi_n \leq A(x'|x_n)$, otherwise the move is *rejected* and one keeps $x_{n+1} = x_n$.

The important simplifications introduced by the Metropolis algorithm are:

1. It is enough to know the desired probability distribution $\bar{\rho}(x)$ up to a normalization constant, because only the ratio $\frac{\bar{\rho}(x')}{\bar{\rho}(x)}$ is needed in calculating the acceptance probability $A(x'|x)$ in Eq. (5.25). This allows us to avoid a useless, and often computationally prohibitive, normalization (e.g., in the variational approach, the normalization factor $\sum_x \psi_g^2(x)$ appearing in Eq. (5.7) need not be calculated).
2. The transition probability $T(x'|x)$ can be chosen to be very simple. For instance, in a one-dimensional example on the continuum, a new coordinate x' can be taken with the rule $x' = x + a\xi$, where ξ is a random number uniformly distributed in $(-1, 1)$, yielding $T(x'|x) = 1/2a$ for $x - a \leq x' \leq x + a$. In this case, we observe that $T(x'|x) = T(x|x')$, a condition which is often realized in practice. Whenever the transition probability is symmetric, i.e., $T(x'|x) = T(x|x')$, the factors in the definition of the acceptance probability $A(x'|x)$, Eq. (5.25), further simplify, so that

$$A(x'|x) = \text{Min} \left\{ 1, \frac{\bar{\rho}(x')}{\bar{\rho}(x)} \right\} .$$

3. As in the example shown in the previous point, the transition probability $T(x'|x)$ allows us to impose that the new configuration x' is very close to x , at least for a small enough. In this limit, all the moves are always accepted, since $\bar{\rho}(x')/\bar{\rho}(x) \approx 1$, and the rejection mechanism is ineffective. A good rule of thumb to speed up the equilibration time, i.e., the number of iterations needed to reach equilibrium distribution, is to tune the transition probability T , for instance by increasing a in the above example, in order to have an average acceptance rate $\langle A \rangle = 0.5$, which corresponds to accepting, on average, only half of the total proposed moves. This criterium is usually the optimal one for computational purposes, but it is not a general rule.

5.7 The bin technique for the estimation of error bars

Let us now go back to our Variational Monte Carlo problem, formulated in Sec. 5.2. As we have seen, we can easily set up a Markov chain in configuration space such that, after discarding a suitable number of initial configurations that are not representative of the equilibrium distribution (we call this initial stage, the *equilibration part*), the Markov process will generate many configuration x_n , $n = 1, \dots, N$, distributed according to the desired probability, Eq. (5.7). We have also seen that, in order to reduce the error bars, we can average the quantity we need to calculate over many realizations N of the same experiment, which in the Markov chain are naturally labeled by the index n of the Markov dynamics:

$$\bar{e}_L = \frac{1}{N} \sum_{n=1}^N e_L(x_n). \quad (5.29)$$

The mean value of the random variable \bar{e}_L is equal to the expectation value of the energy, since all the x_n , after equilibration, are distributed according to the marginal probability p_x , Eq. (5.7). However, the random variables x_n are not independent from each other, and the estimation of the variance with the expression (4.20) will lead, generally, to underestimating the error bars.

In order to overcome the previous difficulty, we divide up a long Markov chain with N steps into several (k) segments (bins), each of length $M = N/k$. On each bin j , $j = 1, \dots, k$, we define the partial average:

$$e_L^j = \frac{1}{M} \sum_{n=(j-1)M+1}^{jM} e_L(x_n), \quad (5.30)$$

so that, clearly,

$$\bar{e}_L = \frac{1}{k} \sum_{j=1}^k e_L^j.$$

We still need to understand how large we have to select M (the length of each bin) in order for the different partial (bin) averages e_L^j to be, effectively, *independent random variables*. This calls for the concept of *correlation time*. After the equilibrium part, that we assume already performed at $n = 1$, the average energy-energy correlation function

$$C(n-m) = \langle e_L(x_n) e_L(x_m) \rangle - \langle e_L(x_n) \rangle \langle e_L(x_m) \rangle, \quad (5.31)$$

depends only on the discrete time difference $n-m$ (stationarity implies time-homogeneity), and it approaches zero exponentially as $C(n-m) \propto e^{-|n-m|/\tau}$, where τ (in units of the discrete time-step) is the correlation time for the local energy in the Markov chain. If we therefore take M (the length of each bin) to be sufficiently larger than τ , $M \gg \tau$, the different bin averages e_L^j can be reasonably considered to be independent random variables, and the variance \bar{e}_L can be easily estimated. Indeed, it can be easily shown that the mean value of the random variable δe_L defined by:

$$\delta e_L = \frac{1}{k(k-1)} \sum_{j=1}^k (e_L^j - \bar{e}_L)^2 \quad (5.32)$$

is equal to $\text{var}(e_L)$, thus δe_L is an estimate of the variance of \bar{e}_L . Strictly speaking, the above equation is valid only when the e_L^j 's are all independent variables, a property that holds for large

M, as one can realize for instance by calculating the bin-energy correlation for two consecutive bins:

$$\langle e^j e^{j+1} \rangle = \langle e_j \rangle \langle e_{j+1} \rangle + \frac{1}{M^2} \left[MC(M) + \sum_{j=1}^{M-1} (C(j) + C(2M-j)) \right]. \quad (5.33)$$

Thus, for the evaluation of the variance, all the bin averages e_L^j can be considered to be independent from each other, up to $O((1/M)^2)$. The estimate of the variance given by Eq. (5.32) is very convenient, because it does not require a difficult estimate of the correlation time associated to the correlation function (5.31).

Exercise 5.1 Consider the one dimensional Heisenberg model with an even number L of sites:

$$H = J \sum_{i=1}^L \vec{S}_i \cdot \vec{S}_{i+1} \quad (5.34)$$

with periodic boundary conditions $\vec{S}_{i+L} = \vec{S}_i$. A good variational wavefunction for the ground state of H can be defined in the basis of configurations $\{x\}$ with definite value of $S_i^z = \pm 1/2$ on each site i and vanishing total spin projection on the z -axis ($\sum_i S_i^z = 0$). In this basis the wavefunction can be written as:

$$\psi(x) = \text{Sign}_M(x) \times \exp \left(\frac{\alpha}{2} \sum_{i \neq j} v_{i,j}^z (2S_i^z)(2S_j^z) \right) \quad (5.35)$$

where $\text{Sign}_M(x) = (-1)^{\sum_{i=1}^{L/2} (S_{2i}^z + 1/2)}$ is the so called Marshall sign determined by the total number of up spins in the even sites, α is a variational parameter, whereas the form of the spin Jastrow factor $v_{i,j}^z = \ln(d_{i,j}^2)$ depends parametrically on the so called cord-distance $d_{i,j}$ between two sites, namely:

$$d_{i,j} = 2 \sin(\pi|i-j|/L) \quad (5.36)$$

- By using the Metropolis algorithm determine the variational energy for the optimal variational parameter α on a finite size $L \leq 100$.
- Using that the energy per site of the Heisenberg model converges to the thermodynamic limit with corrections proportional to $1/L^2$, determine the best upper bound estimate of the energy per site in this model for $L \rightarrow \infty$ and compare it with the exact result: $e_0 = -J(\ln 2 - 1/4) = -J0.44314718$.

Chapter 6

Langevin molecular dynamics for classical simulations at finite T .

There are several ways to simulate a classical partition function

$$Z = \int dx e^{-\beta v(x)} \quad (6.1)$$

at finite inverse temperature $\beta = 1/k_B T$ using a dynamical evolution of the classical particles. In the above expression x may denote the generic positions of the N classical particles, and the corresponding symbol dx stands for a suitable $3N$ -multidimensional integral. Probably the simplest way to simulate such a classical system at finite temperature is given by the so-called first order Langevin dynamics, described by the following equations of motion:

$$\dot{x} = f(x) + \eta_t, \quad (6.2)$$

where $f(x) = -\partial_x v(x)$ represents the classical force acting on the particles, \dot{x} is the usual time derivative of x , and η_t represents a vector in the $3N$ dimensional space, such that each component is a gaussian random variable with zero mean $\langle \eta_t \rangle = 0$, and defined by the following correlator:

$$\langle \eta_t \eta_{t'} \rangle = 2k_B T \delta(t - t'). \quad (6.3)$$

In other words, one assumes that there is no correlation of the noise at different times, namely that the random variables $\eta(t)$ and $\eta(t')$ are always independent for $t \neq t'$. The presence of the noise makes the solution of the above differential equations — a special type of differential equations known as *stochastic differential equations* — also “noisy”.

6.1 Discrete-time Langevin dynamics

In order to solve the above stochastic differential equations, and define an appropriate algorithm for the simulation of classical particles at finite temperature, we integrate both sides of Eq.(6.26)

over finite intervals (t_n, t_{n+1}) , where $t_n = \Delta n + t_0$ are discretized times and t_0 is the initial time (obtained for $n = 0$). In this way we obtain:

$$x_{n+1} - x_n = \Delta f_n + \int_{t_n}^{t_{n+1}} dt \eta(t) + O(\Delta |\Delta f|) \quad (6.4)$$

where we have defined $x_n = x(t_n)$, $f_n = f(x(t_n))$, and we have approximated the integral of the force in this interval with the lowest order approximation Δf_n , where Δf is the maximum variation of the force in this interval. So far, this is the only approximation done in the above integrations. The time-integral in the RHS of the equation (6.4) is a simple enough object: if we introduce, for each time interval (t_{n+1}, t_n) , a random variable z_n which is normally distributed (i.e., a gaussian with zero mean and unit variance), namely:

$$\int_{t_n}^{t_{n+1}} dt \eta(t) = \sqrt{2\Delta k_B T} z_n \quad (6.5)$$

This relation can be understood in the following simple way. First, observe that the “sum” (and therefore also the integral) of gaussian variables with zero mean must be gaussian distributed and with zero mean. If you want to verify that the coefficient appearing in Eq. (6.5) is indeed the correct one, it is enough to verify that the variance of z_n is 1:

$$\begin{aligned} \langle z_n^2 \rangle &= \frac{1}{2\Delta k_B T} \int_{t_n}^{t_{n+1}} dt dt' \int_{t_n}^{t_{n+1}} \langle \eta(t) \eta(t') \rangle \\ &= \frac{1}{\Delta} \int_{t_n}^{t_{n+1}} dt = 1, \end{aligned}$$

where we have used that the correlator $\langle \eta(t) \eta(t') \rangle = 2k_B T \delta(t - t')$ to perform the integral over t' .

By collecting the above results, we can finally write down the final expression for the discretized-time Langevin equation in the following simple form:

$$x_{n+1} = x_n + \Delta f_n + \sqrt{2\Delta k_B T} z_n. \quad (6.6)$$

This is an iteration scheme that defines the new variables x_{n+1} , at time t_{n+1} , in terms of the x_n at time t_n and of a set of normal gaussian distributed variables z_n .

Thus, this iteration represents just a Markov process, that can be implemented by a simple iterative algorithm, once the force can be evaluated for a given position x_n of the N classical particles. It is important to emphasize that, in this iteration scheme, the noise is proportional to $\sqrt{\Delta}$ and dominates, for $\Delta \rightarrow 0$, over the deterministic force contribution, which is linear in Δ . In this way it is simple to estimate that the maximum variation of the force $|\Delta f|$ in each time interval $t_n, t_n + \Delta$ can be large but always bounded by $\simeq \sqrt{(\Delta)}$, so that Eq.(6.6), actually represents a numerical solution of the continuous time Langevin-dynamics up to term vanishing as $\Delta^{3/2}$ because $\Delta f \simeq \sqrt{(\Delta)} |df/dx|$ in Eq.(6.4). For $\Delta \rightarrow 0$ this error is negligible to the actual

change of the position $\Delta x = x_{n+1} - x_n \simeq \sqrt{\Delta}$, so that the continuous time limit can be reached with arbitrary accuracy and is therefore well defined.

Another important remark is that in the limit of zero temperature $T \rightarrow 0$, the noise term disappears from the above equations and the algorithm turns into the simple steepest descent method, which allows to reach the minimum of the potential $v(x)$ in a deterministic fashion, describing correctly the zero-temperature limit of a classical system with potential $v(x)$.

6.2 From the Langevin equation to the Fokker-Planck equation

In the following, we will write all the algebra assuming that x is just a one-dimensional variable. The general case does not present any difficulty (apart for a more cumbersome algebra) and is left to the reader.

Since Eq.(6.6) defines just a Markov process, the corresponding master equation for the probability $P_n(x)$ of the classical variable x can be easily written once the conditional probability $K(x'|x)$ is evaluated. From the Markov process (6.6), we simply obtain that:

$$K(x'|x) = \int \frac{dz}{\sqrt{2\pi}} e^{-z^2/2} \delta(x' - x - \Delta f(x) - \sqrt{2\Delta k_B T} z). \quad (6.7)$$

So, the probability distribution of the classical variable x_n can be obtained at any time t_n by iteratively using the master equation:

$$P_{n+1}(x') = \int dx K(x'|x) P_n(x). \quad (6.8)$$

By replacing the simple form of the kernel (Eq.6.7) in the Master equation, and carrying out the integral over x (recall that $\int dx \delta(f(x)) = 1/|\partial_x f(x)|_{f(x)=0}$) we obtain:

$$P_{n+1}(x') = \int \frac{dz}{\sqrt{2\pi}} e^{-z^2/2} \frac{1}{|1 + \Delta \partial_{x'} f(x')|} P_n(x' - \Delta f(x') - \sqrt{2\Delta k_B T} z) \quad (6.9)$$

valid up to order $O(\Delta^{3/2})$ since in several places we have replaced x with x' . This discrete evolution of the probability can be easily expanded in small Δ , so that the remaining integral over z can be easily carried out. As usual, care should be taken for the term proportional to $\sqrt{\Delta}$. The final results is the following:

$$P_{n+1}(x') = P_n(x') - \Delta \frac{\partial f(x') P_n(x')}{\partial x'} + \Delta k_B T \frac{\partial^2 P_n(x')}{\partial x'^2} \quad (6.10)$$

We finally observe that, for small Δ , $P_{n+1}(x') - P_n(x') \approx \Delta \partial_t P(x')$, and therefore we obtain the so-called Fokker-Planck's equation for the probability density $P(x)$, that reads:

$$\frac{\partial P(x)}{\partial t} = - \frac{\partial f(x) P(x)}{\partial x} + k_B T \frac{\partial^2 P(x)}{\partial x^2}. \quad (6.11)$$

The stationary solution $P_0(x)$ for this equation is verified, by simple substitution in the RHS of Eq. (6.11), to be just the equilibrium Boltzmann distribution $P_0(x) = Z^{-1} e^{-\beta v(x)}$.

6.3 Langevin dynamics and Quantum Mechanics

It was discovered by G. Parisi in the early 80's,¹ that there is a deep relationship between a stochastic differential equation, or more properly the associated Fokker-Planck's equation, and the Schrödinger equation. This is obtained by searching for a solution of Eq. (6.11) of the type:

$$P(x, t) = \psi_0(x)\Phi(x, t) \quad (6.12)$$

where $\psi_0(x) = \sqrt{P_0(x)}$, with $\int dx \psi_0^2(x) = 1$, is an acceptable normalized quantum state. Indeed, it is simple to verify that $\Phi(x, t)$ satisfies the Schrödinger equation in imaginary time:

$$\frac{\partial \Phi(x, t)}{\partial t} = -H_{\text{eff}}\Phi(x, t), \quad (6.13)$$

where H_{eff} , an effective Hamiltonian, is given by:

$$\begin{aligned} H_{\text{eff}} &= -k_B T \partial_x^2 + V(x) \\ V(x) &= \frac{1}{4k_B T} \left(\frac{\partial v}{\partial x} \right)^2 - \frac{1}{2} \frac{\partial^2 v(x)}{\partial x^2} = k_B T \frac{1}{\psi_0(x)} \frac{\partial^2 \psi_0(x)}{\partial x^2}. \end{aligned} \quad (6.14)$$

Notice that the minima of the original potential $v(x)$ are also minima of the effective potential $V(x)$ in the zero temperature limite $T \rightarrow 0$, but the situation is more complicated at finite temperature (as an exercise, try to calculate $V(x)$ for a double-well potential $v(x) = v_0(x^2 - a^2)^2/a^4$). Notice also that the mass of the particle is proportional to the inverse temperature and becomes heavier and heavier as the temperature is lowered.

It is remarkable that the ground state of this effective Hamiltonian can be found exactly, and is just given by $\psi_0(x)$, the corresponding ground state energy being $E_0 = 0$. In this way, the solution of the Schrödinger equation, and the corresponding Fokker-Planck's equation, can be formally given in closed form by expanding in terms of the eigenstates $\psi_n(x)$ of H_{eff} the initial condition $P(x, t = 0)/\psi_0(x) = \sum_n a_n \psi_n(x)$, with $a_n = \int dx \psi_n(x) P(x, t = 0)/\psi_0(x)$, implying that $a_0 = 1$ from the normalization condition on $P(x, t = 0)$. We thus obtain the full evolution of the probability $P(x, t)$ as:

$$P(x, t) = \sum_n a_n \psi_n(x) \psi_0(x) e^{-E_n t} \quad (6.15)$$

and therefore, for large times t , $P(x, t)$ converges *exponentially fast* to the stationary equilibrium distribution $\psi_0(x)^2$. The characteristic time τ for equilibration is therefore given by the inverse gap to the first excitation $\tau = 1/E_1$. The existence of a finite equilibration time is the basic property of Markov chains. Using this property, it is possible to define uncorrelated samples of configurations distributed according to the classical finite temperature partition function, by iterating the discretized Langevin equation for simulation times much larger than this correlation time τ .

Exercise 6.1 Consider a $v(x)$ which is, in one-dimension, a double-well potential:

$$v(x) = \frac{v_0}{a^4} (x^2 - a^2)^2.$$

¹G. Parisi and W. Youghsi, Sci. Sin. **24**, 483 (1981)

Calculate the associated Schrödinger potential $V(x)$, according to Eq. (6.14). Find the lowest-lying eigenvalues and eigenvectors of H_{eff} for several values of the temperature T , by resorting to some numerical technique (for instance, discretization in real space of the Schrödinger problem, and subsequent exact diagonalization of the Hamiltonian).

6.4 Harmonic oscillator: solution of the Langevin dynamics

The discretized version of the Langevin dynamics can be solved, as well, in some special cases. Here we consider the case of a single variable x in a quadratic one-dimensional potential $v(x) = \frac{1}{2}kx^2$. In this case, the discrete-time Langevin equation (6.6) reads:

$$x_{n+1} = x_n(1 - \Delta k) + \sqrt{2\Delta k_B T} z_n \quad (6.16)$$

As we have seen, the Master equation depends on the conditional probability $K(x'|x)$ that in this case can be explicitly derived:

$$K(x'|x) = \frac{1}{\sqrt{\frac{4\pi\Delta}{\beta}}} \exp \left[-\frac{\beta}{4\Delta} (x' - (1 - \Delta k)x)^2 \right] \quad (6.17)$$

This conditional probability satisfies the detailed balance condition (5.17) for a particular distribution $\rho(x) \propto e^{-\beta v(x)}$. Indeed:

$$\frac{K(x'|x)}{K(x|x')} = \frac{\rho(x')}{\rho(x)} = \exp \left(-\frac{\beta}{4\Delta} [\Delta^2 (f_x^2 - f_{x'}^2) - 2\Delta(x' - x)(f_x + f_{x'})] \right) \quad (6.18)$$

which can be easily satisfied by taking the effective inverse temperature $\hat{\beta}$ to be given exactly by the following expression:

$$\hat{\beta} = \beta \left(1 - \frac{\Delta k}{2} \right). \quad (6.19)$$

It is important now to make the following remarks:

- The error in the discretization of the Langevin equation scales correctly to zero for $\Delta \rightarrow 0$ since the correct expected distribution is obtained as $\hat{\beta} \rightarrow \beta$ in this limit.
- At finite Δ , the error in the discretization determines only an increase of the effective temperature of the classical partition function compared to the expected $\Delta \rightarrow 0$ one. The form of the potential remains unchanged.
- It is very interesting that the discretized Langevin equations remain stable only for $\Delta k < 2$. In the opposite case the effective temperature becomes negative and the probability cannot be normalized. In this case the particle diffuse to infinite and the equilibrium distribution is not defined.

Exercise 6.2 Consider a different time discretization of the Langevin dynamics:

$$x_{n+1} = x_n + \frac{\Delta}{2} (f_{x_{n+1}} + f_{x_n}) + \sqrt{2\Delta k_B T} z_n \quad (6.20)$$

where in the time-integral of the deterministic force in (6.6), we have used a trapezoidal rule. Consider the one dimensional case and the harmonic potential $v(x) = \frac{1}{2}kx^2$.

- Show that the corresponding Markov chain is exactly equivalent to the less accurate (6.6) by replacing the inverse temperature $\beta \rightarrow \beta(1 + \frac{\Delta k}{2})$ and the effective spring constant $k \rightarrow \frac{k}{1 + \frac{\Delta k}{2}}$.
- Using the above substitution and the result (6.19), show that this kind of discretized Langevin equation is exact for the harmonic potential.
- Optional: is this still exact in the general multidimensional case, for a generic harmonic potential of, say $3N$ coordinates?

6.5 Second order Langevin dynamic

The most common application of computer simulations is to predict the properties of materials. Since the first works, by Metropolis et al. and Fermi et al. [37, 13], Molecular Dynamics(MD) techniques turned out to be a powerful tool to explore the properties of material in different conditions or to predict them.

The combination of these techniques with the density functional theory (DFT) has become a widely accepted and powerful ab-initio method Car-Parinello Molecular Dynamics (CPMD) [5] that allows to study a broad range of chemical, physical and biological systems. The CPMD approach offers a balance of accuracy and computational efficiency that is well suited for both static and dynamic calculations of numerous properties of systems with hundreds and even thousands of atoms. Although in principle DFT is an exact theory for the electron correlation, it relies on an unknown exchange and correlation functional that must be approximated. The widely used Local Density Approximation (LDA) is difficult to improve systematically. Therefore, in some cases (see for instance [22]) one requires a more accurate computational approach, such as the quantum Monte Carlo (QMC) approach to solve the Schrödinger equation very accurately.

In this chapter, we describe a method[4] that treats the electrons within the many-body QMC and perform Molecular Dynamic "on the fly" on the ions. This method provides an improved dynamical trajectory and significantly more accurate total energy. In the past two different approaches were proposed to couple Quantum Monte Carlo with ionic Molecular Dynamic. The first, called Coupled Electronic-Ionic Monte Carlo (CEIMC) [10], is based on a generalized Metropolis algorithm that takes into account the statistical noise present in the QMC evaluation of the Bohr-Oppenheimer surface energy. In the second approach, called Continuous Diffusion Monte Carlo (CDMC) [18], the Molecular Dynamics trajectories are generated with some empirical models or by DFT, and then the CDMC technique is used to efficiently evaluate energy along the trajectory. Both methods present some drawbacks. In the second method even if all the properties are evaluated using the Diffusion Monte Carlo, the trajectories are generated using empirical models without the accuracy given by the QMC for the structural properties, as radial distribution, bonding lengths and so on. Instead, in the first one the QMC energies are used to perform the Monte Carlo sampling leading to accurate static properties. But this other method has two deficiencies: the first one is that in

order to have a reasonable acceptance rate one has to carry out simulation with an statistical error on the energy of the order of $K_b T$; second, that the correlated sampling, used to evaluate energy differences, is known to have problem with parameters that affect the nodes, as ionic positions. Furthermore, in the correlated sampling, to have a fixed ratio between the current and the initial trial-function the bin length has to be increased exponentially with the size of the system . The method we present here allows to solve two major drawbacks of the previous two techniques. Following the idea of Car and Parrinello [6] we will show that it is possible to perform a feasible *ab-initio* Molecular Dynamics and structural optimization in the framework of the Quantum Monte Carlo by using noisy ionic forces.

6.6 The Born-Oppenheimer approximation

The idea of treating ionic dynamics classically, while electrons are in the ground-state of the Hamiltonian, is based on two very reasonable approximations: the Born-Oppenheimer Approximation(BO) and the Adiabatic one.

In a system of interacting electrons and nuclei there will be usually small momentum transfer between the two types of particles due to their very different masses. The forces between the particles are of similar magnitude because of their similar charge. If one then assumes that the momenta of the particles are also similar, then the nuclei must have much smaller velocities than the electrons due to their heavier mass. On the time-scale of nuclear motion, one can therefore consider the electrons to relax to a ground-state given by the Hamiltonian equation with the nuclei at fixed locations. This separation of the electronic and nuclear degrees of freedom is known as the Born-Oppenheimer approximation. Moreover because the energy scale associated with the electronic excitations is usually very high with respect to the one related to the ionic motion, one can safely consider the electron in their own ground-state. Even in the worst case, the simulation of the hydrogen, Galli et al. [29], using Car-Parinello dynamics with DFT, showed that the electronic band-gap is about $2eV$ and that the first order correction due to the quantistic effects on ions is about $2meV$ for pressure up to $200GPa$.

Although there are techniques, as Path Integral Monte Carlo, to treat finite temperature quantum systems, they become extremely inefficient for low temperature, exactly in the range which we are interested.

6.7 Dealing with Quantum Monte Carlo noise

Recently different method were proposed to evaluate forces by Quantum Monte Carlo with a finite and hopefully small variance [3],[17],[11] (see also section 5.3 for a discussion about zero-variance principle).

It is well known that when forces $\vec{f}_{\vec{R}_i} = -\partial_{\vec{R}_i} E(\vec{R}_1, \vec{R}_2, \dots, \vec{R}_N)$ are given (e.g. by VMC)

with a given noise, there are different way to obtain the canonical distribution. Here the energy $E(\vec{R}_1, \vec{R}_2, \dots \vec{R}_N)$ represents the ground state electronic energy at given ionic positions $\vec{R}_1, \vec{R}_2 \dots \vec{R}_N$, consistently with the Born-Oppenheimer approximation discussed above.

In general the ions have different masses, namely a value M_i can be given for each ion corresponding to the position \vec{R}_i . In the following, for simplicity of notations, we assume that ions have unit mass $M_i = 1$, a simplification that can be generally obtained by a simple rescaling of lengths for each independent ion coordinate $\vec{R}_i \rightarrow \vec{R}_i \sqrt{M_i}$. We often omit the ionic subindices i when not explicitly necessary for clarity and compactness of notations. Moreover matrices (vectors) are indicated by a bar (arrow) over the corresponding symbols, and the matrix (left symbol) vector (right symbol) product is also implicitly understood.

As we have mentioned in the previous section a possible way to simulate the canonical distribution with noisy forces is to use a first order Langevin dynamics:

$$\dot{\vec{R}} = \hat{\beta} [\vec{f}_{\vec{R}} + \vec{\eta}] \quad (6.21)$$

$$\langle \eta_i(t) \rangle = 0 \quad (6.22)$$

$$\langle \eta_{i,\nu}(t) \eta_{j,\mu}(t') \rangle = \hat{\alpha}_{i\nu,j\mu} \delta(t - t'). \quad (6.23)$$

where the matrix α , as well as β , has $3N \times 3N$ entries because for each ion i there are three coordinate components $\nu, \mu = x, y, z$. It is also clear that α is a positive definite symmetric matrix. In this case it is simple to show that, in order to obtain the usual Boltzmann distribution the matrix $\hat{\beta}$ has to satisfy:

$$\hat{\beta} = 2\hat{\alpha}^{-1} K_b T \quad (6.24)$$

whenever $\hat{\alpha}$ is assumed to be independent of \vec{x}_i . In fact by discretizing the above continuous equation and following the same steps as in the previous section we arrive at the following Master equation for the probability density $P_t(\vec{x}_i)$:

$$\partial_t P_t(\vec{R}) = \frac{1}{2} \partial_{\vec{R}} \left[\hat{\beta} \hat{\alpha} \hat{\beta}^\dagger \right] \partial_{\vec{R}} P_t(\vec{R}) - \partial_{\vec{R}} \hat{\beta} \vec{f}_{\vec{R}} P_t(\vec{R}) \quad (6.25)$$

and the result (6.24), obviously follows, because in the stationary solution of the above equation, namely by searching for the equilibrium distribution that allows to vanish identically the RHS of the above equation, it is easily verified that the matrix $\hat{\alpha}^{-1}$ factors out and the equilibrium distribution satisfies the same equation of the conventional Langevin dynamics with uncorrelated noise, i.e. with $\hat{\alpha} = 2k_B T \hat{I}$ and $\hat{\beta} = \hat{I}$, where \hat{I} is the identity matrix.

The above property is not verified in the more realistic case, when the covariance matrix is explicitly dependent on the atomic coordinates \vec{R} . Indeed, even within this assumption this equation turns out to be unstable, because the matrix $\hat{\alpha}$ can be ill-conditioned for the presence of very small eigenvalues, that can be further reduced by statistical fluctuations, and therefore the matrix inversion $\hat{\alpha}^{-1}$ required for the evaluation of $\hat{\beta}$ may often lead to numerical instabilities during the dynamics.

Here we present a method[4] that uses the noisy forces to perform a Molecular Dynamics at a finite temperature without the restriction of a covariance matrix independent of the ionic positions

\vec{R} . In the past the major problem of using QMC to perform *ab-initio* Molecular Dynamic was the presence of the statistical noise, but in this formulation this noise can be efficiently used as thermal bath.

In the corresponding simulation there is a correlated noise associated to the forces, that we assume to be Gaussian with a given covariance matrix. In order to evaluate the covariance matrix in an efficient way during the statistical evaluation of the forces (e.g. by VMC) it is convenient to use the Jackknife re-sampling method (see Appendix A) to estimate the covariance matrix.

It is possible to use this noise to simulate a finite temperature using a Generalized Langevin Equation (GLE), that we are going to describe in the following. The first who used this approach were Schneider and Stoll [31], to study distortive-phase transitions. Later the GLE was used to simulate different systems and also to stabilize the usual Molecular Dynamics [20].

As we will see in the following, the use of a second order Langevin Dynamics doesn't require the inverse evaluation of the matrix $\hat{\alpha}$. Moreover, by properly tuning the friction matrix, and an additional source of noise it is possible to achieve a very fast convergence to equilibrium finite temperature properties.

6.8 Canonical ensemble by Generalized Langevin Dynamics

In order to simulate the canonical ensemble we use a Langevin dynamics and we assume that our system is coupled with a thermal bath due to Quantum Monte Carlo statistical noise plus an additional friction term $\hat{\gamma}$, that here is assumed to be a symmetric matrix:

$$\dot{\vec{v}} = -\hat{\gamma}(\vec{R})\vec{v} + \vec{f}(\vec{R}) + \vec{\eta}(t) \quad (6.26)$$

$$\dot{\vec{R}} = \vec{v} \quad (6.27)$$

$$\langle \eta_{i,\nu}(t) \eta_{j,\mu}(t') \rangle = \hat{\alpha}_{i\nu,j\mu} \delta(t-t'). \quad (6.28)$$

The friction matrix $\hat{\gamma}(\vec{R})$ will be chosen in such a way that the stationary solution of the associated Fokker-Planck equation is the canonical distribution:

$$p_{eq}(\vec{v}_1, \dots, \vec{v}_n, \vec{R}_1, \dots, \vec{R}_n) \simeq e^{-\beta(\frac{1}{2}|\vec{v}|^2 + E(\vec{R}))} \quad (6.29)$$

Following Sec.(6.2), in order to derive the Fokker-Planck equation, we consider a time discretized version of Eq. (6.26), namely for discrete times $t_n = \Delta n$ ($\vec{v}(t_n) = \vec{v}_n$, $\vec{R}(t_n) = \vec{R}_n$), obtained by integrating both sides of Eq.(6.26) in the interval $t_n \leq t \leq t_{n+1}$:

$$\vec{v}_{n+1} = \vec{v}_n + \Delta \vec{f}_{\vec{R}_n} - \Delta \hat{\gamma}(\vec{R})\vec{v}_n + \sqrt{\Delta} \vec{z}_n \quad (6.30)$$

$$\vec{R}_{n+1} = \vec{R}_n + \Delta \vec{v}_n, \quad (6.31)$$

where the covariance matrix of the random vector \vec{z}_n is finite for $\Delta \rightarrow 0$ and is given by:

$$\langle \vec{z}_n \vec{z}_{n'} \rangle = \delta_{n,n'} \hat{\alpha}(\vec{R}_n) \quad (6.32)$$

where the matrix $\hat{\alpha}$, defining the noise acting on the forces has been previously defined in Eq.(6.28). Notice however that here we assume also an explicit dependence on the ionic positions \vec{R} . As

usual the above discretized version of the Langevin equation defines a Markov process, for which the Master equation can be given explicitly, and expanded in small Δ . For this purpose the conditional probability $K(x'|x)$, appearing in the mentioned Master equation, is defined in terms of both velocities and positions, namely $x = (\vec{R}, \vec{v}) = (\vec{R}_n, \vec{v}_n)$ and $x' = (\vec{R}', \vec{v}') = (\vec{R}_{n+1}, \vec{v}_{n+1})$ are $6N$ dimensional vectors, and therefore $K(x'|x)$ reads:

$$K(x'|x) = \int \int d^{3N} \vec{z}_n \delta(\vec{R}' - \vec{R} - \Delta \vec{v}) \delta(\vec{v}' - \vec{v} - \Delta(\vec{f}_{\vec{R}} - \hat{\gamma}(\vec{R})\vec{v}) - \sqrt{\Delta} \vec{z}_n) \exp \left[-\frac{1}{2} (\vec{z}_n \hat{\alpha}^{-1}(\vec{R}) \vec{z}_n) \right] \quad (6.33)$$

we obtain therefore, by using that $P_{n+1}(x') = \int dx K(x'|x) P_n(x)$, and carrying out the $6N$ integral over dx , which is simple due to the corresponding δ functions:

$$P_{n+1}(\vec{R}', \vec{v}') = \int \int d^{3N} \vec{z}_n \exp \left[-\frac{1}{2} (\vec{z}_n \hat{\alpha}^{-1}(\vec{R}) \vec{z}_n) \right] \mu(\vec{R}') P(\vec{R}' - \Delta \vec{v}', \vec{v}' - \Delta(\vec{f}_{\vec{R}'} - \hat{\gamma}(\vec{R}')\vec{v}') - \sqrt{\Delta} \vec{z}_n) \quad (6.34)$$

where the measure term $\mu(\vec{R}')$, coming after integration over the velocities is given simply by:

$$\mu(\vec{R}') = [1 + \Delta (\text{Tr} \hat{\gamma}(\vec{R}'))] + O(\Delta^{3/2}) \quad (6.35)$$

where Tr is the trace of a matrix. By expanding in small Δ and using that $P_{n+1}(x') - P_n(x') = \Delta \partial_t P(x') + O(\Delta^{3/2})$ the corresponding Fokker-Planck equation will be:

$$\frac{\partial P(\vec{R}', \vec{v}', t)}{\partial t} = \left\{ -\frac{\partial}{\partial \vec{R}'} \vec{v}' + \frac{\partial}{\partial \vec{v}'} [\hat{\gamma}(\vec{R}') \vec{v}' - \vec{f}_{\vec{R}'}] + \frac{\partial}{\partial \vec{v}'} \left[\frac{\hat{\alpha}(\vec{R}')}{2} \frac{\partial}{\partial \vec{v}'} \right] \right\} P(\vec{R}', \vec{v}', t) \quad (6.36)$$

It is clear that in the above equation the primed indices can be omitted, and in order to find the matrix $\hat{\gamma}(\vec{R})$ we substitute the Boltzmann distribution

$$P_{eq}(\vec{R}, \vec{v}) = e^{-\frac{|\vec{v}|^2 + V(x)}{k_b T}} \quad (6.37)$$

in the equation 6.36 and we obtain:

$$\vec{\gamma}(\vec{R}) = \frac{\vec{\alpha}(\vec{R})}{2} \beta \quad (6.38)$$

And so for a given noise on the forces $\hat{\alpha}(\vec{R})$ and the temperature we can set the friction tensor in this way to obtain the Boltzmann distribution.

6.9 Integration of the second order Langevin dynamics and relation with first order dynamics

In order to derive the relation between first order and second order Langevin dynamics, we integrate the latter ones using the same approximation we have already employed in the first order dynamics. Since the relation will be obtained in the limit of large friction matrix $\gamma(R)$, we assume that this matrix is diagonal and independent on R . Care should be taken to employ an integration scheme that remains valid even in the limit of $\gamma \rightarrow +\infty$.

Then, in the interval $t_n < t < t_n + \Delta t = t_{n+1}$ and for Δt small, the positions \vec{R} are changing a little and, within a good approximation, the \vec{R} dependence in the Eq.(6.26) can be neglected, so

that this differential equation becomes linear and can be solved explicitly. The closed solution for the velocities can be recasted in the following useful form:

$$\vec{v}_t = e^{-\hat{\gamma}(\vec{R}_n)(t-t_n)}\vec{v}_n + \int_{t_n}^t dt' \exp[\hat{\gamma}(t' - t)][\vec{f}_{R_n} + \vec{\eta}(t')] \quad (6.39)$$

We can then formally solve the second equation $\vec{R} = v$:

$$R_{n+1} = \vec{R}_n + \int_{t_n}^{t_{n+1}} dt' \vec{v}(t) \quad (6.40)$$

by explicitly substituting the RHS of Eq.(6.39) in the above one. The solution can be formally written as:

$$\vec{R}_{n+1} = \left(\frac{\Delta}{\hat{\gamma}(\vec{R})} - \frac{1 - \exp(-\hat{\gamma}(\vec{R})\Delta)}{\hat{\gamma}(\vec{R})^2} \right) \vec{f}_{R_n} + \vec{\eta}_n \quad (6.41)$$

where:

$$\vec{\eta}_n = \int_{t_n}^{t_{n+1}} dt \int_{t_n}^t dt' \exp[\hat{\gamma}(\vec{R}_n)(t' - t)] \quad (6.42)$$

By using relation (6.38), namely $\alpha(\vec{R}) = 2T\gamma(\vec{R})$ and carrying out the related four-fold time integral the correlation of the above gaussian random variables can be explicitly evaluated:

$$\langle \bar{\eta}_i \bar{\eta}_j \rangle = 2T \left[\frac{\Delta}{\hat{\gamma}(\vec{R}_n)} - \frac{1}{2\hat{\gamma}(\vec{R}_n)^2} \left(4 - 3\exp(-\Delta\hat{\gamma}(\vec{R}_n)) - \exp(-2\Delta\hat{\gamma}(\vec{R}_n)) \right) \right]_{i,j} \quad (6.43)$$

For large friction, $\hat{\gamma}(\vec{R}_n)$ is a positive definite matrix with large positive eigenvalues, and all exponentially small quantities vanishing as $\simeq e^{-\Delta\hat{\gamma}(\vec{R}_n)}$ can be safely neglected. The final iteration looks very similar to the discretized version of the first order Langevin equation, namely:

$$\vec{R}_{n+1} = \vec{R}_n + \bar{\Delta}\vec{f}(\vec{R}_n) + \sqrt{2T\bar{\Delta}}\vec{z}_n \quad (6.44)$$

with $\bar{\Delta} = \frac{\Delta}{\hat{\gamma}}$, being indeed a matrix. In the particular case the friction is proportional to the identity matrix, we obtain therefore exact matching between the first order Langevin equation with time step discretization $\frac{\Delta}{\hat{\gamma}}$, where Δ is the discrete time used in the second order Langevin equation. The temperature appears in the noisy part exactly in the same way $\sqrt{2T}$.

Chapter 7

Stochastic minimization

Optimization schemes are divided into two categories: variance and energy minimization. The former is widely used, since it has proven to be stable and reliable, even for a poor sampling of the variational wave function. Nevertheless, a lot of effort has been put recently into developing new energy minimization methods, which could be as efficient and stable as the variance based optimizations. Indeed the use of the energy minimization is generally assumed to provide “better” variational wave functions, since the aim of either the VMC or the DMC calculations is to deal with the lowest possible energy, rather than the lowest variance. Moreover the latest energy minimization schemes based on the stochastic evaluation of the Hessian matrix (SRH) [34] are shown to be robust, stable and much more efficient than the previously used energy optimization methods, like e.g. the Stochastic Reconfiguration (SR) algorithm [33].

7.1 Wave function optimization

As already mentioned in the introduction, there has been an extensive effort to find an efficient and robust optimization method with the aim to improve the variational wave function. Indeed, a good wave function yields results with greater statistical accuracy both in VMC and in DMC simulations. Moreover, within the DMC framework, the FNA and the LA (used in the case of non local potentials), benefit from an optimized wave function since all these approximations become exact as the trial state approaches an exact eigenstate of the Hamiltonian. Therefore a well optimized variational ansatz is crucial to obtain reliable and accurate results. The usual trial wave function used in QMC calculation is the product of an antisymmetric part and a Jastrow factor. The antisymmetric part can be either a single Slater determinant or a multi configuration state, while the Jastrow factor is a bosonic many body function which accounts for the dynamical correlations in the system.

Two different approaches exist for the wave function optimization: the variance and the energy minimization. The former has been presented by Umrigar *et al.*[40] in 1988 and widely used in

the last two decades. Let $\{\alpha_i\}$ be the variational parameters contained in the trial wave function. These are obtained by minimizing the variance of the local energy over a set of M configurations $\{\mathbf{R}_1, \mathbf{R}_2, \dots, \mathbf{R}_M\}$ sampled from the square of the initial guess $\Psi_T(\mathbf{R}, \alpha^0)$:

$$\sigma^2(\alpha) = \sum_i^M \left[\frac{H\Psi_T(\mathbf{R}_i, \alpha)}{\Psi_T(\mathbf{R}_i, \alpha)} - \bar{E} \right]^2 w(\mathbf{R}_i, \alpha) / \sum_i^M w(\mathbf{R}_i, \alpha), \quad (7.1)$$

where

$$\bar{E} = \sum_i^M \frac{H\Psi_T(\mathbf{R}_i, \alpha)}{\Psi_T(\mathbf{R}_i, \alpha)} w(\mathbf{R}_i, \alpha) / \sum_i^M w(\mathbf{R}_i, \alpha), \quad (7.2)$$

is the average energy over the sample of configurations. The weights $w(\mathbf{R}_i, \alpha) = |\Psi_T(\mathbf{R}_i, \alpha) / \Psi_T(\mathbf{R}_i, \alpha^0)|^2$ take into account the change of the variational wave function due to the change of the parameters, while the set of configurations remains the same. In this way, it is enough to generate about 2000 points from the starting guessed distribution in order to find the minimum of $\sigma^2(\alpha)$ and to iterate few times the procedure until the starting set of parameters is close to the optimal one. A different version of the algorithm is the unweighted variance minimization[21, 12], i.e. with all unitary weights, which is more stable since it avoids weights fluctuations. The advantage of the variance minimization method is that $\sigma^2(\alpha)$ is the sum of all positive terms, therefore the optimization iterated over a fixed sample leads to a *real* minimization of the variance, once it is calculated over a wider sample based on the new wave function. Instead, for a naive minimization of energy over a limited sample, it is not guaranteed that the new energy will be really lower than the starting one, and often the minimum does not even exist.

Despite the efficiency and robustness of the existing variance minimization, the possibility to develop an energy minimization method is still appealing, since the structural optimization of a compound is feasible only within an energy based approach, and also because it has been observed[32] that an energy optimized wave function gives better expectation values for operators which do not commute with the Hamiltonian. Therefore a lot of energy based optimization methods for QMC calculations have been proposed during these last few years, ranging from the simplest steepest descent (SD) approach [19] to the more sophisticated Newton method [24, 23, 39]. The goal is always to design a scheme which is stable even in the presence of the statistical noise of QMC sampling, and which converges quickly to the global minimum of the estimator. In the two next subsections we will present the Stochastic Reconfiguration (SR) method and the Stochastic Reconfiguration method with Hessian accelerator (SRH). Both of them are energy minimization procedures largely used in the present study, the latter is an evolution of the former after the introduction of a reliable and efficient scheme to estimate the Hessian matrix.

7.2 Stochastic reconfiguration method

We introduce the *stochastic minimization* of the total energy based upon the SR technique, already exploited for lattice systems [33]. Let $\Psi_T(\alpha^0)$ be the wavefunction depending on an initial set of p variational parameters $\{\alpha_k^0\}_{k=1, \dots, p}$. Consider now a small variation of the parameters $\alpha_k = \alpha_k^0 +$

$\delta\alpha_k$. The corresponding wavefunction $\Psi_T(\alpha)$ is equal, within the validity of the linear expansion, to the following one:

$$\Psi'_T(\alpha) = \left(\Psi_T(\alpha^0) + \sum_{k=1}^p \delta\alpha_k \frac{\partial}{\partial\alpha_k} \Psi_T(\alpha^0) \right) \quad (7.3)$$

Therefore, by introducing local operators defined on each configuration $x = \{\mathbf{r}_1, \dots, \mathbf{r}_N\}$ as the logarithmic derivatives with respect to the variational parameters:

$$O^k(x) = \frac{\partial}{\partial\alpha_k} \ln \Psi_T(x) \quad (7.4)$$

and for convenience the identity operator $O^0 = 1$, we can write Ψ'_T in a more compact form:

$$|\Psi'_T(\alpha)\rangle = \sum_{k=0}^p \delta\alpha_k O^k |\Psi_T\rangle, \quad (7.5)$$

where $|\Psi_T\rangle = |\Psi_T(\alpha_0)\rangle$ and $\delta\alpha_0 = 1$. However, as a result of the iterative minimization scheme we are going to present, $\delta\alpha_0 \neq 1$, and in that case the variation of the parameters will be obviously scaled

$$\delta\alpha_k \rightarrow \frac{\delta\alpha_k}{\delta\alpha_0} \quad (7.6)$$

and Ψ'_T will be proportional to $\Psi_T(\alpha)$ for small $\frac{\delta\alpha_k}{\delta\alpha_0}$.

Our purpose is to set up an iterative scheme to reach the minimum possible energy for the parameters α , exploiting the linear approximation for $\Psi_T(\alpha)$, which will become more and more accurate close to the convergence, when the variation of the parameters is smaller and smaller. We follow the stochastic reconfiguration method and define

$$|\Psi'_T\rangle = P_{SR}(\Lambda - H)|\Psi_T\rangle \quad (7.7)$$

where Λ is a suitable large shift, allowing Ψ'_T to have a lower energy than Ψ_T [33], and P_{SR} is a projection operator over the $(p+1)$ -dimensional subspace, spanned by the basis $\{O_k|\Psi_T\rangle\}_{k=0,\dots,p}$, over which the function $|\Psi'_T\rangle$ has been expanded (Eq. 7.5). In a continuous system, if its energy is unbounded from above, Λ should be infinite. However, in this case, the optimal Λ is finite, since the basis is finite, and the spectrum of the Hamiltonian diagonalized in this basis is bounded from above as in a lattice system. In order to determine the coefficients $\{\delta\alpha_k\}_{k=1,\dots,p}$ corresponding to Ψ'_T defined in Eq.7.7, one needs to solve the SR conditions:

$$\langle \Psi_T | O^k (\Lambda - H) | \Psi_T \rangle = \langle \Psi_T | O^k | \Psi'_T \rangle \quad \text{for } k = 0, \dots, p \quad (7.8)$$

that can be rewritten in a linear system:

$$\sum_l \delta\alpha_l s_{l,k} = f^k, \quad (7.9)$$

where $s_{l,k} = \langle \Psi_T | O^l O^k | \Psi_T \rangle$ is the covariance matrix and $f^k = \langle \Psi_T | O^k (\Lambda - H) | \Psi_T \rangle$ is the known term; both $s_{l,k}$ and f^k are computed stochastically by a Monte Carlo integration. These linear equations (7.9) are very similar to the ones introduced by Filippi and Fahy [15] for the energy minimization of the Slater part. In our formulation, there is no difficulty to optimize the Jastrow and the Slater part of the wavefunction at the same time. The present scheme is also much simpler

because does not require to deal with an effective one body Hamiltonian, but it seems to be less efficient, since it treats all energy scales at the same footing (see Subsection “Different energy scales” and Ref. [30]).

After the system (7.9) has been solved, we update the variational parameters

$$\alpha_k = \alpha_k^{(0)} + \frac{\delta\alpha_k}{\delta\alpha_0} \quad \text{for } k = 1, \dots, p \quad (7.10)$$

and we obtain a new trial wavefunction $\Psi_T(\alpha)$. By repeating this iteration scheme several times, one approaches the convergence when $\frac{\delta\alpha_k}{\delta\alpha_0} \rightarrow 0$ for $k \neq 0$, and in this limit the SR conditions (7.8) implies the Euler equations of the minimum energy. Obviously, the solution of the linear system (7.9) is affected by statistical errors, yielding statistical fluctuations of the final variational parameters α_k even when convergence has been reached, namely when the $\{\alpha_k\}_{k=1, \dots, p}$ fluctuate without drift around an average value. We perform several iterations in that regime; in this way, the variational parameters can be determined more accurately by averaging them over all these iterations and by evaluating also the corresponding statistical error bars.

It is worth noting that the solution of the linear system (7.9) depends on Λ only through the $\delta\alpha_0$ variable. Therefore the constant Λ indirectly controls the rate of change in the parameters at each step, i.e. the speed of the algorithm for convergence and the stability at equilibrium: a too small value will produce uncontrolled fluctuations for the variational parameters, a too large one will allow convergence in an exceedingly large number of iterations. The choice of Λ can be controlled by evaluating the change of the wavefunction at each step as:

$$\frac{|\Psi'_T - \Psi_T|^2}{|\Psi_T|^2} = \sum_{k, k' > 0} \delta\alpha_k \delta\alpha_{k'} s_{k, k'} \quad (7.11)$$

By keeping this value small enough during the optimization procedure, one can easily obtain a steady and stable convergence. Moreover, we mention that the stochastic procedure is able in principle to perform a global optimization, as discussed in Ref. [33] for the SR and in Ref. [19] for the Stochastic Gradient Approximation (SGA), because the noise in the sampling can avoid the dynamics of the parameters to get stuck into local minima.

7.2.1 Stochastic reconfiguration versus steepest descent method

SR is similar to a standard SD calculation, where the expectation value of the energy $E(\alpha_k) = \frac{\langle \Psi | H | \Psi \rangle}{\langle \Psi | \Psi \rangle}$ is optimized by iteratively changing the parameters α_i according to the corresponding derivatives of the energy (generalized forces):

$$f_k = -\frac{\partial E}{\partial \alpha_k} = -\frac{\langle \Psi | O_k H + H O_k + (\partial_{\alpha_k} H) | \Psi \rangle}{\langle \Psi | \Psi \rangle} + 2 \frac{\langle \Psi | O_k | \Psi \rangle \langle \Psi | H | \Psi \rangle}{\langle \Psi | \Psi \rangle^2}, \quad (7.12)$$

namely:

$$\alpha_k \rightarrow \alpha_k + \Delta t f_k. \quad (7.13)$$

Δt is a suitable small time step, which can be taken fixed or determined at each iteration by minimizing the energy expectation value. Indeed the variation of the total energy ΔE at each step

is easily shown to be negative for small enough Δt because, in this limit

$$\Delta E = -\Delta t \sum_i f_i^2 + O(\Delta t^2).$$

Thus the method certainly converges at the minimum when all the forces vanish. Notice that in the definition of the generalized forces (7.12) we have generally assumed that the variational parameters may appear also in the Hamiltonian. This is particularly important for the structural optimization since the atomic positions that minimize the energy enter both in the wave function and in the potential.

In the following we will show that similar considerations hold for the SR method, that can be therefore extended to the optimization of the geometry. Indeed, by eliminating the equation with index $k = 0$ from the linear system (7.9), the SR iteration can be written in a form similar to the steepest descent:

$$\alpha_i \rightarrow \alpha_i + \Delta t \sum_k \bar{s}_{i,k}^{-1} f_k \quad (7.14)$$

where the reduced $p \times p$ matrix \bar{s} is:

$$\bar{s}_{j,k} = s_{j,k} - s_{j,0} s_{0,k} \quad (7.15)$$

and the Δt value is given by:

$$\Delta t = \frac{1}{2(\Lambda - \frac{\langle \Psi | H | \Psi \rangle}{\langle \Psi | \Psi \rangle} - \sum_{k>0} \Delta \alpha_k s_{k,0})}. \quad (7.16)$$

From the latter equation the value of Δt changes during the simulation and remains small for large enough energy shift Λ . However, using the analogy with the steepest descent, convergence to the energy minimum is reached also when the value of Δt is sufficiently small and is kept constant for each iteration (we have chosen to determine Δt by verifying the stability and the convergence of the algorithm at fixed Δt value). Indeed the energy variation for a small change of the parameters is:

$$\Delta E = -\Delta t \sum_{i,j} \bar{s}_{i,j}^{-1} f_i f_j.$$

It is easily verified that the above term is always negative because the reduced matrix \bar{s} , as well as \bar{s}^{-1} , is positive definite, being s an overlap matrix with all positive eigenvalues.

For a stable iterative method, such as the SR or the SD one, a basic ingredient is that at each iteration the new parameters α' are close to the previous α according to a prescribed distance. The fundamental difference between the SR minimization and the standard steepest descent is just related to the definition of this distance. For the SD it is the usual one defined by the Cartesian metric $\Delta_\alpha = \sum_k |\alpha'_k - \alpha_k|^2$, instead the SR works correctly in the physical Hilbert space metric of the wave function Ψ , yielding $\Delta_\alpha = \sum_{i,j} \bar{s}_{i,j} (\alpha'_i - \alpha_i)(\alpha'_j - \alpha_j)$, namely the square distance between the two normalized wave functions corresponding to the two different sets of variational parameters $\{\alpha'\}$ and $\{\alpha_k\}$ ¹. Therefore, from the knowledge of the generalized forces f_k , the most

¹ Δ_α is equivalent to the quantity of Eq. 7.11, but the variation of the wave function is expressed in the orthogonal basis $\{(O_k - \langle O_k \rangle) | \Psi_T \rangle\}_{k=1, \dots, p}$

convenient change of the variational parameters minimizes the functional $\Delta E + \bar{\Lambda}\Delta_\alpha$, where ΔE is the linear change in the energy $\Delta E = -\sum_i f_i(\alpha'_i - \alpha_i)$ and $\bar{\Lambda}$ is a Lagrange multiplier that allows a stable minimization with small change Δ_α of the wave function Ψ . The final iteration (7.14) is then easily obtained.

The advantage of SR compared with SD is obvious because sometimes a small change of the variational parameters correspond to a large change of the wave function, and the SR takes into account this effect through the Eq. 7.14. In particular the method is useful when a non orthogonal basis set is used as we have done in this work. Indeed by using the reduced matrix \bar{s} it is also possible to remove from the calculation those parameters that imply some redundancy in the variational space. A more efficient change in the wave function can be obtained by updating only the variational parameters that remain independent within a prescribed tolerance, and therefore, by removing the parameters that linearly depend on the others. A more stable minimization is obtained without spoiling the accuracy of the calculation. A weak tolerance criterium $\epsilon \simeq 10^{-3}$, provides a very stable algorithm even when the dimension of the variational space is large. For a small atomic basis set, by an appropriate choice of the Jastrow and Slater orbitals, the reduced matrix \bar{s} is always very well conditioned even for the largest system studied, and the above stabilization technique is not required. Instead the described method is particularly important for the extension of QMC to complex systems with large number of atoms and/or higher level of accuracy, because in this case it is very difficult to select - e.g. by trial and error - the relevant variational parameters, that allow a well conditioned matrix \bar{s} for a stable inversion in (7.14).

Once all the parameters are independent, that can be checked by explicit calculation of the spectrum of the reduced matrix \bar{s} , the simulation is stable whenever $1/\Delta t > \Lambda_{cut}$, where Λ_{cut} is an energy cutoff that is strongly dependent on the chosen wave function and is generally weakly dependent on the bin length. Whenever the wave function is too much detailed, namely has a lot of variational freedom, especially for the high energy components of the core electrons, the value of Λ_{cut} becomes exceedingly large and too many iterations are required for obtaining a converged variational wave function. In fact a rough estimate of the corresponding number of iterations P is given by $P\Delta t \gg 1/G$, where G is the typical energy gap of the system, of the order of few eV in small atoms and molecules. Within the SR method it is therefore extremely important to work with a bin length rather small, so that many iterations can be performed without much effort.

7.2.2 Statistical bias of forces

In a Monte Carlo optimization framework the forces f_k are always determined with some statistical noise η_k , and by iterating the procedure several times with a fixed bin length the variational parameters will fluctuate around their mean values. These statistical fluctuations are similar to the thermal noise of a standard Langevin equation:

$$\partial_t \alpha_k = f_k + \eta_k, \quad (7.17)$$

where

$$\langle \eta_k(t) \eta_{k'}(t') \rangle = 2T_{noise} \delta(t - t') \delta_{k,k'}. \quad (7.18)$$

Within a QMC scheme, one needs to control T_{noise} , by increasing the bin length as clearly $T_{noise} \propto 1/\text{Bin length}$, because the statistical fluctuations of the forces, obviously decreasing by increasing the bin length, are related to the thermal noise by Eq. 7.18. On the other hand, the number of iterations necessary to reach the convergence is weakly dependent on the bin length, but it depends mainly on the energy landscape of the system. The optimal value for the bin length is the smallest one that provides T_{noise} within the desired accuracy.

The variational parameters α_k , averaged over the Langevin simulation time will be close to the true energy minimum, but the corresponding forces $f_k = -\partial_{\alpha_k} E$ will be affected by a bias that scales to zero with the thermal noise T_{noise} , due to the presence of non quadratic terms in the energy landscape. The systematic bias on the forces should be controlled through an appropriate choice of the bin length in order to not exceed the statistical error of the averaged parameters.

7.2.3 Structural optimization

In the last few years remarkable progress has been made in developing Quantum Monte Carlo (QMC) techniques which are able in principle to perform structural optimization of molecules and complex systems [1, 2, 9, 35]. Within the Born-Oppenheimer approximation the nuclear positions \mathbf{R}_i can be considered as further variational parameters included in the set $\{\alpha_i\}$ used for the SR minimization (7.14) of the energy expectation value. For clarity, in order to distinguish the conventional variational parameters from the ionic positions, in this section we indicate with $\{c_i\}$ the former ones, and with \mathbf{R}_i the latter ones. It is understood that $R_i^\nu = \alpha_k$, where a particular index k of the whole set of parameters $\{\alpha_i\}$ corresponds to a given spatial component ($\nu = 1, 2, 3$) of the i -th ion. Analogously the forces (7.12) acting on the ionic positions will be indicated by capital letters with the same index notations.

The purpose of the present section is to compute the forces \mathbf{F} acting on each of the T nuclear positions $\{\mathbf{R}_1, \dots, \mathbf{R}_T\}$, being T the total number of nuclei in the system:

$$\mathbf{F}(\mathbf{R}_a) = -\nabla_{\mathbf{R}_a} E(\{c_i\}, \mathbf{R}_a), \quad (7.19)$$

with a reasonable statistical accuracy, so that the iteration (7.14) can be effective for the structural optimization. In this work we have used a finite difference operator $\frac{\Delta}{\Delta \mathbf{R}_a}$ for the evaluation of the force acting on a given nuclear position a :

$$\mathbf{F}(\mathbf{R}_a) = -\frac{\Delta}{\Delta \mathbf{R}_a} E = -\frac{E(\mathbf{R}_a + \Delta \mathbf{R}_a) - E(\mathbf{R}_a - \Delta \mathbf{R}_a)}{2\Delta R} + O(\Delta R^2) \quad (7.20)$$

where $\Delta \mathbf{R}_a$ is a 3 dimensional vector. Its length ΔR is chosen to be 0.01 atomic units, a value that is small enough for negligible finite difference errors. In order to evaluate the energy differences in Eq. 7.20 we have used the space-warp coordinate transformation [38, 16] briefly summarized in the following paragraphs. According to this transformation the electronic coordinates \mathbf{r} will also be translated in order to mimic the right displacement of the charge around the nucleus a :

$$\bar{\mathbf{r}}_i = \mathbf{r}_i + \Delta \mathbf{R}_a \omega_a(\mathbf{r}_i), \quad (7.21)$$

where

$$\omega_a(\mathbf{r}) = \frac{F(|\mathbf{r} - \mathbf{R}_a|)}{\sum_{b=1}^T F(|\mathbf{r} - \mathbf{R}_b|)}. \quad (7.22)$$

$F(r)$ is a function which must decay rapidly; here we used $F(r) = \frac{1}{r^4}$ as suggested in Ref. [16].

The expectation value of the energy depends on $\Delta\mathbf{R}$, because both the Hamiltonian and the wave function depend on the nuclear positions. Now let us apply the space-warp transformation to the integral involved in the calculation; the expectation value reads:

$$E(\mathbf{R} + \Delta\mathbf{R}) = \frac{\int d\mathbf{r} J_{\Delta\mathbf{R}}(\mathbf{r}) \Psi_{\Delta\mathbf{R}}^2(\bar{\mathbf{r}}(\mathbf{r})) E_L^{\Delta\mathbf{R}}(\bar{\mathbf{r}}(\mathbf{r}))}{\int d\mathbf{r} J_{\Delta\mathbf{R}}(\mathbf{r}) \Psi_{\Delta\mathbf{R}}^2(\bar{\mathbf{r}}(\mathbf{r}))}, \quad (7.23)$$

where J is the Jacobian of the transformation and here and henceforth we avoid for simplicity to use the atomic subindex a . The importance of the space warp in reducing the variance of the force is easily understood for the case of an isolated atom a . Here the force acting on the atom is obviously zero, but only after the space warp transformation with $\omega_a = 1$ the integrand of expression (7.23) will be independent of $\Delta\mathbf{R}$, providing an estimator of the force with zero variance.

Starting from Eq. 7.23, it is straightforward to explicitly derive a finite difference differential expression for the force estimator, which is related to the gradient of the previous quantity with respect to $\Delta\mathbf{R}$, in the limit of the displacement tending to zero:

$$\begin{aligned} \mathbf{F}(\mathbf{R}) &= -\left\langle \lim_{|\Delta\mathbf{R}| \rightarrow 0} \frac{\Delta}{\Delta\mathbf{R}} E_L \right\rangle \\ &+ 2 \left(\langle H \rangle \left\langle \lim_{|\Delta\mathbf{R}| \rightarrow 0} \frac{\Delta}{\Delta\mathbf{R}} \log(J^{1/2} \Psi) \right\rangle - \left\langle H \lim_{|\Delta\mathbf{R}| \rightarrow 0} \frac{\Delta}{\Delta\mathbf{R}} \log(J^{1/2} \Psi) \right\rangle \right), \end{aligned} \quad (7.24)$$

where the brackets indicate a Monte Carlo like average over the square modulus of the trial wave function, $\frac{\Delta}{\Delta\mathbf{R}}$ is the finite difference derivative as defined in (7.20), and $E_L = \frac{\langle \Psi | H | x \rangle}{\langle \Psi | x \rangle}$ is the local energy on a configuration x where all electron positions and spins are given. In analogy with the general expression (7.12) of the forces, we can identify the operators O_k corresponding to the space-warp change of the variational wave function:

$$O_k = \frac{\Delta^\nu}{\Delta R} \log(J_{\Delta\mathbf{R}}^{1/2} \Psi_{\Delta\mathbf{R}}) \quad (7.25)$$

The above operators (7.25) are used also in the definition of the reduced matrix \bar{s} for those elements depending on the variation with respect to a nuclear coordinate. In this way it is possible to optimize both the wave function and the ionic positions at the same time, in close analogy with the Car-Parrinello[7] method applied to the minimization problem. Also Tanaka [36] tried to perform Car-Parrinello like simulations via QMC, within the less efficient steepest descent framework.

An important source of systematic errors is the dependence of the variational parameters c_i on the ionic configuration \mathbf{R} , because for the final equilibrium geometry all the forces f_i corresponding to c_i have to be zero, in order to guarantee that the true minimum of the potential energy surface (PES) is reached [8]. As shown clearly in the previous subsection, within a QMC approach it is possible to control this condition by increasing systematically the bin length, when the thermal bias T_{noise} vanishes. In Fig. 7.1 we report the equilibrium distance of the Li molecule as a function of the inverse bin length, for two different basis sets, so that an accurate evaluation of such an

important quantity is possible even when the number of variational parameters is rather large, by extrapolating the value to an infinite bin length.

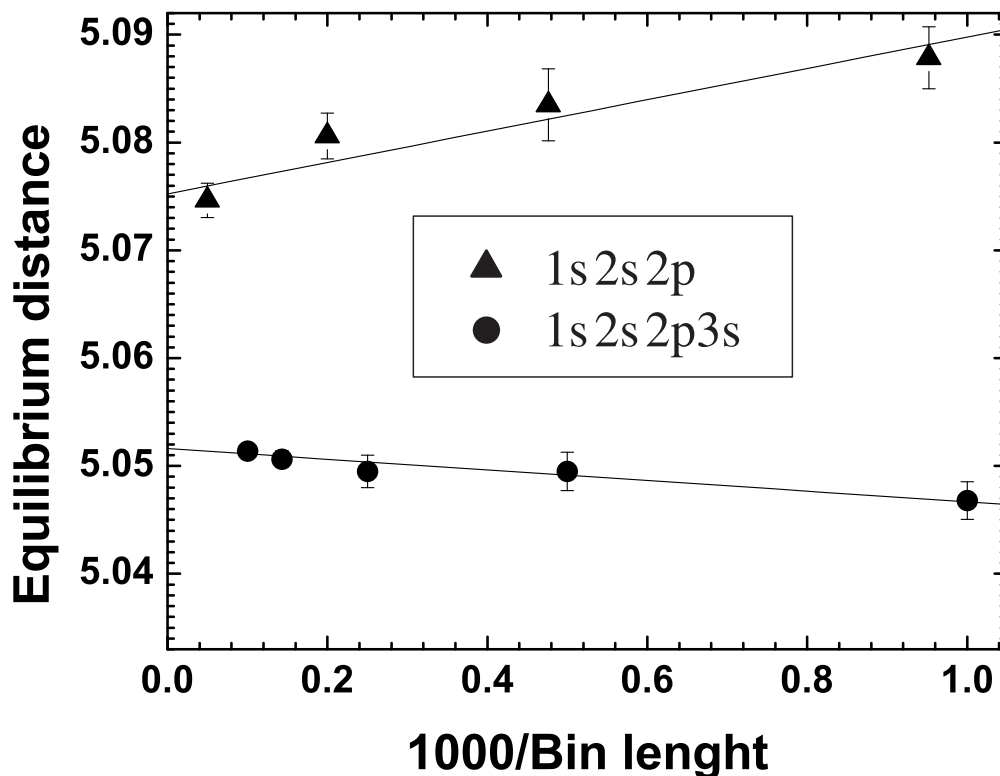


Figure 7.1: Plot of the equilibrium distance of the Li_2 molecule as a function of the inverse bin length. The total energy and the binding energy are reported in Chapter ?? (HERE DEFINE) in Tables ?? and ?? (HERE DEFINE) respectively. The triangles (full dots) refer to a simulation performed using 1000 (3000) iterations with $\Delta t = 0.015H^{-1}$ ($\Delta t = 0.005H^{-1}$) and averaging over the last 750 (2250) iterations. For all simulations the initial wavefunction is optimized at $Li - Li$ distance 6 a.u.

We have not attempted to extend the geometry optimization to the more accurate DMC, since there are technical difficulties [27], and it is computationally much more demanding.

Different energy scales

The SR method performs generally very well, whenever there is only one energy scale in the variational wave function. However if there are several energy scales in the problem, some of the variational parameters, e.g. the ones defining the low energy valence orbitals, converge very slowly with respect to the others, and the number of iterations required for the equilibration becomes

exceedingly large, considering also that the time step Δt necessary for a stable convergence depends on the high energy orbitals, whose dynamics cannot be accelerated beyond a certain threshold.

If the interest is limited to a rather small atomic basis, the SR technique is efficient, and general enough to perform the simultaneous optimization of the Jastrow and the determinantal part of the wave function, a very important feature that allows to capture the most non trivial correlations contained in our variational ansatz. Moreover, SR is able to perform the structural optimization of a chemical system, which is another appealing characteristic of this method. However, to optimize an extended atomic basis, it is necessary to go beyond the SR method, and the use of the second energy derivatives (the Hessian matrix) will be necessary to speed up the convergence to the minimum energy wave function.

Chapter 8

Green's function Monte Carlo

8.1 Exact statistical solution of model Hamiltonians: motivations

As we have seen in the Introduction, it is important to go beyond the variational approach, because, for correlated systems with a large number of electrons, it is very difficult to prepare a variational wavefunction with a good enough variational energy. Remember that a good accuracy in the energy per particle does not necessarily imply a sufficient quality for the correlation functions, which is indeed the most important task of a numerical approach. For that, you would need an accuracy of the variational energy below the gap to the first excited state, which is generally impossible.

8.2 Single walker technique

In the following we will denote by x the discrete labels specifying a given state of the N -electron Hilbert space of our system (for instance, specifying all the electron positions and spins). We will also assume that, given the Hamiltonian H , the matrix elements $\langle x'|H|\mathbf{x}\rangle = H_{x',x}$, for given x , can be computed efficiently for each x' . Typically, for a lattice Hamiltonian, though the dimension of the Hilbert space spanned by $\{x'\}$ increases exponentially with the system size L , the number of vanishing entries of the matrix representing H , $H_{x',x} = 0$, is very large, so that the non-zero column elements in $H_{x',x}$, for given x , are of the order of the system size L , and can be therefore computed with a reasonable computational effort.

Using the above property, it is possible to define a stochastic algorithm that allows to perform the power method (see the Introduction) in a statistical way, in the sense that the wavefunction

$$\psi_n(x) = \langle x|(\Lambda\mathbf{1} - H)^n|\psi_G\rangle, \quad (8.1)$$

with $|\psi_G\rangle$ some initial trial state, is evaluated with a stochastic approach. To this purpose, we

define the basic element of this stochastic approach, the so called *walker*. A walker is basically determined by an index x , labelling a configuration $|x\rangle$ in the Hilbert space of our system, with an associated weight w (roughly speaking associated to the amplitude of the wavefunction at x , see below).

The walker “walks” in the Hilbert space of the matrix H , by performing a Markov chain with a discrete iteration time n , and thus assuming configurations (x_n, w_n) according to a given probability density $P_n(x_n, w_n)$. (Recall that a walker is associated to the pair (x, w) , so that the Markov chain involves both the weight w and the configuration x .)

The goal of the Green's function Monte Carlo (GFMC) approach is to define a Markov process, yielding after a large number n of iterations a probability distribution for the walker, $P_n(w, x)$, which determines the ground state wavefunction ψ_{GS} . To be specific, in the most simple formulation we would require:

$$\int dw w P_n(x, w) = \langle x | \psi_n \rangle, \quad (8.2)$$

i.e., the probability that, at time n , a walker is at x , multiplied by w and integrated over all weights w , is just the amplitude of the wavefunction $|\psi_n\rangle$ at x .

In order to apply a statistical algorithm for solving the ground state of the Hamiltonian H , it is necessary to assume that all the matrix elements of the so called Green's function

$$G_{x',x} = \langle x' | \Lambda \mathbf{1} - H | x \rangle = \Lambda \delta_{x',x} - H_{x',x}, \quad (8.3)$$

appearing in (9.1) are *positive definite*, so that they may have a meaning of probability. For the diagonal element $G_{x,x}$ there is no problem: we can always satisfy this assumption by taking a sufficiently large shift Λ . However, the requirement of positiveness is indeed important, and non trivial, for the *non-diagonal* elements of G , and is fulfilled only by particularly simple Hamiltonians. If it is not fulfilled, i.e., if $G_{x',x} < 0$ for some pairs (x', x) , we say that we are in presence of the so-called *sign problem*, that will be discussed in the forthcoming chapters.

Once positiveness ($G_{x',x} \geq 0$) is assumed to hold, we can divide up the Green's function into the product of two factors: a stochastic matrix $p_{x',x}$ – by definition, a matrix with all positive elements $p_{x',x} \geq 0$, and with the normalization condition $\sum_{x'} p_{x',x} = 1$ for all columns – times a scale factor b_x . Indeed, if we define $b_x = \sum_{x'} G_{x',x} > 0$ to be such a scale factor, then $p_{x',x} = G_{x',x}/b_x$ is trivially positive and column normalized, and is therefore the stochastic matrix we are looking for. In summary, we have split G into:

$$\begin{aligned} G_{x',x} &= p_{x',x} b_x \\ b_x &= \sum_{x'} G_{x',x} \\ p_{x',x} &= G_{x',x}/b_x. \end{aligned} \quad (8.4)$$

We now want to devise a simple Markov process that guarantees Eq. (8.2). Indeed, given (w_n, x_n) , we can, by using the decomposition (8.4),

- a) generate $x_{n+1} = x'$ with probability p_{x',x_n}
 - b) update the weight with $w_{n+1} = w_n b_x$.
- (8.5)

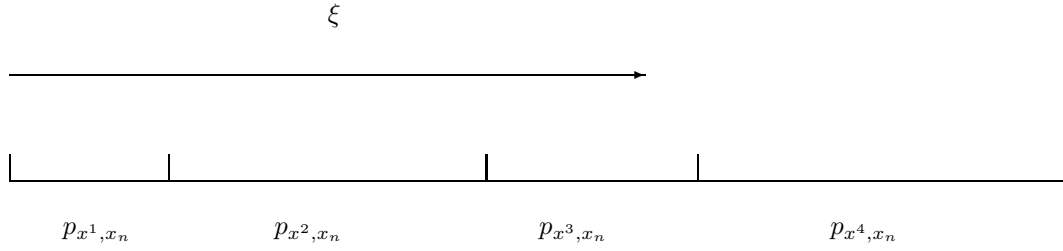


Figure 8.1: The interval $(0,1]$ is divided up into sub-intervals of length equal to the probability p_{x^i, x_n} , for all i 's labelling the possible configurations x' with non zero probability p_{x^i, x_n} (the example shown has only four entries). Then a random number $0 < \xi \leq 1$ is generated, and the new configuration $x_{n+1} = x^3$ (in the example shown) is selected, as ξ lies in the corresponding interval. The index n indicates the Markov chain iteration number.

The reader should pose here, to get fully convinced that this Markov process leads to Eq. (8.2). This Markov process can be very easily implemented for generic correlated Hamiltonians on a lattice, since the number of non-zero entries in the stochastic matrix p_{x', x_n} , for given x_n , is small, and typically growing only as the number of lattice sites L . Thus, in order to define x_{n+1} , given x_n , it is enough to divide the interval $(0, 1)$ into smaller intervals (see Fig. 8.2) of lengths p_{x', x_n} for all possible $\{x'\}$ connected to x_n with non-zero probability p_{x', x_n} . Then, a pseudo-random number ξ between 0 and 1 is generated. This ξ will lie in one of the above defined intervals, with a probability of hitting the interval corresponding to a certain x' exactly equal to p_{x', x_n} . This clearly defines x_{n+1} according to the desired Markov chain (8.5). From Eq. (8.5) it is immediate to verify that the conditional probability K of the new walker (x_{n+1}, w_{n+1}) , given the old one at (x_n, w_n) , is simply:

$$K(x_{n+1}, w_{n+1} | x_n, w_n) = p_{x_{n+1}, x_n} \delta(w_{n+1} - w_n b_{x_n}) . \quad (8.6)$$

Thus, the Master equation corresponding to the probability density $P_n(x_n, w_n)$ is given by (see Eq.5.15):

$$P_{n+1}(x', w') = \sum_x \int dw K(x', w' | x, w) P_n(x, w) . \quad (8.7)$$

Hereafter, the integration limits over the variable w are assumed to run over the whole range $-\infty, \infty$, the probability density $P(x, w)$ being *zero* for the values of w that are not allowed by the Markov chain (e.g., $w < 0$).

Finally, it is simple enough to show that the walker – defined by the stochastic variables x_n and w_n – determines statistically the state $\psi_n(x)$ in Eq. (9.1) by means of the relation:

$$\psi_n(x) = \langle w_n \delta_{x, x_n} \rangle = \int dw_n w_n P_n(x, w_n) , \quad (8.8)$$

where the first average, intended over infinitely many independent realizations of the Markov chain, is rarely pursued in actual practice as there is too much information contained in $\psi_n(x)$ for every configuration x in the Hilbert space. The Quantum Monte Carlo approach is based on the possibility that for physical correlation functions, like e.g. the energy, it is not necessary to have an accurate statistical information of the wavefunction, namely to have each component $\psi_n(x)$ of the

wavefunction with a standard deviation much smaller than its value. In a many body system with an Hilbert space exponentially large, this information cannot even be stored. Moreover, in order to have an adequate error bar on all configurations, each of them has to be visited at least once, implying an exponentially large computation time. It turns out that the standard deviation on the total energy or other physical quantities corresponding to the same state $\psi_n(x)$ is instead adequate even when the number of configurations generated by the Monte Carlo algorithm is much smaller than the Hilbert space. In the Monte Carlo scheme, there are random variables like $w_n \delta_{x,x_n}$ in Eq.(8.8) that cannot even be sampled. Eventually physical correlation functions can be computed, with reasonable accuracy corresponding to the well defined state $\psi_n(x)$.

Indeed, once the relation (8.8) is supposed to hold for some n , using the Master equation (8.7) we will immediately obtain:

$$\begin{aligned} \int dw_{n+1} w_{n+1} P_{n+1}(x', w_{n+1}) &= \int dw_{n+1} w_{n+1} \sum_x \int dw_n p_{x',x} \delta(w_{n+1} - w_n b_x) P_n(x, w_n) \\ &= \sum_x \int dw_n p_{x',x} b_x w_n P_n(x_n, w_n) \\ &= \sum_x G_{x',x} \psi_n(x) = \psi_{n+1}(x'), \end{aligned} \quad (8.9)$$

where in the latter equality we have used the assumed form of $\psi_n(x)$, Eq. (8.8), and the Green's function decomposition (8.4). Eq. (8.9), therefore, allows us to state that (8.8) holds also for $n+1$, and, by induction, it is valid for each n , once the initial condition $\psi_0(x) = \langle w_0 \delta_{x,x_0} \rangle$ is imposed, e.g., by $P_0(x, w) = \delta(w-1) \delta_{x,x_0}$, representing a walker with weight 1 in the configuration x_0 , i.e., an initial wavefunction completely localized at x_0 , $\psi_0(x) = \delta_{x,x_0}$. For large n , as explained in the Introduction, the power method converges to the ground state of H and thus the walker w_n, x_n contains, for large n , the information of the ground state wavefunction $\psi_{GS}(x)$, namely:

$$\psi_{GS}(x) = \langle w_n \delta_{x,x_n} \rangle .$$

8.2.1 Correlation functions

In principle, using the basic relation (8.8) we can have information on the ground-state wavefunction amplitudes for each configuration x , when n is large enough. However this information is too large for being physically relevant, especially for large number of sites, when the Hilbert space is huge. The most important physical quantities are, as usual, ground state energy and correlation functions over the state (8.8). In particular, the ground state energy can be obtained by averaging the random variable

$$e(x) = \sum_{x'} H_{x',x} = \Lambda - b_x . \quad (8.10)$$

Indeed, if we take the ratio between the means of the two random variables $w_n e(x_n)$ and w_n over the Markov chain (8.5), by using (8.8), we easily obtain:

$$\frac{\langle w_n e(x_n) \rangle}{\langle w_n \rangle} = \frac{\sum_{x_n} \int dw_n w_n e_L(x_n) P_n(x_n, w_n)}{\sum_{x_n} \int dw_n w_n P_n(x_n, w_n)} = \frac{\sum_{x_n} e_L(x_n) \psi_n(x_n)}{\sum_{x_n} \psi_n(x_n)} . \quad (8.11)$$

Thus, for large n , when $\psi_n(x)$ is equal to the ground-state wavefunction $\psi_{GS}(x)$ (up to a normalization constant) the numerator will converge exactly to the ground state energy E_{GS} times the denominator,

$$\sum_x e(x)\psi_{GS}(x) = \sum_{x',x} H_{x',x}\psi_{GS}(x) = \sum_{x'} \langle x'|H|\psi_{GS}\rangle = E_{GS} \sum_{x'} \psi_{GS}(x'),$$

where in the latter equality we have used that $H|\psi_{GS}\rangle = E_{GS}|\psi_{GS}\rangle$.

At variance with the Variational Monte Carlo, the statistical evaluation of the energy shown above is obtained by taking the ratio of two random variables $e(x_n)w_n$ and w_n , which leads to some complications in the evaluation of the error bars. Moreover, there is a difficulty for computing generic operator averages, because the Green's function Monte Carlo does not give explicit information of the *square* of the wavefunction $\psi_n(x)$. Before explaining how to remedy to these problems, we consider in more detail the convergence properties of the Markov process (8.5), and (8.7), which will be useful for the forthcoming sections.

8.2.2 Convergence properties of the Markov process

First of all we consider the marginal probability $\bar{\psi}_n(x_n) = \int dw_n P_n(x_n, w_n)$ of the configuration x_n , regardless of what the random weight w_n is ($\bar{\psi}_n$ should not be confused with the wavefunction ψ_n , where the weight factor w_n appears explicitly). It is straightforward to derive, using the Markov iteration (8.5), that this marginal probability evolves in a simple way:

$$\bar{\psi}_{n+1}(x_{n+1}) = \sum_{x_n} p_{x_{n+1},x_n} \bar{\psi}_n(x_n), \quad (8.12)$$

as p_{x_{n+1},x_n} is just the conditional probability of having x_{n+1} , once x_n is given. Since the matrix $G_{x',x}$ is symmetric, by using the definitions in (8.4) it is simple to show that the probability function

$$\bar{\psi}(x) = \frac{b_x}{\sum_{x'} b_{x'}} \quad (8.13)$$

is a *right eigenvector* of the stochastic matrix p with unit eigenvalue, namely $\sum_x p_{x',x} \bar{\psi}(x) = \bar{\psi}(x)$. It is also possible to show that, under the iteration (8.12), the probability $\bar{\psi}_n(x)$ will converge to $\bar{\psi}(x)$ no matter what is the initial condition, and exponentially fast, provided the stochastic matrix p , alias the Hamiltonian H itself, satisfy the following:

Definition 8.1 (Ergodicity.) *Any configuration x' can be reached, in a sufficiently large number of Markov iterations, starting from any initial configuration x , formally for each couple of configurations x and x' belonging to the Hilbert space considered, there exists an integer M such that $(p^M)_{x',x} \neq 0$.*

As we have shown in Sec.(5.5), it is possible to define an effective Hamiltonian $\bar{H}_{x',x}$ corresponding to the above Markov iteration (8.12) defined by $p_{x',x}$. Indeed using the same notations of Sec.(5.5) with $g(x) = \sqrt{\psi(x)}$ and:

$$\bar{H}_{x',x} = -\frac{1}{\sqrt{b_x b_{x'}}} G_{x',x}. \quad (8.14)$$

the Markov process (8.5) defines a Master equation (8.12), whose solution is independent of the initial condition, and the speed of convergence to the so-called equilibrium distribution $\bar{\psi} = g^2(x)$ (8.13) is related to the spectrum of the effective Hamiltonian \bar{H} (11.1), which is in turn closely related to the physical one H .

8.3 Importance sampling

According to Eq. (8.10), the calculation of the energy in the above described Green's function technique will not satisfy the "zero variance property" because the random quantity e_L does not depend on any variational guess ψ_g , as in the variational Monte Carlo (see Eq.(5.6), where, by improving ψ_g , one can substantially reduce the statistical fluctuations.

It is possible to recover this important property of the variational Monte Carlo, by a slight modification of the iteration technique. To this purpose, it is enough to consider the so-called *importance sampling* Green's function:

$$\bar{G}_{x',x} = \psi_g(x')G_{x',x}/\psi_g(x). \quad (8.15)$$

In general, $\bar{G}_{x',x}$ is no longer symmetric. Whenever $\bar{G}_{x',x} \geq 0$ for all (x',x) , it is possible to apply the same decomposition in (8.4) to \bar{G} , defining the corresponding Markov chain (8.5) with:

$$\begin{aligned} p_{x',x} &= \bar{G}_{x',x}/b_x \\ b_x &= \sum_{x'} \bar{G}_{x',x} = \Lambda - \frac{\sum_{x'} \psi_g(x')H_{x',x}}{\psi_g(x)} = \Lambda - e_L(x). \end{aligned} \quad (8.16)$$

Quite amusingly, if the guess wavefunction ψ_g used in the importance sampling procedure is the correct ground state wavefunction $\psi_g(x) = \psi_{GS}(x)$, then $e_L(x) = E_{GS}$ is a constant, and statistical fluctuations vanish exactly. Another useful property of the importance sampling procedure is a possible remedy to the sign problem. There are cases, in practical applications, where the original Green's function $G_{x',x}$ does not satisfy the positivity condition for all off-diagonal matrix elements. The antiferromagnetic nearest-neighbor Heisenberg model on the square lattice is a particularly important example of such a case. On the square lattice, we can define two sublattices A and B, the sites $R_i = (x_i, y_i)$, with $x_i, y_i \in \mathbb{Z}$, belonging to the A(B)-sublattice whenever $(-1)^{x_i+y_i} = +1(-1)$. In this case the standard Monte Carlo approach is defined with configurations $\{x\}$ where electrons have definite spin along the z -axis. In this basis, all the spin-flip terms in the Hamiltonian, $(S_i^+ S_j^- + \text{H.c.})$, act on antiparallel spins located at nearest-neighbor lattice points i and j that belong to opposite sublattices. These terms generate positive matrix elements for H , $H_{x',x} = J/2$, and hence *negative* matrix elements for G , $G_{x',x} = -J/2$. On the other hand, by choosing *any* guiding function $\psi_g(x)$ satisfying the so-called *Marshall sign rule*, i.e.,

$$\text{Sign } \psi_g(x) = (-1)^{\text{Number of spin up in A sublattice for configuration } x}, \quad (8.17)$$

it is readily verified that the importance sampled Green's function \bar{G} in (8.15) has instead all *positive* matrix elements $\bar{G}_{x',x} \geq 0$ ($\Lambda = 0$ can be chosen in this case).

All the derivations of Section 8.2 can be repeated exactly in the same way for the importance sampled \bar{G} , with trivial factors of ψ_g appearing here and there. We thus obtain, for instance, that:

$$\langle w_n \delta_{x, x_n} \rangle = \psi_g(x) \psi_n(x) \quad (8.18)$$

where $\psi_n(x)$ is defined in Eq. (9.1). On the other hand, for large n , the configurations x_n will be distributed according to $\bar{\psi}(x) = \frac{\psi_g^2(x) b_x}{\sum_{x'} \psi_g^2(x') b_{x'}}$, where $g(x) = \sqrt{\bar{\psi}(x)}$ remains the scale factor in the similarity transformation (5.19) defining the effective Hamiltonian \bar{H} in Eq. (11.1). Using the results of Sec.(5.5), assuming that at $n = 0$ the configurations are already equilibrated according to $\bar{\psi}$, we obtain:

$$E_{GS} = \lim_{n \rightarrow \infty} \frac{\langle w_n e_L(x_n) \rangle}{\langle w_n \rangle} = \frac{\langle \psi_g | H (\Lambda - H)^n | \bar{\phi} \rangle}{\langle \psi_g | (\Lambda - H)^n | \bar{\phi} \rangle}. \quad (8.19)$$

where $\langle x | \bar{\phi} \rangle = b_x \psi_g(x)$.

Since the convergence of the above limit is exponentially fast in n (at least for any finite size lattice, where a finite gap to the first excitation exists) it is enough to stop the iteration to a reasonably small finite $n = l$. Instead of repeating the Markov chain several times up to $n = l$, to accumulate statistics, it is clearly more convenient to average over a long Markov chain with $N \gg l$, where N is the total number of iterations of (8.5), and considering the corresponding estimates in (8.19):

$$E_{GS} = \lim_{l \rightarrow \infty} \frac{\langle \psi_g | H (\Lambda - H)^l | \bar{\phi} \rangle}{\langle \psi_g | (\Lambda - H)^l | \bar{\phi} \rangle} = \frac{\sum_{n > n_0}^N G_n^l e_L(x_n)}{\sum_{n > n_0}^N G_n^l} \quad (8.20)$$

where n_0 is the number of iterations required for the statistical equilibration of the Markov process and the weighting factors G_n^l are given by:

$$G_n^l = \prod_{i=1}^l b_{x_{n-i}}. \quad (8.21)$$

The above equations (8.20,8.21) are easily explained. At each discrete time $n - l$ we can take an equilibrated configuration distributed according to $\bar{\psi}(x)$, and consider l iterations of the Markov process (8.5) with initial condition $w_{n-l} = 1$, namely

$$P_{n-l}(x, w) = \delta(w - 1) \bar{\psi}(x), \quad (8.22)$$

leading, after l iterations, to a final weight $w_l = G_n^l$ at time n .

The relation (8.20) is exact in the statistical sense relating exact quantum averages to corresponding averages of random variables (G_n^l and $e_L(x_n)$), and allows us to compute the energy with an error bar decreasing like the inverse square root of the Markov chain length N . In order to estimate this error bar, it is useful to apply the ‘‘bin technique’’ of Section 5.7, especially because, in this case, the numerator and the denominator in (8.20) are highly correlated. After computing the bin average of the ratio \bar{e}^j in each bin (8.20), the error bar of the total average \bar{e} over the whole Markov chain can be estimated by assuming that each bin average is not correlated with the other

ones, leading to:

$$\sigma_{\bar{e}}^2 = \frac{1}{k(k-1)} \sum_{j=1}^k (\bar{e} - \bar{e}^j)^2, \quad (8.23)$$

where $\sigma_{\bar{e}}$ is the estimated standard deviation of \bar{e} . The above expression is valid only when the bin length $M = N/k$ is large enough compared to the correlation time, and $k \gtrsim 30$ for a good statistical accuracy of the estimated variance. A practical implementation of the above algorithm is given in App.(B.1).

8.4 The limit $\Lambda \rightarrow \infty$ for the power method, namely continuous time approach

The constant Λ appearing in $G_{x',x} = \Lambda - \delta_{x',x}$, which defines the the Green function with importance sampling \bar{G} in Eq.(8.15) has to be taken large enough to determine that all the diagonal elements of \bar{G} are non-negative (by definition the off-diagonal ones of \bar{G} are always non-negative). This requirement often determines a very large constant shift which increases with larger size and is not known a priori. The trouble in the simulation may be quite tedious, as if for the chosen Λ a negative diagonal element is found for \bar{G} , one needs to increase Λ and start again with a completely new simulation. The way out is to work with exceedingly large Λ , but this may slow down the efficiency of the algorithm as in the stochastic matrix $p_{x',x}$ the probability to remain in the same configuration p_d may become very close to one

$$p_d = \frac{\Lambda - H_{x,x}}{\Lambda - e_L(x)} \quad (8.24)$$

where $e_L(x)$ is the local energy Eq. (5.6) that do not depend on Λ given the configuration x .

In the following we will show that The problem of working with large Λ can be easily solved with no loss of efficiency. We report this simple idea applied to the simple algorithm introduced so far for a single walker. If Λ is large it is possible to remain a large number k_p of times (of order Λ) in the same configuration before a new one is accepted. The idea is that one can determine a priori, given p_d what is the probability $t(k)$ to make k diagonal moves before the first acceptance of a new configuration with $x' \neq x$. This is given by $t(k) = p_d^k(1 - p_d)$ for $k = 0, \dots, L - 1$ and $t(L) = p_d^L$ if no off-diagonal moves are accepted during the L trials.

It is a simple exercise to show that, in order to sample $t(k)$ one needs one random number $0 < \xi < 1$, so that the stochastic integer number k can be computed by the simple formula

$$k = \min(L, \lceil \frac{\ln \xi}{\ln p_d} \rceil), \quad (8.25)$$

where the brackets indicate the integer part. During the total L iterations one can iteratively apply this formula by bookkeeping the number of iterations L_{left} , that are left to complete the loop of L iterations. At the first iteration $L_{left} = L$, then k is extracted using (8.25), and the weight w of the walker is updated according to k diagonal moves, namely $w \rightarrow w b_x^k$ and if $k < L_{left}$ a new

configuration is extracted randomly according to the transition probability $t_{x',x}$ defined by:

$$t_{x',x} = \begin{cases} \frac{p_{x',x}}{Z(x)/b_x} & \text{for } x \neq x' \\ 0 & \text{for } x = x' \end{cases} \quad (8.26)$$

where:

$$Z(x) = \sum_{x' \neq x} \bar{G}_{x',x} = -e_L(x) + H_{x,x} \quad (8.27)$$

Finally, if $k < L_{left}$, L_{left} is changed to $L_{left} - k - 1$, so that one can continue to use Eq. (8.25) until $L_{left} = 0$, meaning that all the L steps are executed, with a finite number of steps even when Λ and $L \propto \Lambda$ is extremely large.

Indeed it is interesting to observe that this method can be readily generalized for $\Lambda \rightarrow \infty$ by increasing L with Λ , namely $L = [\Lambda\tau]$, where τ represents now exactly the imaginary time evolution of the exact propagator $e^{-H\tau}$ applied statistically. To this purpose it is enough to bookkeep the corresponding time left t_{left} remaining to complete the imaginary time propagation of length τ . Indeed before generating a new configuration according to the same transition probability (8.26), one needs only to generate a random time interval:

$$t_{try} = \text{Min}(-\ln z/Z(x), t_{left}) \quad (8.28)$$

where z is a random number uniformly distributed in the interval $(0, 1]$ and update the weights and t_{left} according to:

$$t_{left} \rightarrow t_{left} - t_{try} \quad (8.29)$$

$$w \rightarrow w \exp(-t_{try}e_L(x)) \quad (8.30)$$

The loop is completed when $t_{left} = 0$.

8.4.1 Local operator averages

The Green's function Monte Carlo can be also used efficiently to compute expectation values of local operators \hat{O} , i.e., operators which are diagonal on all the elements of the configuration basis $|x\rangle$,

$$\hat{O}|x\rangle = O_x|x\rangle, \quad (8.31)$$

where O_x is the eigenvalue corresponding to the configuration x . For instance, in the Heisenberg model a particularly important operator is the square of the order parameter along the z direction:

$$\hat{O} = \left[\frac{1}{L} \sum_R e^{i\vec{Q}\cdot\vec{R}} S_R^z \right]^2, \quad (8.32)$$

where $Q = (\pi, \pi)$ in two-dimensions. This operator allows us to verify the existence of antiferromagnetic long-range order, by evaluating the expectation value $\langle \psi_{GS} | \hat{O} | \psi_{GS} \rangle$ on any finite system. The limiting $L \rightarrow \infty$ value, when finite, implies a finite antiferromagnetic order parameter, the so-called *staggered magnetization* m^\dagger , for the infinite system.

For local operators, the local estimator is simply $\frac{\langle \psi_g | \hat{O} | x \rangle}{\langle \psi_g | x \rangle} = O_x$. Moreover, the Markov chain (8.5) is easily modified for accounting for the application, at a selected iteration time $n - m$, of the operator \hat{O} . This is in fact exactly equivalent – in the statistical sense – to modifying the weight $w'_{n-m} \rightarrow O_{x_{n-m}} w_{n-m}$. In this way, it is simple to verify that:

$$\frac{\langle w_n O_{x_{n-m}} \rangle}{\langle w_n \rangle} = \frac{\langle \psi_g | (\Lambda - H)^m \hat{O} (\Lambda - H)^{l-m} | \bar{\phi} \rangle}{\langle \psi_g | (\Lambda - H)^l | \bar{\phi} \rangle} \rightarrow \langle \psi_{GS} | \hat{O} | \psi_{GS} \rangle. \quad (8.33)$$

In the above equation, $w_{n-l} = 1$ is assumed, according to the initial condition (8.22) for the definition of the weighting factors G_n^l in (8.21), implying that $m \leq l$, so that the practical expression of Eq.(8.33) becomes:

$$\langle \psi_{GS} | \hat{O} | \psi_{GS} \rangle \simeq \frac{\sum_n G_n^l O_{x_{n-m}}}{\sum_n G_n^l}. \quad (8.34)$$

valid for $l - m, m \gg 1$. Indeed the latter equation (8.34) is satisfied for $l \rightarrow \infty$, provided also $m \rightarrow \infty$ in this limit. Indeed, only with a very large m , we can filter out the ground state from the left-hand side state $\langle \psi_g |$. A practical implementation of the above algorithm is given in App.(B.1).

By using (8.33) for $m = 0$, the so called *mixed averaged* $\langle \hat{O} \rangle_{MA}$ is obtained, a biased estimator of the exact quantum average:

$$\langle \hat{O} \rangle_{MA} = \frac{\langle \psi_g | \hat{O} | \psi_{GS} \rangle}{\langle \psi_g | \psi_{GS} \rangle}. \quad (8.35)$$

The calculation of these mixed averages is possible for any type of operator, not only the local ones. For operators that are defined on the ground state, $\hat{O} | \psi_{GS} \rangle = \gamma_O | \psi_{GS} \rangle$ (γ_O being the eigenvalue), such as the total spin S^2 or the total energy, the mixed average estimator is exact (as we have seen in particular for the energy in (8.19)). For all other operators, a well known scheme to evaluate the ground state expectation value is known as the *Ceperley correction*:

$$\frac{\langle \psi_{GS} | \hat{O} | \psi_{GS} \rangle}{\langle \psi_{GS} | \psi_{GS} \rangle} \approx 2 \langle \hat{O} \rangle_{MA} - \langle \hat{O} \rangle_{VMC}, \quad (8.36)$$

where $\langle \hat{O} \rangle_{VMC} = \frac{\langle \psi_g | \hat{O} | \psi_g \rangle}{\langle \psi_g | \psi_g \rangle}$ is the simple variational estimate corresponding to ψ_g . This approach is justified provided the variational wavefunction ψ_g is very close to ψ_{GS} and can be written as $\psi_g = \psi_{GS} + \epsilon \psi'$, with ψ_{GS} and ψ' normalized, and $\epsilon \ll 1$. The expression (8.36) clearly holds up to $O(\epsilon^2)$.

8.5 Many walkers formulation

The practical reason for taking l as small as possible in (8.20) is that for large l the variance of the weight factors G_n^l diverges exponentially, leading to uncontrolled fluctuations, as we will now show. To this purpose it is enough to compute the variance of the G_n^l factors

$$\text{var } G_n^l = (\delta G^l)^2 = \langle w_l^2 \rangle - \langle w_l \rangle^2$$

and show that it diverges. We use the Master equation (8.7), with the initial condition (8.22), and consider the following quantity $\Phi_n(x) = \langle w_n^2 \delta_{x, x_n} \rangle$, that is easily related to the desired quantity,

since $\langle w_l^2 \rangle = \sum_x \Phi_l(x)$. Then, following (8.9) we write:

$$\begin{aligned}
\Phi_{n+1}(x') &= \langle w_{n+1}^2 \delta_{x',x_{n+1}} \rangle = \int dw_{n+1} w_{n+1}^2 P_{n+1}(x', w_{n+1}) \\
&= \int dw_{n+1} w_{n+1}^2 \sum_x \int dw_n p_{x',x} \delta(w_{n+1} - b_x w_n) P_n(x, w_n) \\
&= \sum_x \int dw_n p_{x',x} b_x^2 w_n^2 P_n(x, w_n) \\
&= \sum_x (G_{x',x} b_x) \Phi_n(x). \tag{8.37}
\end{aligned}$$

According to Eq.(8.37), $\langle w_l^2 \rangle = \sum_x \Phi_l(x)$ will diverge, for large l , exponentially fast, as $\propto \lambda_2^l$, where λ_2 is the maximum eigenvalue of the matrix Gb (b is here a diagonal matrix $(b)_{x,x'} = \delta_{x,x'} b_x$). At the same time, $\langle w_l \rangle$ will diverge as $\langle w_l \rangle \sim \lambda^l$, where $\lambda = \Lambda - E_{GS}$ is the maximum eigenvalue of the Green's function G . In general $\lambda_2 \geq \lambda^2$ as $\langle w_l^2 \rangle$ has to be bounded by $\langle w_l \rangle^2$ by the Schwartz inequality. The equality sign holds only if the matrix b is a constant times the identity matrix, namely, by Eq.(8.16), when the guiding function is exact and the local energy has zero variance. It is therefore clear that, quite generally, we get an exponential increase of the fluctuations

$$(\delta G^l)^2 \sim (\lambda_2^l - \lambda^{2l}) \rightarrow \infty,$$

as $l \rightarrow \infty$.

In order to overcome this problem of an exponentially increasing variance, we will discuss in the following section a way to propagate a set of M walkers simultaneously defined by weights w_i and configurations x_i , for $i = 1, \dots, M$. By evolving them independently, clearly no improvement is obtained for the aforementioned large fluctuations. Instead, we will consider the following reconfiguration of the walkers: before the variance of the weights w_i becomes too large, we will redefine the set of walkers by dropping out those with a weight which is too small, and correspondingly generate copies of the more important ones, in such a way that after this reconfiguration all the walkers have approximately the same weight. By iterating this process, the weights of all the walkers will be kept approximately equal during the simulation. This property yields a considerable reduction of statistical errors, as the variance of the average weight $\bar{w} = \frac{1}{M} \sum_i w_i$ is reduced by a factor $\propto \sqrt{M}$. This allows therefore a more stable propagation even for large l .

8.5.1 Carrying many configurations simultaneously

Given the M walkers we indicate the corresponding configurations and weights with a couple of vectors $(\underline{x}, \underline{w})$, with each vector component x_i, w_i $i = 1, \dots, M$, corresponding to the i^{th} walker. It is then easy to generalize the Master equation Eq. (8.7) to many *independent* walkers. If the evolution of P is done without further restrictions, each walker is uncorrelated from any other one, and we have:

$$P_n(x_1, x_2, \dots, x_M, w_1, w_2, \dots, w_M) = P_n(x_1, w_1) P_n(x_2, w_2) \cdots P_n(x_M, w_M).$$

Old walkers		New Walkers	
$w_1 x_1$	\longrightarrow	$\bar{w} x'_1 = x_{j(1)}$	with probability p_j
$w_2 x_2$	\longrightarrow	$\bar{w} x'_2 = x_{j(2)}$	with probability p_j
$w_3 x_3$	\longrightarrow	$\bar{w} x'_3 = x_{j(3)}$	with probability p_j
\vdots	\vdots	\vdots	\vdots
$w_M x_M$	\longrightarrow	$\bar{w} x'_M = x_{j(M)}$	with probability p_j

Table 8.1: Reconfiguration scheme with bias control. Here $\bar{w} = \frac{1}{M} \sum_{k=1}^M w_k$ and the probability $p_j = \frac{w_j}{\sum_{k=1}^M w_k}$ can be sampled by using a random number for each walker according to the same scheme reported in Fig.(8.2) for $p_{x',x}$. This allows to define the table $j(i)$ for $i = 1, \dots, M$ corresponding to the selected new configurations.

Similarly to the previous case (8.18), we can define the state evolved at iteration n with the Green's function G (with importance sampling implemented) by:

$$\begin{aligned}
\psi_n(x)\psi_g(x) &= \left\langle \frac{1}{M} \sum_{i=1}^M w_i \delta_{x,x_i} \right\rangle \\
&= \int dw_1 \int dw_2 \cdots \int dw_M \sum_{\underline{x}} \left(\frac{w_1 \delta_{x,x_1} + w_2 \delta_{x,x_2} + \cdots + w_M \delta_{x,x_M}}{M} \right) P_n(\underline{x}, \underline{w}).
\end{aligned} \tag{8.38}$$

Since we are interested in the state ψ_n , we can define a reconfiguration process that changes the probability distribution P_n *without changing the statistical average* $\left\langle \frac{1}{M} \sum_{i=1}^M w_i \delta_{x,x_i} \right\rangle$ that is relevant in the calculations of ψ_n . This can be obtained by a particular Markov process applied to the configurations (x_j, w_j) , which leads to new walkers (x'_j, w'_j) . Each new walker (x'_j, w'_j) , with $j = 1 \cdots M$, will have the same weight $w'_j = \bar{w} = \frac{\sum_j w_j}{M}$ and an arbitrary configuration x'_j , among the M possible old configurations x_k , $k = 1 \cdots M$, chosen with a probability p_k proportional to the weight of that configuration, $p_k = w_k / \sum_j w_j$ (see picture 8.5.1).

It is clear that, after this reconfiguration, the new set of M walkers have by definition the same weights $w'_j = \bar{w}$, and most of the irrelevant walkers with small weights have dropped out. This reconfiguration plays the same stabilization effect of the conventional *branching* scheme, but with a few extra advantages that we will mention later on.

It is easy to derive the Master equation corresponding to this reconfiguration Markov process (see previous chapter) and show that indeed the relevant average (8.38), is not statistically modified. The corresponding conditional probability K is simple, in this case, because all the new walkers are independent from each other, and K factorizes for each walker:

$$P'_n(\underline{x}', \underline{w}') = \sum_{\underline{x}} \int [d\underline{w}] K(\underline{x}', \underline{w}' | \underline{x}, \underline{w}) P_n(\underline{x}, \underline{w}) \tag{8.39}$$

$$K(\underline{x}', \underline{w}' | \underline{x}, \underline{w}) = \prod_{j=1}^M \left(\frac{\sum_i w_i \delta_{x'_j, x_i}}{\sum_i w_i} \right) \delta \left(w'_j - \frac{\sum_i w_i}{M} \right). \tag{8.40}$$

Hereafter $\int [d\underline{w}]$ will be a convenient shorthand notation for the multiple integrals over all the w_i variables. Notice, finally, that the conditional probability K is correctly normalized

$$\sum_{\underline{x}'} \int [d\underline{w}'] K(\underline{x}', \underline{w}' | \underline{x}, \underline{w}) = 1 .$$

The proof that this reconfiguration scheme does not influence the relevant average we are interested in is detailed in the next section. For an efficient implementation of this reconfiguration scheme, see the Appendix (B).

8.5.2 Bias control

One of the problem of the traditional branching scheme adopted in GFMC in order to control the walker population size M and the fluctuations of the weights, is that, in so doing, one introduces a *bias* in the simulation, i.e., a sistematic error which is simply due to some kind of correlation between the walkers that the reconfiguration introduces. For high accuracy calculations, this bias often becomes the most difficult part of the error to control. In this section we will prove that the present reconfiguration scheme, defined in Eq. (8.39), does a much better job: Though it clearly introduces some kind of correlation among the walkers, we can rigorously prove that the average

$$\Gamma_n(x) = \psi_n(x) \psi_g(x) = \langle \frac{1}{M} \sum_i w_i \delta_{x, x_i} \rangle$$

calculated with the probability P_n is exactly equal to the corresponding average $\Gamma'_n(x)$ calculated with the probability P'_n , obtained after reconfiguration (see Eq. (8.39)),

$$\Gamma'_n(x) = \Gamma_n(x) . \quad (8.41)$$

This means that there is no loss of information in the present reconfiguration process.

Proof: By definition, using (8.39), we have:

$$\Gamma'_n(x) = \sum_{\underline{x}, \underline{x}'} \int [d\underline{w}] \int [d\underline{w}'] \left(\frac{\sum_j w'_j \delta_{x, x'_j}}{M} \right) K(\underline{x}', \underline{w}' | \underline{x}, \underline{w}) P_n(\underline{x}, \underline{w}) .$$

The first term in the integrand contains a sum. It is simpler to single out each term of the sum $w'_k \delta_{x, x'_k} / M$, and to integrate over all the possible variables $\underline{x}', \underline{w}'$ but x'_k and w'_k . It is then easy to show that this contribution to Γ'_n , which we will indicate by $[\Gamma'_n]_k$, is given by:

$$[\Gamma'_n]_k = \sum_{\underline{x}, x'_k} \int [d\underline{w}] \int [dw'_k] \frac{w'_k}{M} \delta_{x, x'_k} \left(\frac{\sum_i w_i \delta_{x'_k, x_i}}{\sum_i w_i} \right) \delta \left(w'_k - \frac{\sum_i w_i}{M} \right) P_n(\underline{x}, \underline{w}) .$$

Then, by integrating simply in dw'_k and summing over x'_k in the previous expression, we easily get that $[\Gamma'_n]_k = \frac{1}{M} \Gamma_n$, independent of k . Therefore, by summing over k we have proven the statement in (8.41).

8.6 The GFMC scheme with bias control

We are finally in the position of presenting a GFMC scheme that works well in practice, because of the control of the weight fluctuations that the reconfiguration scheme introduced provides. It is straightforward to generalize the equations (8.20,8.33), to many walkers (configurations). We assume that the reconfiguration process described in the previous sections is applied repeatedly, each k_b steps of independent walker propagation. The index n appearing in the old expressions (8.21) will now label the n^{th} reconfiguration process. The measurement of the energy can be done *immediately after* the reconfiguration process, when all the walkers have the same weight, thus in Eq. (8.20) we would need to substitute:

$$e_L(x_n) \rightarrow \frac{1}{M} \sum_{j=1}^M e_L(x_j^n), \quad (8.42)$$

or, for a better statistical error, the energy can be sampled *just before* the reconfiguration, taking properly into account the weight of each single walker:

$$e_L(x_n) \rightarrow \frac{\sum_{j=1}^M w_j e_L(x_j^n)}{\sum_{j=1}^M w_j}. \quad (8.43)$$

It is useful, after each reconfiguration, to store the quantity $\bar{w} = \frac{1}{M} \sum_{j=1}^M w_j$ resetting to $w'_n = 1$ the weights of all the walkers (instead of taking $w'_j = \bar{w}$). Thus, the total weights G_n^l correspond to the application of $l \times k_b$ iterations of the power method (as in Eq. 9.1) towards the equilibrium distribution $\bar{\psi}(x) = \langle \frac{1}{M} \sum_j \delta_{x,x_j} \rangle$, equilibrium distribution that is independent of n for large enough n , as in the single walker formulation. The value of the weighting factor G_n^l can be easily recovered by following the evolution of the M walkers weights in the previous l reconfiguration processes, and reads:

$$G_n^l = \prod_{j=0}^{l-1} \bar{w}_{n-j}, \quad (8.44)$$

where the average weight of the walkers \bar{w} after each reconfiguration has been defined previously.

An example of how the method works for the calculation of the ground state energy of the Heisenberg model on a 4×4 square lattice is shown in Fig. (8.2). Remarkably, the method converges very fast, as a function of l , to the exact result, with smaller error bars as compared to traditional branching schemes. The fact that the reconfiguration scheme does not need to be applied at every iteration, leads to a much smaller bias (the $l = 1$ value for $k_b = 4$, dotted line, is five times closer to the exact result than the corresponding $k_b = 1$ value). In all cases, the bias introduced by the reconfigurations is corrected by a sufficiently large value of l , which keeps the correct weighting factors into account. An extra advantage of the present reconfiguration scheme is that the number of walkers M is maintained strictly fixed, while some of the traditional branching schemes work with a fluctuating number of walkers M .

Exercise 8.1 Consider a single spinless particle in a one dimensional chain described by lattice points $|x_i \rangle = |i \rangle$, where $|i \rangle$ is the state with the particle at site i . The particle can move to the

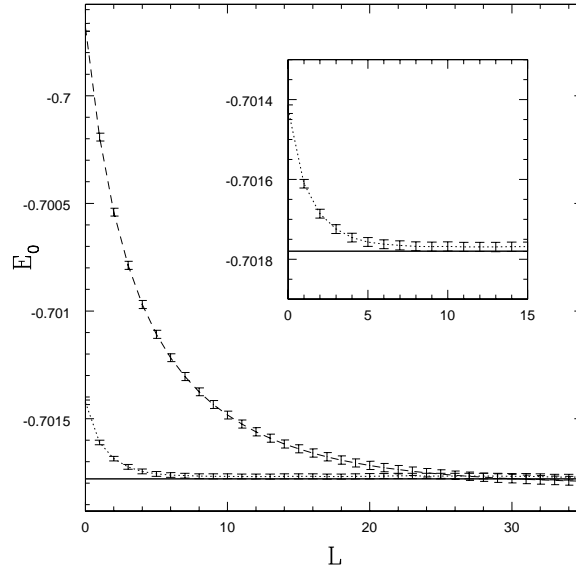


Figure 8.2: Energy per site for a 4×4 Heisenberg model cluster. The x-label L is simply what we denote by l in the text, and should not be confused with the lattice size. The continuous line is the exact result, obtained by exact diagonalization, while the dotted (dashed) line connects GFMC data as a function of the number l of weight factors included in G_n^l . The number of walkers was in all cases $M = 10$, and the reconfiguration scheme was applied at each iteration ($k_b = 1$, slower convergence – dashed line), or every four iterations ($k_b = 4$, dotted line). The guiding wavefunction $\psi_g(x)$ is a standard one for the Heisenberg model, satisfying the Marshall sign rule (8.17), which we do not specify further here. All the data are obtained with the same amount of computer time. The inset shows an enlargement of the bottom-left part of the main plot.

left or to the right, with hopping matrix elements $-t$, apart for the boundary site $i = 1$ ($i = L$) where the particle can move only to the right (left). The particle is also subject to a linear potential increasing with the distance from the $i = 1$ boundary, thus the Hamiltonian reads:

$$H = -t \sum_{i=1}^{L-1} (c_i^\dagger c_{i+1} + \text{H.c.}) + V \sum_{i=1}^L (i-1) c_i^\dagger c_i \quad (8.45)$$

and V/t represents the dimensionless coupling of the model.

1. Write the matrix elements of the Hamiltonian in configuration space, namely in the basis $|x_i\rangle = |i\rangle$.
2. For $V/t = 10$, $L = 30$ compute, using the variational Monte Carlo, the expectation value of the energy on the variational state $\psi_g(x) = e^{-g|i|}$, where g is a variational parameter to be optimized (finding the g which gives the minimum energy expectation value).

3. Compute the exact ground state energy for $V/t = 10$ using the single walker technique described by the Markov chain (8.5).
4. Compute the mixed average and the exact expectation value on the ground state of the average position of the particle, corresponding to the operator $\hat{O} = \sum_i ic_i^\dagger c_i$.

Chapter 9

Reptation Monte Carlo

9.1 motivations

As we have seen it is possible to solve the problem of the exponential growth of the weights in the Green's function Monte Carlo technique (GFMC), by introducing many walkers and iteratively propagate them with approximately the same weight. This technique, though widely used, can be inefficient when the number of walkers necessary to carry out a simulation becomes too large. This may happen when the wavefunction used for importance sampling is rather poor or it is necessary to compute correlation functions without biased estimator (e.g. mixed average) or the too much expensive forward walking technique.

The reptation Monte Carlo algorithm has been introduced recently[25] as a simpler and more efficient way to make importance sampling on the walker weights. In principle this technique requires only one walker, and represents a straightforward change of the basic single walker GFMC technique introduced in the previous chapter.

9.2 A simple path integral technique

As before we will denote by x the discrete labels specifying a given state of the N -electron Hilbert space of our system (for instance, specifying all the electron positions and spins). We will also assume that, given the Hamiltonian H , the matrix elements $\langle x'|H|\mathbf{x}\rangle = H_{x',x}$, for given x , can be computed efficiently for each x' . Typically, for a lattice Hamiltonian, though the dimension of the Hilbert space spanned by $\{x'\}$ increases exponentially with the system size L , the number of vanishing entries of the matrix representing H , $H_{x',x} = 0$, is very large, so that the non-zero column elements in $H_{x',x}$, for given x , are of the order of the system size L , and can be therefore computed with a reasonable computational effort.

Using the above property, it is possible to define a stochastic algorithm that allows to perform

the power method (see the Introduction) in a statistical way, in the sense that the wavefunction

$$\psi_n(x) = \langle x | (\Lambda \mathbf{1} - H)^n | \psi_t \rangle, \quad (9.1)$$

with $|\psi_t\rangle$ some initial trial state, is evaluated with a stochastic approach.

The goal of the Reptation Monte Carlo (RMC) approach is to define a Markov process, that allows to sample a sort of partition function:

$$Z(\psi_t) = \langle \psi_t | (\Lambda I - H)^T | \psi_t \rangle \quad (9.2)$$

where T is a large integer power, where it is understood that several physical quantities like the energy expectation value, can be written as a classical average, where $Z(\psi_t)$ represents the partition function. In order to achieve this target, we use in RMC the same decomposition of the Green's function with importance sampling, that has been previously adopted for the GFMC, namely:

$$G_{x',x} = \psi_t(x') (\Lambda \delta_{x,x'} - H_{x',x}) / \psi_t(x) = b_x p_{x',x} \quad (9.3)$$

By means of this decomposition, by inserting the completeness $\sum_x |x\rangle \langle x| = I$ before and after each $\Lambda I - H$ power in Eq.(9.4), and some simple algebra, we obtain:

$$Z(\psi_t) = \sum_{x_0, x_1, \dots, x_T} b_{x_{T-1}} b_{x_{T-2}} \cdots b_{x_0} p_{x_T, x_{T-1}} \cdots p_{x_1, x_0} \psi_t(x_0)^2 \quad (9.4)$$

The above partition function is defined in terms of a generalized coordinate R -the Reptile- where the coordinates x are specified at all integer times $T = 0, \dots, T$:

$$R = x_T \cdots, x_2, x_1, x_0 \quad (9.5)$$

In this way it is simple to convince ourselves that the energy and many correlation functions (the operators diagonal in the local basis as in the forward walking) can be written in a classical looking form.

For instance the energy estimator can be conveniently written as:

$$E(T) = \frac{\sum_R W(R) (e_L(x_0) + e_L(x_T)) / 2}{\sum_R W(R)} \quad (9.6)$$

where $e_L(x) = \frac{\langle \psi_t | H | x \rangle}{\langle \psi_t | x \rangle} = \frac{\langle x | H | \psi_t \rangle}{\langle x | \psi_t \rangle}$ is the local energy already met in GFMC and the classical weight is:

$$W(R) = b_{x_{T-1}} b_{x_{T-2}} \cdots b_{x_0} p_{x_T, x_{T-1}} \cdots p_{x_1, x_0} \psi_t(x_0)^2 \quad (9.7)$$

Notice that $E(T)$, by the variational principle, is an upper bound of the true ground state energy, because it corresponds to the energy expectation value of the energy over the state $(\Lambda I - H)^{T/2} | \psi_t \rangle$. On the other hand for $T \rightarrow \infty$, $E(T)$ converges to the exact ground state energy E_0 , due to the power method projection. Analogously all correlation functions that are defined in the given local basis (corresponding operators are diagonal) can be computed at the middle interval for $|x\rangle = x_{T/2}$ and averaged over the same classical weight $W(R)$.

9.3 Sampling $W(R)$

In order to sample this weight we need to define two basic moves $R \rightarrow R'$, that are used to update globally the reptile, and considered at this stage with equal probability. It is convenient to indicate these two updates with the label $d = \pm 1$. For $d = 1$ ($d = -1$) we adopt the convention that the reptile is moving right (left) in time. The variable d in the standard RMC is chosen randomly at each step with equal probability for a left or a right move.

9.3.1 Move RIGHT $d = 1$

$$R' = \{x'_T, x'_{T-1} \cdots, x'_1, x'_0\} = \{\bar{x}, x_T, \cdots, x_2, x_1\} \quad (9.8)$$

where \bar{x} , the trial move at the rightmost side of the reptile, is obtained by sampling the matrix $p_{\bar{x}, x_T}$, i.e. the transition probability $T^d(R'|R)$, defining this process is given by:

$$T^1(R'|R) = \frac{1}{2} p_{\bar{x}, x_T} \quad (9.9)$$

The corresponding weight on the new reptile R' is given by:

$$W(R') = b_{x_T} b_{x_{T-1}} \cdots b_{x_1} p_{\bar{x}, x_T} p_{x_T, x_{T-1}} \cdots p_{x_2, x_1} \psi_t(x_1)^2 \quad (9.10)$$

Thus the ratio $W(R')/W(R)$ required to implement the Metropolis algorithm(5.25) is easily evaluated:

$$W(R')/W(R) = \frac{b_{x_T} p_{\bar{x}, x_T} \psi_t(x_1)^2}{b_{x_0} p_{x_1, x_0} \psi_t(x_0)^2} \quad (9.11)$$

9.3.2 Move LEFT $d = -1$

$$R' = \{x'_T, \cdots, x'_1, x'_0\} = \{x_{T-1}, \cdots, x_1, x_0, \bar{x}\} \quad (9.12)$$

where \bar{x} , the trial move at the leftmost side of the reptile, is obtained by sampling the matrix $p_{\bar{x}, x_0}$, i.e. the transition probability $T^d(R'|R)$, defining this process is given by:

$$T^{-1}(R'|R) = \frac{1}{2} p_{\bar{x}, x_0} \quad (9.13)$$

The corresponding weight on the new reptile R' is given by:

$$W(R') = b_{x_{T-2}} b_{x_{T-3}} \cdots b_{x_0} b_{\bar{x}} p_{x_{T-1}, x_{T-2}} p_{x_{T-2}, x_{T-3}} \cdots p_{x_0, \bar{x}} \psi_t(\bar{x})^2 \quad (9.14)$$

Thus the ratio $W(R')/W(R)$ required to implement the Metropolis algorithm(5.25) is easily evaluated:

$$W(R')/W(R) = \frac{b_{\bar{x}} p_{\bar{x}_0, \bar{x}} \psi_t(\bar{x})^2}{b_{x_{T-1}} p_{x_T, x_{T-1}} \psi_t(x_0)^2} \quad (9.15)$$

Now we are in the position to simplify the term appearing in the Metropolis algorithm (Eq.5.25).

For the right move the opposite one that brings back $R' \rightarrow R$ is a left move $d = -1$ with $\bar{x} = x_0$ and (notice that the leftmost configuration of the R' reptile is x_1), namely by using Eq.(9.13):

$$T^{-1}(R|R') = \frac{1}{2}p_{x_0,x_1} \quad (9.16)$$

Therefore the right move will be accepted with probability:

$$a(R'|R) = \overline{Min(1, r(R', R))} \quad (9.17)$$

where:

$$r(R', R) = W(R')/W(R)T^{-d}(R|R')/T^d(R'|R) \quad (9.18)$$

where we have used that for the step labeled by $d = \pm 1$ that brings $R \rightarrow R'$ the reverse move can be obtained only by applying the opposite move $-d = \mp 1$. The global transition probability of the Markov process is given by $K(R'|R) = a(R'|R)T^d(R'|R)$ for $R \neq R'$ and d univocally determined by the choice of R' and R . Then it is simple to show that the detailed balance condition is always verified.

Moreover, by using the Eqs.(9.11,9.9,9.16) we can simplify the above ratio and obtain for $d = 1$:

$$r(R', R) = \frac{b_{x_T}\psi_t(x_1)^2 p_{x_0,x_1}}{b_{x_0}p_{x_1,x_0}\psi_t(x_0)^2} \quad (9.19)$$

Now using the definition of the stochastic matrix and the symmetry of the Hamiltonian

$$p_{x_0,x_1}/p_{x_1,x_0} = \frac{b_{x_0}\psi_t(x_0)^2}{b_{x_1}\psi_t(x_1)^2}$$

which further simplify the final expression for r when $d = 1$:

$$r(R', R) = b_{x_T}/b_{x_1} \quad (9.20)$$

With analogous steps we can also derive the expression for $r(R', R)$ in Eq.(9.18) with the left move $d = -1$:

$$r(R', R) = b_{x_0}/b_{x_{T-1}} \quad (9.21)$$

which completely define in a simple way the rules for accepting or rejecting the new proposed reptile R' in the standard Metropolis algorithm (5.25).

9.4 Bounce algorithm

The bounce algorithm is more efficient than the standard one because one can obtain a shorter autocorrelation time by doing many steps in one direction (only right or only left), and was introduced recently for an efficient simulation of electrons and protons at finite temperature[28]. In practice the algorithm is easily explained. The variable $d = \pm 1$ is no longer randomly sampled, but d changes sign only when the move is rejected in Eq.(9.17), so that the transition probability used in the bounce algorithm is simply multiplied by a factor two: $T_B^d(R'|R) = 2T^d(R'|R)$.

In order to prove that the bounce algorithm samples the correct distribution $W(R)$ we need to include in the state space also the direction d , namely $R \rightarrow R, d$, and prove that the conditional probability associated to this Markov process $K_B(R', d'|R, d)$ determines an equilibrium distribution $\Pi(R, d) = W(R)/\sum_{R'} W(R')$, that does not depend on d . In more details the conditional probability describing this Markov process is given by:

$$\begin{aligned} K_B(R', d'|R, d) &= T_B^d(R'|R)a(R'|R)\delta_{d',d} \\ &+ \delta(R' - R)B(R, d)\delta_{d',-d} \end{aligned} \quad (9.22)$$

where R' is the proposed move in the right or left direction according to the running value of d and $B_d(R)$ can be easily obtained by using that the conditional probability is normalized, namely $\sum_{R', d'} K_B(R', d'|R, d) = 1$, yielding:

$$\begin{aligned} B(R, d) &= 1 - \left[\sum_{R'} T_B^d(R'|R)(1 - a(R'|R)) \right] \\ &= \sum_{R'} T_B^d(R'|R)a(R'|R) \end{aligned} \quad (9.23)$$

where the latter equality follows from the normalization condition of the transition probability $T_B^d(R', R)$, i.e. $\sum_R T_B^d(R', R) = 1$.

In this way, though the transition probability K_B does not satisfy the detailed balance condition, it is possible to show that the master equation:

$$\sum_{R, d} K_B(R', d'|R, d)P_n(R, d) = P_{n+1}(R', d') \quad (9.24)$$

remains stationary for the desired equilibrium distribution $P_n(R, d) = \frac{W(R)}{2}$. Indeed by assuming to apply the above Markov iteration in Eq.(8.19) with $P_n(R, d) = \frac{W(R)}{2}$, we obtain:

$$P_{n+1}(R', d') = \frac{W(R')}{2}B(R', -d') + \frac{1}{2} \sum_R T^{d'}(R', R)a^{d'}(R', R)W(R). \quad (9.25)$$

In the last term of the above equation, in order to carry out the formal integration over R , we apply the following relation:

$$T_B^d(R'|R)a(R'|R)W(R) = W(R')T_B^{-d}(R|R')a(R|R') \quad (9.26)$$

that can be obtained as a consequence of Eqs.(9.17,9.18) and the definition of $T_B^d = 2T^d$. Then, after simple substitution, we get:

$$P_{n+1}(R', d') = \frac{W(R')}{2}B(R', -d') + \frac{W(R')}{2} \sum_R T^{-d'}(R, R')a^{-d'}(R, R') \quad (9.27)$$

Finally by noticing that $\sum_R T^{-d'}(R, R')a^{-d'}(R, R')$, in the above equation is nothing but the definition of $B(R', -d')$ in Eq.(9.23) we easily get:

$$P_{n+1}(R') = \frac{W(R')}{2}B(R', -d') + \frac{W(R')}{2} [1 - B(R', -d')] = \frac{W(R')}{2} \quad (9.28)$$

that proves the stationarity of the distribution.

In order to prove that the Markov process converges certainly to this equilibrium distribution one has to assume that the equilibrium distribution is unique even though the bounce Markov chain does not satisfy the detailed balance condition (see exercise). I was not able to prove in a simple way this more general property of Markov chains even though there is some attempt in the literature to have a simple proof[26], which is however wrong. Rigorous proof that a Markov chain converges to a unique distribution can be obtained by a generalization of the Perron-Frobenius theorem to non symmetric matrices. This is a well known result and can be applied to this case, as we have done for a Markov chain satisfying the detailed balance condition.

Exercise 9.1 *Prove that the detailed balance condition is not satisfied in the bounce algorithm.*

Chapter 10

Fixed node approximation

10.1 Sign problem in the single walker technique

In the previous chapter we have described a method that allows to compute the ground state property of a given Hamiltonian H , once the matrix elements:

$$G_{x',x} = \psi_g(x')\Lambda\delta_{x',x} - H_{x',x}/\psi_g(x) \geq 0$$

for a suitable guiding function $\psi_g(x)$ and a sufficiently large constant shift Λ . In principle the approach (8.5) can be easily generalized to a non positive definite Green function, for the simple reason that we can apply the scheme (8.5) to the positive Green function $\tilde{G}_{x',x} = |G_{x',x}|$, and take into account the overall sign of the Green function $s_{x',x} = \text{Sign}G_{x',x}$ in the walker weight w . Indeed the approach will change for an additional operation:

- a) generate $x_{n+1} = x'$ with probability p_{x',x_n}
 - b) update the weight with $w_{n+1} = w_n b_x$
 - c) update the weight with $w_{n+1} \rightarrow w_{n+1} s_{x_{n+1},x_n}$.
- (10.1)

10.2 An example on the continuum

It is convenient to consider the following toy model:

$$H = -1/2\partial_x^2 + V(x) \tag{10.2}$$

of a particle in a segment $0 \leq x \leq L$, under a potential $V(x)$ which is symmetric under the reflection around the center $x_c = L/2$, namely $P_+V = V$, where P_+ (P_-) is the projection operation over this symmetric subspace for even (odd) wavefunctions. The operator P_{\pm} acts on a wavefunction $\phi(x)$ in the simple way:

$$P_{\pm}\phi = 1/2(\phi(x) \pm \phi(L-x)) \tag{10.3}$$

and clearly commutes with the hamiltonian. In the following we will define an algorithm that will allow to sample the lowest excitation ψ_0 with odd reflection symmetry ($\psi_0(L-x) = -\psi_0(x)$) around the center.

This toy-model is a very simplified version of the many electron problem calculation. The ground state of the many body hamiltonian is always bosonic if we do not take into account the antisymmetry of the fermionic wavefunction. The projection P in this case is just the projection over this antisymmetric subspace and, just like in the toy model problem, the physical eigenvalue of the many-electron system is the one corresponding to the lowest energy antisymmetric subspace. In the following all the properties derived for the toy model will be also valid for the more complicated many-fermion realistic model, upon the identification of P as the projector onto the fully antisymmetric fermionic subspace.

The antisymmetry under permutations just like the reflection over the center in the toy model, implies that the wavefunction is no longer positive, and there should exist regions of both positive and negative signs.

In the continuous case we cannot apply the power method to filter the ground state wavefunction because of the presence of unbounded positive eigenvalues. In this case, the Green function has to be written in an exponential form:

$$G(x', x) = \langle x' | e^{-H\tau} | x \rangle \simeq \frac{1}{\sqrt{2\pi\tau}} e^{-\frac{1}{2\tau}(x'-x)^2} e^{-\tau V(x)} \quad (10.4)$$

where in the latter expression we have neglected terms of order τ as τ is assumed to be small. The first term can be taught as a diffusion process, and the second is the responsible of the branching scheme. An algorithm implementing the above iteration is given in (8.5), where $b_x = e^{-\tau V(x)}$ and $p_{x',x} = \frac{1}{\sqrt{2\pi\tau}} e^{-\frac{1}{2\tau}(x'-x)^2}$ defines the diffusion process as the normalization condition:

$$\sum_{x'} p_{x',x}$$

is verified (summation replaced by integral is understood). This term can be implemented by the Markov iteration:

$$x_{n+1} = x_n + \sqrt{\tau}\eta_n \quad (10.5)$$

where η_n is a random number distributed according to the Gaussian probability distribution.

Similarly to the power method, after applying several times the Green function multiplication:

$$\psi_{n+1}(x') = \sum_x G(x', x)\psi_n(x) \quad (10.6)$$

we obtain the lowest energy eigenstate non orthogonal to the initial one $\psi_0(x) = \psi_g(x)$, that can have a definite symmetry under reflection (or permutation in the many-body case).

Consider now the simpler case $V = 0$. We know exactly the lowest state of the model with odd reflection:

$$\phi_0(x) = \sqrt{2/L} \sin(2\pi x/L) \quad (10.7)$$

with energy

$$E_0 = 1/2\left(\frac{2\pi}{L}\right)^2 \quad (10.8)$$

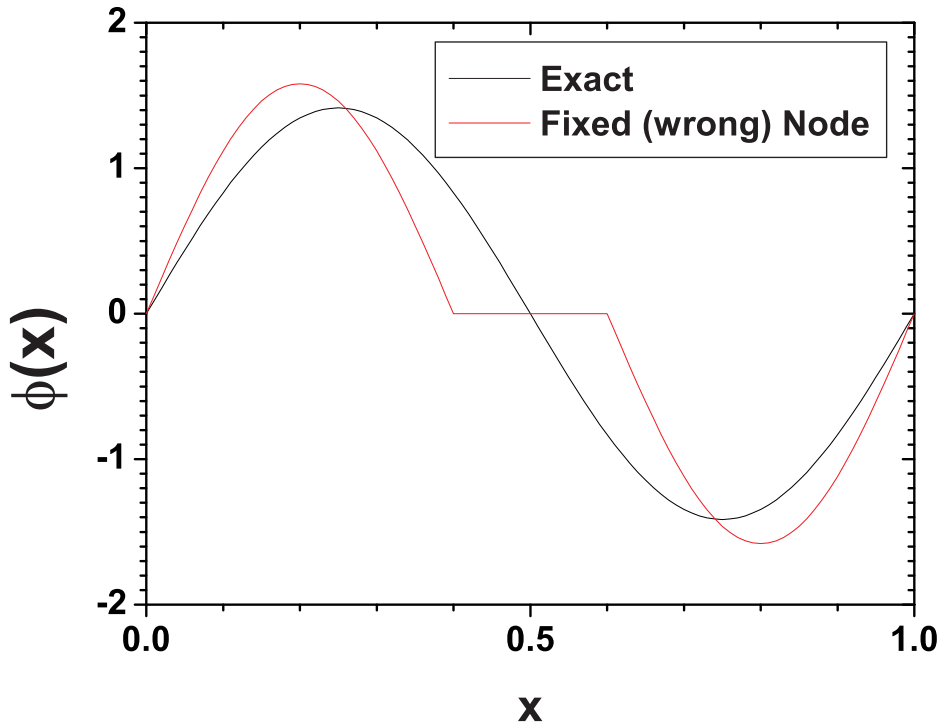


Figure 10.1: Comparison of the exact first excited state for the toy model considered in the text with $L = 1$ and $V = 0$, with the Fixed node approximate excited state with a wrong node located at $l = 0.4$ ($l = L/2 = 0.5$ being the exact node in this case).

The iteration (8.5) cannot be applied in this case as the initial wavefunction cannot have a meaning of probability. In order to solve this problem, we consider the restricted space $\bar{\mathcal{H}}$ of wavefunctions that vanish outside a given interval (see Fig.10.1)

$$0 < x \leq l$$

After acting with a projector P_- on such a wavefunction we obtain a well defined odd reflection symmetry state that can be used as a variational wavefunction of H :

$$\phi_P(x) = P_- \phi \quad (10.9)$$

as indicated in Fig.(10.1) by the red curve.

It is simple to convince that this extended wavefunction $\phi_P(x)$ has the same energy expectation

value of the wavefunction $\phi(x)$ restricted in the nodal pocket because simply:

$$E_{FN} = \frac{\int_0^L dx \phi_P(x) (-1/2\partial_x^2) \phi_P(x)}{\int_0^L \phi_P(x)^2} = \frac{\int_0^l dx \phi(x) (-1/2\partial_x^2) \phi(x)}{\int_0^l dx \phi(x)^2} \quad (10.10)$$

It is important to emphasize that this equality holds despite the fact the wave function has a discontinuous first derivative at the wrong nodal point (see Fig.10.1), yielding:

$$(-1/2\partial_x^2)\phi_P(x) = -1/4\partial_x^2[\phi(x) - \phi(L-x)] + 1/4[\delta(x-l) - \delta(L-l-x)]\phi'(l) \quad (10.11)$$

where $\phi'(l) = \lim_{x \rightarrow l | x < l} \partial_x \phi(x)$. In fact the singular contribution coming from this δ function does not play any role in the integrals appearing in Eq.(10.10) because the wave function $\phi_P(x) = 0$ at the nodal point $x = l$.

Given the equality (10.10) valid for any function $\phi(x)$ defined in the nodal pocket $0 < x \leq l \leq L/2$ it is clear that the lowest possible energy can be obtained by optimizing the wave function just in the nodal pocket, which turns in a bosonic nodeless problem, suitable for the Green Function Monte Carlo. In this simple case we can also provide the best $\phi(x)$ analytically because is the standing wave satisfying $\phi(0) = \phi(l) = 0$:

$$\phi(x) = \sqrt{2/l} \sin(\pi x/l) \quad (10.12)$$

and is displayed by the red curve in Fig.(10.1). The corresponding variational energy E_{FN} can be immediately computed as:

$$E_{FN} = 1/2(\pi/l)^2 > E_0 \quad (10.13)$$

With this simple example it is possible to emphasize the most important properties of the Fixed node approximation:

- the method is clearly variational as the projected wavefunction $\phi_P = P_- \phi$ has exactly the energy E_{FN} obtained with a bosonic ground state calculation in the nodal region $0 < x \leq l$.
- In this simple example the error in the node position is simply given by $\epsilon = L/2 - l$. It is important to observe that the corresponding error in the Fixed node energy is not quadratic in this error but *linear*, namely from Eqs. (10.13,10.8) we obtain: $E_{FN} = E_0(1 + 4\epsilon/L + O(\epsilon^2))$. This property is the main reason why the energy is very sensitive to the accuracy of the nodes of a variational wave function. Therefore it is reasonable to expect accurate nodes by using the variational approach. On the contrary, low energy effects are expected to be determined mainly by the amplitude of the wave function. The diffusion Monte Carlo applied to a good variational wave function optimized with the variational approach, appears so far a rather accurate method for strongly correlated fermion systems.
- Though the energy corresponding to the projected wavefunction $\phi_P(x)$ and the one defined in the nodal pocket $\phi(x)$ coincide due to Eq.(10.10), the same does not hold for the variance (5.12) calculated for $\phi_P(x)$ and $\phi(x)$. It is simple to show that the variance of the Fixed

node ground state (10.12) is zero in the nodal pocket, but when the physical projected wave function is considered in the whole space $0 \leq x \leq L$ an infinite contribution to the variance comes from the δ functions in the RHS of Eq.(10.11). In this case in fact the infinite terms $\int \delta(x-l)^2 + \delta(L-x-l)^2 - 2\delta(x-l)\delta(L-x-l)$ cancels only *when the node position is exact* $l = L/2$. As expected the variance calculated correctly in the total space can be zero *only if the wave function $\phi_P(x)$ is just an exact eigenstate of the hamiltonian H .*

10.3 Effective hamiltonian approach for the lattice fixed node

In the lattice case, that should be more simple, the fixed node approximation was introduced much later, because in a lattice the hamiltonian can have non zero matrix elements that connect two regions of opposite signs in the guiding function $\psi_g(x)$. In this case the basic equality (10.10), which defines the fixed node method in the continuous case, no longer applies. In order to overcome this difficulty one can generalize the Fixed node to the lattice case, considering that the fixed node method can be thought as a systematic improvement of a variational guess, that is defined by an effective Hamiltonian:

$$H^{eff} = -\frac{\Delta}{2} + \frac{\Delta\psi_g}{2\psi_g}(x) \quad (10.14)$$

in the nodal pocket region where $\psi_g(x)$ does not change sign. Here we use shorthand notations for the N -electron laplacian $\Delta = \sum_{i=1}^N \Delta_i$, and x , as usual, denotes the N -electron configurations defined by the N positions $\vec{r}_i, i = 1, \dots, N$ and their spins. A simple inspection leads to the following important properties, the first one is that:

$$H^{eff}\psi_g = 0 \quad (10.15)$$

which means that ψ_g is an exact eigenstate of H^{eff} and actually is the ground state, since in the nodal pocket where the effective Hamiltonian is defined, $\psi_g(x)$ represents just the true bosonic ground state. The second property is to realize that the fixed node approximation, corresponds to define a better Hamiltonian H^{FN} , defined in the nodal pocket, by realizing that in this region of space:

$$H^{FN} = H = H^{eff} + e_L(x) \quad (10.16)$$

where $e_L(x) = \frac{\langle \psi_g | H | x \rangle}{\langle \psi_g | x \rangle} = -\frac{1}{2} \frac{\Delta\psi_g}{\psi_g} + V(x)$, where $V(x)$ defines formally the Coulomb interactions acting on a given configuration x .

Can we do a similar thing in a lattice model?

Given any Hamiltonian and *any* guiding function $\psi_g(x)$ defined on a lattice, it is possible to define an effective Hamiltonian H^{eff} with the same property of Eq.(10.15).

$$H_\gamma^{eff} = \begin{cases} H_{x,x} + (1 + \gamma)\mathcal{V}_{sf}(x) - e_L(x) & \text{for } x' = x \\ H_{x',x} & \text{if } x' \neq x \text{ and } s_{x',x} < 0 \\ -\gamma H_{x',x} & \text{if } x' \neq x \text{ and } s_{x',x} > 0 \end{cases} \quad (10.17)$$

where:

$$s_{x',x} = \begin{cases} \psi_g(x')H_{x',x}\psi_g(x) & \text{if } x' \neq x \\ 0 & \text{if } x' = x \end{cases} \quad (10.18)$$

With the above definitions that may appear quite cumbersome, but indeed are quite simple and general, one can easily prove that Eq.(10.15) is indeed satisfied by definition. With a little inspection we can easily realize that the Hamiltonian H^{eff} is non frustrated, as a unitary transformation

$$|x\rangle \rightarrow \text{Sgn}\psi_g(x)|x\rangle \quad (10.19)$$

transforms the Hamiltonian into a "bosonic one" with all negative off diagonal matrix elements, implying that the ground state $|\psi_g(x)\rangle$ is unique and the lowest energy is zero.

Now, following the fixed node scheme, we can improve the above effective Hamiltonian for any value of γ , by adding to the diagonal part a term proportional to the local energy, namely:

$$H_\gamma^{FN} = H^{eff} + \delta_{x',x}e_L(x) \quad (10.20)$$

This hamiltonian will also satisfy the Perron-Frobenius property defined before and the sign of its ground state will be the same as the one defined by $\psi_g(x)$. With the above definition it also follows that

$$\frac{\langle \psi_g | H_\gamma^{FN} | \psi_g \rangle}{\langle \psi_g | \psi_g \rangle} = \frac{\langle \psi_g | H_\gamma | \psi_g \rangle}{\langle \psi_g | \psi_g \rangle} = E_{VMC} \quad (10.21)$$

Therefore the ground state energy E_γ^{FN} of the hamiltonian H_γ^{FN} is certainly below or at most equal to the variational energy E_{VMC} .

We have now to prove that E_γ^{FN} is a variational upper bound of the true ground state energy E_0 of H . To this purpose we note that, by using its definition (10.20) and Eq.(10.17)

$$H_\gamma^{FN} = H + (1 + \gamma)O \quad (10.22)$$

where O is a positive definite operator defined in terms of a guiding function $\psi_g(x)$, that does not vanish in any configuration x of a subspace \mathcal{S} of the total Hilbert space \mathcal{H} (typically $\mathcal{S} = \mathcal{H}$ otherwise the guiding function provides a restriction of the Hilbert space, where the variational upper bound holds a fortiori) where the Markov process is ergodic. More specifically the operator O is defined in the following way:

$$O_{x',x} = \begin{cases} -H_{x',x} & \text{if } s_{x',x} > 0 \\ \sum_{x'} s_{x',x} / \psi_g(x)^2 & \text{if } x' = x \end{cases} \quad (10.23)$$

Now if O is semipositive definite, as it is shown in the Appendix (C), we can consider the ground state ψ_γ^{FN} (assumed here normalized) as a variational state of the true Hamiltonian H , and we have:

$$E_0 \leq \langle \psi_\gamma^{FN} | H | \psi_\gamma^{FN} \rangle = \langle \psi_\gamma^{FN} | H_\gamma^{FN} - (1 + \gamma)O | \psi_\gamma^{FN} \rangle \leq E_\gamma^{FN} \quad (10.24)$$

This concludes the proof that E_γ^{FN} improves the variational estimate in the sense that the state ψ_γ^{FN} has an expectation value of the energy lower than the variational estimate E_{VMC} , and that $E_\gamma^{FN} \geq E_0$. An important remark is that in the lattice case, not necessarily E_γ^{FN} is the lowest energy compatible with the nodes of the guiding function, as indeed, numerical calculations shows that E_γ^{FN} has a weak dependence on the parameter γ . This is also easily understood because E_γ^{FN} at least on a finite system has to be an analytic function of γ . We can formally continue this function to negative value of γ where for $\gamma = -1$, by means of Eq.(10.22) we have to obtain the exact ground state energy. Hence, whenever E^{FN} is not exact there should be some dependence on γ .

We can establish also another important property of this effective Hamiltonian approach. Indeed, by using the Hellmann-Feynman theorem and Eq.(10.22), we have:

$$\langle \psi_\gamma^{FN} | O | \psi_\gamma^{FN} \rangle = \frac{dE_\gamma^{FN}}{d\gamma} \quad (10.25)$$

Therefore the expectation value of the energy E_γ^{FNA} of the exact hamiltonian on the fixed node ground state $|\psi_\gamma^{FN}\rangle$ can be numerically evaluated by using again the simple relation (10.22):

$$E_\gamma^{FNA} = E_\gamma^{FN} - (1 + \gamma) \frac{dE_\gamma^{FN}}{d\gamma} \quad (10.26)$$

E_γ^{FNA} further improves the variational estimate given by E_γ^{FN} , and shows also that the fixed node ground state is a variational state better than the original VMC ansatz given here by ψ_g . As a last remark we can easily show that E_γ^{FNA} is minimum for $\gamma = 0$ because:

$$\frac{dE_\gamma^{FNA}}{d\gamma} = -(1 + \gamma) \frac{d^2 E_\gamma^{FN}}{d\gamma^2} > 0 \quad (10.27)$$

where the latter inequality comes from the convexity property (see App.D) of the ground state energy (E_γ^{FN}) of an Hamiltonian (H_γ^{FN}) depending linearly upon a parameter (γ).

Chapter 11

Auxiliary field quantum Monte Carlo

One of the most important advantages of the Hartree-Fock or more generally of mean field theories is that a complete and efficient numerical solution is possible in terms of simple linear algebra operations and at most the diagonalization of small matrices. The main task of the auxiliary field technique is to reduce the many-body problem to the solution of several mean-field Hartree-Fock calculations. This is generally possible by using the stochastic method, and therefore the statistical errors are under control provided the sign problem do not appear during the mentioned transformation, that is indeed possible in many interesting cases. Moreover, as we will see in the following, when the sign problem appears with this technique, it is milder than the conventional case, obtained in a configuration space of distinguishable particles. In fact the sign problem instability is not related to the bosonic-fermionic instability, because in this approach explicit antisymmetric Slater determinant are sampled.

11.1 Trotter approximation

We define an effective Hamiltonian \bar{H} , implicitly depending on $\Delta\tau$, by the following relation:

$$\exp(-\Delta\tau\bar{H}) = \exp(-\frac{\Delta\tau}{2}K) \exp(-\Delta\tau V) \exp(-\frac{\Delta\tau}{2}K) \quad (11.1)$$

Since both the LHS and the RSH of the above equation are Hermitian and positive definite operators the solution of the above equation exists and can be made explicit by using perturbation theory in small $\Delta\tau$. In this limit we find that:

$$\begin{aligned} \bar{H} &= H + \Delta\tau^2 O \\ O &= \frac{1}{12} [[K, V], V] + \frac{1}{24} [[K, V], K] \end{aligned} \quad (11.2)$$

The kinetic energy K and the potential energy V are extensive operators, namely with a number of terms localized around a given site and proportional to the number of sites, namely can be written as:

$$\begin{aligned} V &= \sum_i V_i \quad V_i = U n_{i,\uparrow} n_{i,\downarrow} \\ K &= \sum_i K_i \quad K_i = -t/2 \sum_{\tau,\sigma} (c_{i+\tau,\sigma}^\dagger c_{i,\sigma} + \text{h.c.}) \end{aligned}$$

The operator O , at first sight, appears to contain a number of terms proportional to the cube of the number of sites, because by expanding the commutators we get terms such as KVK , a product of three extensive operators. However a closer inspection, by evaluating for instance the commutator between K and V , leads us to conclude that the commutator of two extensive operators is again an extensive operator, and therefore the operator O defined in Eq.(11.2) is a perfectly consistent extensive operator. All properties therefore that we can compute at fixed $\Delta\tau$ refers to the ones of an effective Hamiltonian \tilde{H} , that differs by the correct one by means of a small extensive perturbation. This clearly suggests that, in this case, the error associated to the Trotter decomposition is perfectly under control as it can be reduced systematically by decreasing $\Delta\tau^2$. Moreover, for a given accuracy on thermodynamic quantities (e.g. the energy per site), one does not need to decrease the Trotter time $\Delta\tau$ as one increases the system size, i.e. the error associated to the Trotter approximation is size consistent.

11.2 Auxiliary field transformation

The generalization of the continuous auxiliary field transformation:

$$\int_{-\infty}^{\infty} \frac{d\sigma}{\sqrt{2\pi}} \exp\left(-\frac{1}{2}\sigma^2\right) \exp \lambda \sigma (n_\uparrow - n_\downarrow) = \exp\left(\frac{g}{2}(n_\uparrow - n_\downarrow)^2\right) \quad (11.3)$$

with $lambda^2 = g$ is given by the much more efficient expression:

$$\sum_{\sigma=\pm 1} \frac{1}{2} \exp \lambda \sigma (n_\uparrow - n_\downarrow) = \exp\left(\frac{g}{2}(n_\uparrow - n_\downarrow)^2\right) \quad (11.4)$$

that is valid upon an appropriate change of $lambda$ obtained by solving the simple equation $\cosh \lambda = \exp(g/2)$. This expression can be easily proved by Taylor expanding $\exp(\lambda n_\uparrow)$ and noting that all powers different from zero contribute with $\lambda^k/k!$, because $n_\uparrow^k = n_\uparrow$ for $k \geq 1$. Therefore:

$$\exp(\lambda n_\uparrow) = 1 + (\exp \lambda - 1)n_\uparrow \quad (11.5)$$

With similar algebra it can be readily shown that:

$$\begin{aligned} \exp(-g/2(n_\uparrow - n_\downarrow)^2) &= 1 + (\exp(g/2) - 1)(n_\uparrow + n_\downarrow) + 2(1 - \exp(g/2))n_\uparrow n_\downarrow \\ \sum_{\sigma=\pm 1} \frac{1}{2} \exp \lambda \sigma (n_\uparrow - n_\downarrow) &= 1 + (\cosh \lambda - 1)(n_\uparrow + n_\downarrow) + 2(1 - \cosh \lambda)n_\uparrow n_\downarrow, \end{aligned}$$

namely that Eq.(11.4) is indeed verified.

The above transformation is very useful because simplifies a very complicated many-body operator $\exp\left(\frac{g}{2}(n_\uparrow - n_\downarrow)^2\right)$, namely containing in the exponent the square of a simple one-body operator $n_\uparrow - n_\downarrow$, i.e. quadratic when expressed in terms of c and c^\dagger . By means of the so called Hubbard-Stratonovich transformation (HST) it is written as a superposition of simple one body propagation $\exp\lambda\sigma(n_\uparrow - n_\downarrow)$, depending upon an auxiliary field σ .

In particular the many-body propagator can be recasted, using again that $n_\sigma^2 = n_\sigma$, in a form suitable for HST:

$$\exp(-\Delta\tau V) = \exp\left(-\frac{\Delta\tau}{2}N\right) \prod_i \exp\left(U\Delta\tau(n_{i\uparrow} - n_{i\downarrow})^2\right) \quad (11.6)$$

where N is the total number operator. In this way, by introducing an independent Ising field $\sigma_i = \pm 1$ for each site, we can write:

$$\exp(-\Delta\tau V) = \sum_{\sigma_i = \pm 1} \exp\left(\sum_i \lambda\sigma_i(n_{i\uparrow} - n_{i\downarrow})\right) \quad (11.7)$$

apart for an irrelevant constant $C = \exp(-\frac{\Delta\tau}{2}N)/2^L$, because we assume in the following that the total number of particles N is fixed and L is the number of sites.

Finally we have to remark that there are several ways to recast the many body term \hat{V} in a form suitable for HST decomposition, for instance a famous one starts from the consideration that \hat{V} can be also written as a sum of local density operators- $n_i = \sum_\sigma n_{i\sigma}$ - squared

$$\hat{V} = \frac{U}{2} \sum_i n_i^2 - \frac{UN}{2} \quad (11.8)$$

A transformation similar to Eq.(11.3) is possible, by using an imaginary constant $\lambda \rightarrow i\lambda$, because in this case the propagator $\exp(-\hat{V})$ contains squared one body operators with *negative* prefactors. This introduces some phase problem in quantum Monte Carlo, that however disappears at half filling, or can be afforded by using some approximation, namely the Constrained Path Quantum Monte Carlo (CPQMC), introduced long time ago by S. Zhang and collaborators. To our knowledge no systematic study has been done, aimed to identify the most efficient HST for a given model, namely the one that minimizes the statistical errors for a given computational time. In our experience the real HST introduced above is the most efficient for the Hubbard model at least away from the half filling conditions. Instead for electronic structure applications, though the long range Coulomb interaction can be formally recasted as a sum of squared one body operators with *negative* prefactors, a complex HST where the field σ is coupled to the density appears unavoidable for affordable computations, because the real HST introduces too large fluctuations at large momenta.

11.3 A simple path integral technique

Now we are in the position to compute exactly all properties of the ground state of the effective Hamiltonian \bar{H} , that can be set arbitrarily close to the exact Hubbard Hamiltonian, with an error

vanishing as $\Delta\tau^2$.

To this purpose we consider the quantity:

$$Z = \langle \psi_t | [\exp(-\bar{H}\Delta\tau)]^{(2T)} | \psi_t \rangle \quad (11.9)$$

where $2T$ is the total number of times the propagator is applied to a trial function $|\psi_t\rangle$. For $T \rightarrow \infty$ the many-body state

$$|\psi_T\rangle = [\exp(-\Delta\tau\bar{H})]^T |\psi_t\rangle = \exp(-T\Delta\tau\bar{H})|\psi_t\rangle$$

converges obviously to the exact ground state of \bar{H} and Z can be useful to compute correlation functions O over the ground state $|\bar{\psi}_0\rangle$ of \bar{H} :

$$\langle \bar{\psi}_0 | O | \bar{\psi}_0 \rangle = \lim_{T \rightarrow \infty} \frac{\langle \psi_T | O | \psi_T \rangle}{Z} \quad (11.10)$$

We then replace both in Z and in the numerator of the above equation, the auxiliary field transformation (11.7) for each Trotter slice, so that the field $\sigma_i^j = \pm 1$ acquires also a discrete time index $1 \leq j \leq 2T$, thus for instance the quantity Z is expressed as an Ising partition function over this discrete field:

$$\begin{aligned} Z &= \sum_{\sigma_i^j = \pm 1} \langle \psi_t | \exp(-\frac{\Delta\tau}{2}K) \exp[\lambda \sum_i \sigma_i^{2T} (n_{i\uparrow} - n_{i\downarrow})] \exp(-\Delta\tau K) \exp[\lambda \sum_i \sigma_i^{2T-1} (n_{i\uparrow} - n_{i\downarrow})] \\ &\quad \cdots \exp(-\Delta\tau K) \exp[\lambda \sum_i \sigma_i^1 (n_{i\uparrow} - n_{i\downarrow})] \exp(-\frac{\Delta\tau}{2}K) | \psi_t \rangle \\ &= \sum_{\sigma_i^j = \pm 1} \langle \psi_t | U_\sigma(2T, 0) | \psi_t \rangle \end{aligned} \quad (11.11)$$

where we have introduced the compact definition of the one body propagator $U_\sigma(2T, 1)$, acting from the first time slice to the last one, from left to right. This one body propagator has the property that, if applied to a Slater determinant, transforms it to a Slater determinant, and therefore if the trial function ψ_T is chosen as a Slater determinant, for a fixed field configuration the quantity $\langle \psi_T | U_\sigma(2T, 0) | \psi_T \rangle$ can be numerically evaluated.

This is the basis of the auxiliary field transformation, as, using the same fields also the numerator in expression (11.10) can be computed and we obtain:

$$\frac{\langle \psi_T | O | \psi_T \rangle}{\langle \psi_T | \psi_T \rangle} = \frac{\sum_{\sigma_i^j = \pm 1} \langle \psi_t | U_\sigma(2T, T) O U_\sigma(T, 0) | \psi_t \rangle}{\sum_{\sigma_i^j = \pm 1} \langle \psi_t | U_\sigma(2T, 0) | \psi_t \rangle} \quad (11.12)$$

The Monte Carlo can be done by using a positive weight dependent on the fields σ_i^j given by:

$$W(\sigma_i^j) = |\langle \psi_t | U_\sigma(2T, 0) | \psi_t \rangle| \quad (11.13)$$

we indicate also with $S(\sigma_i^j)$ the sign of $\langle \psi_t | U_\sigma(2T, 0) | \psi_t \rangle$. In order to compute any correlation function it is enough to compute the average of two random variables over configurations $\{\sigma_i^j\}$ distributed according to $W(\sigma_i^j)$, namely:

$$\frac{\langle \psi_T | O | \psi_T \rangle}{\langle \psi_T | \psi_T \rangle} = \frac{\langle \frac{\langle \psi_t | U_\sigma(2T, T) O U_\sigma(T, 0) | \psi_t \rangle}{W(\sigma_i^j)} \rangle_W}{\langle S(\sigma_i^j) \rangle_W} \quad (11.14)$$

where the symbol $\langle A \rangle_W$ indicates the statistical average of the random variable A over the distribution defined by the weight W . It is important to emphasize that the algorithm is in principle defined here, because all quantities (random variables and weights), can be computed numerically in polynomial time once the fields σ_i^j are given: ψ_T is a Slater determinant and can be characterized by an orbital matrix $N \times 2L$, ψ_{ij} .

11.4 Some hint for an efficient and stable code

11.4.1 Stable imaginary time propagation of a Slater Determinant

The method described in the previous sections is essentially defined for infinite precision arithmetic. Unfortunately real computations are affected by truncation errors, namely the basic limitation is that summing two real numbers differing by several order of magnitudes leads to loss of information, namely:

$$1 + \epsilon = 1 \quad (11.15)$$

if $\epsilon \leq \sim 10^{-15}$ in double precision arithmetic.

This limitation of finite precision arithmetic leads to an instability problem, when trying to apply a one-body propagator $U(\tau, 0)$ to a Slater determinant for large imaginary time τ . Consider for instance $U(\tau, 0) = \exp(-H_0\tau)$, where H_0 is a one body hamiltonian with single particle eigenvalues E_i -assumed in ascending order, E_1 being the lowest one and E_N representing the finite size Fermi energy- and corresponding eigenvectors $\phi_i(r, \sigma)$. As we have seen in the previous chapters the propagation of a Slater determinant of the type:

$$|SD\rangle = \left(\prod_{j=1}^N \sum_{r,\sigma} \psi_j(r, \sigma) c_{r,\sigma}^\dagger \right) |0\rangle \quad (11.16)$$

leads to another Slater determinant $|SD(\tau)\rangle = \exp(-H_0\tau)|SD\rangle$, which is obtained by propagating each orbital $\psi_j \rightarrow \psi_j(\tau)$ independently:

$$\psi_j(\tau) = \sum_i \exp(-\tau E_i) \langle \phi_i | \psi_j \rangle \phi_i \quad (11.17)$$

which means that for large enough time τ , most of the eigenvector components of ψ_i will disappear for the limitation given in Eq.(11.15). More precisely, whenever $\exp[-(E_N - E_1)\tau] \leq \sim 10^{-15}$, there will be only $N - 1$ linearly independent orbitals within numerical accuracy, leading to an ill defined Slater determinant. In order to overcome this problem a simple solution can be found. One can divide the large time propagation in several much shorter ones, with propagation time $\tilde{\tau} = \tau/p$ where p is chosen in a way that:

$$(E_N - E_1)\tau/p \ll \ln 10^{15} \quad (11.18)$$

Notice also that the condition given in Eq.(11.18) is also size consistent (as the Trotter approximation), because for instance in a lattice model the band width of the single particle eigenvalues is finite in the thermodynamic limit (e.g. $4Dt$ for the Hubbard model where D is the dimensionality)

After each short propagation $|SD(t + \bar{\tau})\rangle = \exp(-H_0\bar{\tau})|SD(t)\rangle$ the propagated orbitals in Eq.(11.17) can be orthogonalized without losing information of the Slater determinant. One can use indeed that any linear transformation:

$$\psi_i \rightarrow \sum_k U_{ik} \psi_k \quad (11.19)$$

leaves unchanged the Slater determinant apart for an overall constant equal to $\det U$, which can be saved and updated during the total propagation obtained after applying p times an orthogonalization between the orbitals. The Gram-Schmidt orthogonalization is the most simple to code for this purpose, but we have found that a more efficient one is obtained by applying the Cholesky decomposition. In this technique the $N \times N$ overlap matrix is considered:

$$S_{i,j} = \langle \psi_i | \psi_j \rangle \quad (11.20)$$

Since it is obviously positive definite (for N independent orbitals), it can be decomposed as $S = LL^\dagger$, where L is an upper triangular matrix. Then the new orbitals:

$$\psi' = L^{-1} \psi \quad (11.21)$$

will be obviously orthogonal each other, and will describe the same determinant apart for an overall constant equal to $1/\det L$, which is rather simple to compute as L is an upper triangular matrix and its determinant is simply the product of its diagonal terms. After the orthogonalization the new orbitals start to be again orthonormal and another stable propagation can be done without facing any instability problems, until for large p we obtain the exact N lowest eigenstates of the one body Hamiltonian H_0 .

11.4.2 Sequential updates

In order to speed up each Metropolis update, it is important to propose new values of the fields σ_{ij} for all sites in a given time slice $j = 1, \dots, 2T$. On each time slice j we have two Slater determinants the left one $\langle \psi_L^j |$ and the right one $|\psi_R^j\rangle$ that do not change if we change the site index i , namely:

$$\begin{aligned} \langle \psi_t | U_\sigma(2T, 0) | \psi_t \rangle &= \langle \psi_L^j | \exp \left(\lambda \sum_i \sigma_{i,j} (n_{i\uparrow} - n_{i\downarrow}) \right) | \psi_R^j \rangle \\ &= \langle \psi_L^j | \exp V_j | \psi_R^j \rangle. \end{aligned} \quad (11.22)$$

where $|\psi_R^j\rangle = \exp(-\frac{\Delta\tau}{2}K)U(j-1, 1)|\psi_t\rangle$ and $\langle \psi_L^j| = \langle \psi_t|U(2T, j+1)\exp(-\frac{\Delta\tau}{2}K)$.

A flip of the field on a given site k , $\sigma_{kj} \rightarrow -\sigma_{kj}$ can be employed by first computing the generalized Green's function between the left and right states, and including also the $\exp V_j$ term:

$$g_{r'\sigma', r\sigma} = \frac{\langle \psi_L^j | c_{r',\sigma'}^\dagger c_{r,\sigma} \exp V_j | \psi_R^j \rangle}{\langle \psi_L^j | \exp V_j | \psi_R^j \rangle}. \quad (11.23)$$

We assume for generality that the above Green function can have also off-diagonal spin components $\sigma \neq \sigma'$, that allows the implementation of a rather general wave function (e.g. also the BCS wave

function. In this case the anomalous averages can be replaced, after a simple particle-hole on the spin-down electrons, with the off-diagonal spin elements).

This quantity can be evaluated by scratch at the beginning of the loop over the sites and the time slices ($j = 2T$), by using standard linear algebra operations:

$$g_{r'\sigma',r\sigma} = [\psi_L^j S^{-1} \bar{\psi}_R^{Tj}] \quad (11.24)$$

where the column (row) index in ψ_L^j and ψ_R^j is the orbital index (site and spin σ) in the matrix products defined in the RHS of the above equation, T is the symbol for the transpose of a matrix, and $\bar{\psi}_R = \exp V_j \psi_R$, $S = \psi_R^T \psi_L$ is the overlap matrix between the right and the left determinants. The recomputation by scratch of the Green's function is required for stability reasons (see later) and it is therefore convenient to perform it at selected time slices, e.g. $j = k \times p$, where p is a sufficiently small number (in the Hubbard case $p \times \Delta\tau t \leq 1/2$ is usually enough).

After any computation by scratch of the Green's function one can employ much faster updates for computing the Green's function itself and all the quantity necessary to the Markov chain.. For instance the ratio of the new and old determinant corresponding to the change of one spin can be written as (by applying the Wick's theorem):

$$\begin{aligned} \frac{\langle \psi_t | U'_\sigma(2T, 0) | \psi_t \rangle}{\langle \psi_t | U_\sigma(2T, 0) | \psi_t \rangle} &= \frac{\langle \psi_L^j | \exp(\mp 2\sigma_{kj}(n_\uparrow - n_\downarrow)) | \bar{\psi}_R^j \rangle}{\langle \psi_L^j | \bar{\psi}_R^j \rangle} \\ &= (1 + \lambda_\uparrow g_{k\uparrow, k\uparrow})(1 + \lambda_\downarrow g_{k\downarrow, k\downarrow}) - \lambda_\uparrow \lambda_\downarrow g_{k\uparrow, k\downarrow} g_{k\downarrow, k\uparrow} \end{aligned} \quad (11.25)$$

where $\lambda_{\pm\frac{1}{2}} = \exp(\mp 2\lambda\sigma_{kj}) - 1$. Once accepted the move the Green's function can be updated with similar algebra (not shown), basically using again the Wicks' theorem, with a computational effort that scales at most as the square of the number of sites. First one can compute the new Green's function corresponding to the spin-up update $\exp V_j^\uparrow \rightarrow \exp(-2\lambda\sigma_j n_\uparrow) \exp V_j$:

$$g_{r'\sigma',r\sigma}^\uparrow = g_{r'\sigma',r\sigma} + \frac{\lambda_\uparrow}{1 + \lambda_\uparrow g_{k\uparrow, k\uparrow}} g_{r'\sigma',k\uparrow} (\delta_{k,r} \delta_{\sigma,\uparrow} - g_{k\uparrow, r\sigma}) \quad (11.26)$$

then the final one obtained by employing the spin down flip $\exp V_j^\uparrow \rightarrow \exp(2\lambda\sigma_j n_\downarrow) \exp V_j^\uparrow$:

$$g'_{r'\sigma',r\sigma} = g_{r'\sigma',r\sigma}^\uparrow + \frac{\lambda_\downarrow}{1 + \lambda_\downarrow g_{k\downarrow, k\downarrow}^\uparrow} g_{r'\sigma',k\downarrow}^\uparrow (\delta_{k,r} \delta_{\sigma,\downarrow} - g_{k\downarrow, r\sigma}) \quad (11.27)$$

A better and numerically more stable algorithm is obtained by updating directly g' in term of the original g , by substituing g^\uparrow given by Eq.(11.26) in Eq.(11.27).

So far the loop over all the sites at given time slice can be done with $\simeq L^3$ operations. In order to go from one time slice to a neighboring time slice one needs to propagate the left and right Slater Determinants ψ_L^j and ψ_R^j with matrix-matrix operations, amounting again at most to L^3 operations. Also the green function does not need to be computed by scratch but can be propagated backward with analogous matrix matrix operations. Thus a sweep over all the time slices costs at most $L^3 T$ operations. This algorithm is therefore particularly efficient for ground state properties since the $T \rightarrow \infty$ limit can be reached with a cost proportional to the number of time slices only.

11.4.3 Delayed updates

The basic operation in Eqs.(11.26,11.27) is the so called rank-1 update of a generic $2L \times 2L$ matrix:

$$g'_{i,j} = g_{i,j} + a_i b_j \quad (11.28)$$

where L is the number of sites here and henceforth we omit the spin indices for simplicity. This operation can be computationally inefficient, when, for large size, the matrix g is not completely contained in the cache of the processor. A way to overcome this drawback is to delay the update of the matrix g , without losing its information. This can be obtained by storing a set of left and right vectors and the initial full matrix g^0 , from which we begin to delay the updates:

$$g_{i,j} = g_{i,j}^0 + \sum_{l=1}^m a_i^l b_j^l \quad (11.29)$$

as, each time we accept a new configuration, a new pair of vectors a_i^{m+1} and b_j^{m+1} can be easily computed in few operations in term of g^0 , a_i^l , b_j^l $l = 1, \dots, m$, by substituting Eq.(11.29) into the RHS of Eqs.(11.26):

$$a_i^{m+1} = g_{r_i \sigma_i, k \uparrow} \quad (11.30)$$

$$b_j^{m+1} = \frac{\lambda_{\uparrow}}{1 + \lambda_{\uparrow} g_{k \uparrow, k \uparrow}} (\delta_{k, r_j} \delta_{\sigma_j, \uparrow} - g_{k \uparrow, r_j \sigma_j}). \quad (11.31)$$

where here the index j of the vector b runs over the $2L$ possible values of $\{r, \sigma\}$. Notice that the number of operations required to evaluate the above expressions in term of g written in the form (11.29) is $\simeq m(2L + N)$, negligible compared to the full update for $m \ll L$. Analogous and obvious expressions can be found for the spin down update to be done sequentially to the spin up update as shown in Eq.(11.27).

In this way we can find an optimal $m = k_{rep}$, when we can evaluate the full matrix $g_{i,j}$ by a standard matrix matrix multiplication:

$$g = g^0 + AB^T \quad (11.32)$$

where A and B are $2L \times k_{rep}$ and $2L \times k_{rep}$ matrices made of the $l = 1, 2, \dots, k_{rep}$ column vectors a_i^l and b_j^l , respectively. After this standard matrix-matrix product one can continue with a new delayed update with a new $g^0 = g$, by initializing again to zero the integer m in Eq.(11.29). The clear advantage of this is that after a cycle of k_{rep} Markov steps the bulk of the computation is given by the evaluation of the matrix-matrix product in Eq.(11.32), that is much more efficient and is not cache limited compared with the k_{rep} rank-1 original updates of g given in Eq.(??). With the k_{rep} delayed algorithm, once the optimal k_{rep} is found one can improve the speed of the variational Monte Carlo code by about an order of magnitude for large number of electrons (see Fig.11.1)

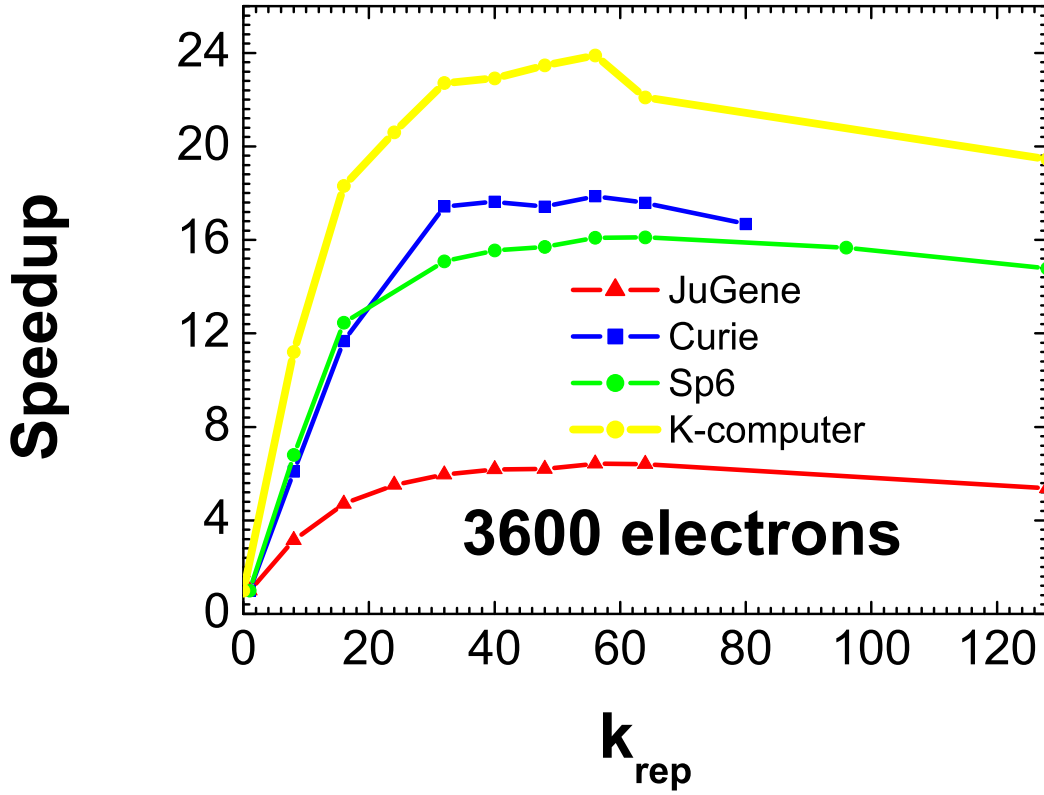


Figure 11.1: Speedup obtained by using delayed updates in quantum Monte Carlo for the auxiliary field method applied to the half-filled Hubbard model for a 3600 sites cluster with 3600 electrons. With the same number of Metropolis updates and calculation of the various correlation functions the algorithm described in this appendix is several times faster compared with the conventional one ($k_{rep} = 1$). Test calculations were done in the JuGene supercomputer in Jülich (maximum speedup 6.4 with $k_{rep} = 56$), in the Curie machine (maximum speedup 17.9 with $k_{rep} = 56$) hosted in Bruyeres-le-Chatel France, in the K-computer hosted in Kobe Japan (maximum speedup 23.9 for $k_{rep} = 56$), and in the sp6-CINECA (maximum speedup 16.1 for $k_{rep} = 64$) in Bologna

11.4.4 No sign problem for attractive interactions, half-filling on bipartite lattices

In order to understand why the auxiliary field technique is not vexed by the so called fermion sign problem in some non trivial cases, it is better to understand first the case of attractive interaction $U < 0$. In this case an auxiliary field transformation is possible with a real field σ coupled only to the total density $\sigma(n_{\uparrow} + n_{\downarrow} - 1)$. The transformation (11.4) can be readily generalized in this case:

$$\sum_{\sigma=\pm 1} \frac{1}{2} \exp \lambda \sigma (n_{\uparrow} + n_{\downarrow} - 1) = \exp \left(\frac{g}{2} (n_{\uparrow} + n_{\downarrow} - 1)^2 \right) \quad (11.33)$$

where $\cosh \lambda = \exp(g/2)$ with $g = |\frac{U\Delta\tau}{2}|$. If we take as a trial function ψ_t one with the same spin-up and spin-down orbitals $\psi_t = \psi_t^\uparrow \otimes \psi_t^\downarrow$, where:

$$|\psi_t^\sigma\rangle = \left[\prod_{i=1}^{N/2} \sum_j \psi_{ij} c_{j,\sigma}^\dagger \right] |0\rangle \quad (11.34)$$

, it is easy to realize that the functional Z introduced previously becomes:

$$Z = \sum_{\sigma_{ij}=\pm 1} |\langle \psi^\uparrow | U^\dagger(2T, 1) | \psi^\uparrow \rangle|^2 \quad (11.35)$$

simply because the total propagation acts in the same way over the spin up and the spin down component of the wave function. One immediately see that in this case the integrand is strictly positive because it is the square of a real number.

This is a general property of the auxiliary field transformation. For attractive spin-independent interaction there is no sign problem when the number of spin down particles is exactly equal to the number of spin down ones.

The half filled case in bipartite lattice can be easily mapped to the attractive case, by the so called particle-hole transformation on the spin down particles:

$$c_{i\downarrow}^\dagger \rightarrow (-1)^i c_{i\downarrow} \quad (11.36)$$

where $(-1)^i = 1$ (-1) if i is a site belonging to the A (B) sublattice of the bipartite lattice. The above transformation changes a positive interaction to a negative one, and, as it can be easily checked, Eq.(11.33) turns exactly to Eq.(11.4). Therefore one concludes that there is no sign problem when the number of spin-down electrons after the particle hole transformation $L - N_\downarrow$ is exactly equal to the number of spin up electrons, namely

$$N_\downarrow + N_\uparrow = L$$

, which is exactly the half-filled condition.

Exercise 11.1 Consider the error of the energy at the middle interval as a function of $\Delta\tau$ as defined in Eq.(11.10):

$$E_0(\Delta\tau) = \lim_{T \rightarrow \infty} \frac{\langle \psi_T | H | \psi_T \rangle}{\langle \psi_T | \psi_T \rangle} = \langle \bar{\psi}_0 | H | \bar{\psi}_0 \rangle \quad (11.37)$$

where $\bar{\psi}_0$ is the ground state of the effective hamiltonian \bar{H} defined by the Trotter approximation in Eq.(11.1). Show that:

1. $\bar{H} = H + V$ where V can be expanded as $V = \Delta\tau^2 O_2 + \Delta\tau^3 O_3 + \dots$ and that therefore perturbation theory in V can be generally applied if i) the ground state of H is non degenerate (or unique) and ii) $\Delta\tau$ is sufficiently small.
2. Using perturbation theory show that:

$$E_0(\Delta\tau) = E_0 + O(\Delta\tau^4) \quad (11.38)$$

and therefore $E(\Delta\tau)$ can be fitted by $E(\Delta\tau) = E_0 + A\Delta\tau^4 + B\Delta\tau^5 + \dots$ (see Fig. 11.2)

3. This extremely fast convergence of the energy as a function of $\Delta\tau$ has not been appreciated so far, because for laziness or irrelevant gains in computational time, it is usually adopted the asymmetric decomposition in the Trotter formula:

$$\exp(-\Delta\tau H) = \exp(-\Delta\tau K) \exp(-\Delta\tau V) + O(\Delta\tau^2) \quad (11.39)$$

Show that in this case the calculation of the ground state energy as a function of the Trotter time amounts to compute:

$$E(\Delta\tau) = \langle \bar{\psi}_0 | \exp(\frac{\Delta\tau}{2} K) H \exp(-\frac{\Delta\tau}{2} K) | \bar{\psi}_0 \rangle \quad (11.40)$$

leading to the much larger $O(\Delta\tau^2)$ Trotter error for the energy.

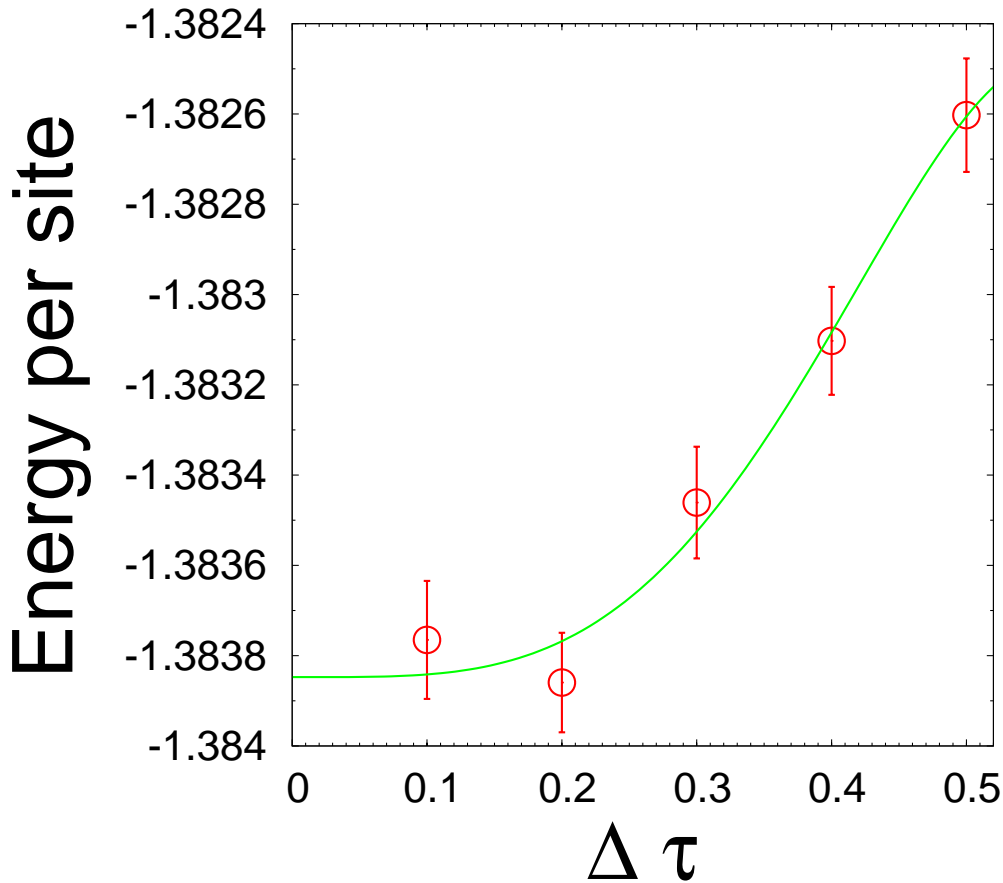


Figure 11.2: Energy per site of the 32 site cluster Hubbard model at $U/t = 1$ as a function of the Trotter time discretization $\Delta\tau$. Antiperiodic boundary conditions are assumed in both the independent directions $\tau_{\pm} = (\pm 4, 4)$ defining the cluster. The number of electrons is fixed at the half-filling condition $N = L = 32$ and the total imaginary time projection $\Delta\tau t T = 3$ large enough to obtain ground state properties for this cluster.

Appendix A

Re-sampling methods

There is a simple motivation to use re-sampling methods. In fact let's consider a set of independent and identically distributed data sample of size n of an unknown probability distribution F :

$$X_1, X_2, \dots, X_n \sim F \quad (\text{A.1})$$

We can compute the sample average $\bar{x} = \sum_{i=1}^n x_i/n$, and then we can estimate the accuracy of \bar{x} using standard deviation:

$$\hat{\sigma} = \sqrt{\frac{1}{n(n-1)} \sum_{i=1}^n (x_i - \bar{x})^2} \quad (\text{A.2})$$

The trouble with this formula is that it does not, in any obvious way, extend to estimators other than \bar{x} . For this reason a generalized version of A.2 is introduced such that it reduces to the usual standard deviation when the chosen estimator is the average.

A.1 Jackknife

Now we briefly describe how is possible to obtain the standard deviation of a generic estimator using the Jackknife method. For simplicity we consider the average estimator. Lets consider the variables:

$$\bar{x}_i = \frac{n\bar{x} - x_i}{n-1} = \frac{1}{n-1} \sum_{j \neq i} x_j, \quad (\text{A.3})$$

where \bar{x} is the sample average. \bar{x}_i is the sample average of the data set deleting the i th point. Then we can define the average of \bar{x}_i :

$$\bar{x}_{(\cdot)} = \sum_{i=1}^n \bar{x}_i/n. \quad (\text{A.4})$$

The jackknife estimate of standard deviation is then defined as:

$$\hat{\sigma}_{JACK} = \sqrt{\frac{n-1}{n} \sum_{i=1}^n (\bar{x}_i - \bar{x}_{(\cdot)})^2} \quad (\text{A.5})$$

The advantage of this formula is that it can be used for any estimator, and it reduces to the usual standard deviation for the mean value estimator.

In this lecture notes we always used the Jackknife re-sampling method. Here we want to show that the connection between the Jackknife and another very used re-sampling method the Bootstrap. Consider a generic estimator $\theta(F)$ evaluated on set of data x_1, x_2, \dots, x_n of the unknown distribution F . Let's take a *re-sampling vector*

$$P^* = (P_1^*, P_2^*, \dots, P_n^*) \quad (\text{A.6})$$

such that

$$\begin{aligned} P_i^* &\geq 0 \\ \sum_{i=1}^n P_i^* &= 1 \end{aligned}$$

in other words, a probability vector. We can re-weight our data sample with the vector P^* and then evaluate the estimator $\hat{\theta}$ on the re-sampled data:

$$\hat{\theta}^* = \hat{\theta}(P^*) \quad (\text{A.7})$$

The difference between Bootstrap and Jackknife is in the choice of this re-sampling probability vector. In the Bootstrap we use:

$$P^0 = \left(\frac{1}{n}, \frac{1}{n}, \dots, \frac{1}{n} \right) \quad (\text{A.8})$$

while in the Jackknife

$$P_{(i)} = \left(\frac{1}{n-1}, \frac{1}{n-1}, \dots, 0, \frac{1}{n-1}, \dots, \frac{1}{n-1} \right). \quad (\text{A.9})$$

The estimate of the standard deviation is then given by eq. A.2, for a good discussion about Jackknife, Bootstrap and other re-sampling methods see Ref. [14].

Appendix B

A practical reconfiguration scheme

In this Appendix we follow the notations of Sec.(8.5.2) to describe an efficient implementation of the reconfiguration process needed to stabilize the GFMC method.

According to the basic algorithm shown in Tab.(8.5.1) the new walker configurations x'_i , at each reconfiguration, are chosen among the old ones x_j , $j = 1 \cdots M$, with probability p_j . In order to do that, in principle M^2 operations are required, as for each walker one has to scan all the M intervals to realize where the random number falls. A more efficient algorithm can be defined by sorting the M random numbers before defining the index function $j(i)$, $i = 1, \cdots M$, denoting the old walker index j corresponding to the i th new walker (see Tab. 8.5.1). Notice that this index table $j(i)$ contains all the information required for the forward walking technique in Eq. (8.33).

After the described process, some of the old configurations (most likely those with large weights, hence large p_j) may appear in many copies, while others (most likely those with small weights, hence small p_j) have disappeared. This happens even if the distribution p_j is roughly uniform $p_j \sim 1/M$, yielding clearly some loss of information in the statistical process. A better way of implementing the reconfiguration process, without losing information and without introducing any source of systematic error, is obtained by the following simple variation of the scheme presented so far, which we simply state without proof. The main idea is that the permutation of the walker index, obviously does not introduce any bias in the average quantity (8.38). and therefore we can assume that the M random numbers \bar{z}_i required for the reconfiguration process, are already sorted in ascending order as:

$$\bar{z}_i = (\xi + (i - 1))/M \quad i = 1 \cdots M, \quad (\text{B.1})$$

where ξ is a pseudo-random number in $(0, 1)$, so that the random numbers \bar{z}_i are correlated among each others. This set of numbers \bar{z}_i , now uniformly distributed in the interval $(0, 1)$ (more precisely, \bar{z}_1 is uniformly distributed in $(0, 1/M]$, \bar{z}_2 in $(1/M, 2/M]$, etc.), is then used to select the new configurations, yielding a more efficient implementation of the desired reconfiguration process. In fact with this choice, that is still unbiased for the wavefunction average (8.38), there is no loss of information if all the walkers have the same weights. Each of them will remain after the

reconfiguration with the same weight. Instead with the previous scheme the probability that a walker interval is never visited by any random number is $(1 - 1/M)^M \simeq e^{-1}$, leading to remove about 37% of the old walker configurations (see Tab.8.5.1). The choice (B.1) is therefore about 37% more efficient than the previous one. It is also obviously fast as it takes only $O(M)$ operations because it is not necessary to sort the random numbers \bar{z}_i in this case, and the index matrix $j(i)$ is naturally ordered $j(i+1) \geq j(i)$.

B.1 An efficient implementation of the single walker algorithm

In this appendix we describe briefly an efficient way to implement the described algorithm.

We assume that a computer is given and that

1. pseudo random number ξ can be generated uniformly distributed in the interval $(0,1]$
2. an essentially infinite memory space is given in the hard disk.
3. a random initial configuration x_n is selected for $n = 0$. The integer counter n associated to the Markov iteration time is initialized to zero ($n = 0$).

The Markov chain of a given number of iterations N is easily simulated in such a computer according to (8.5):

- a) Compute $b_{x_n} = \sum_x G_{x,x_n}$, and the new table $p_{x',x_n} = G_{x',x_n}/b_{x_n}$, for the (few) non zero matrix elements.
- b) generate $x_{n+1} = x'$ with probability p_{x',x_n} .
To this purpose only a pseudo random number ξ is required and the new configuration is selected according to Fig.(8.2).
- c) Store in the file the configuration x_n and the related weight b_{x_n} .
- d) Set $n = n + 1$ and go to (c) until $n = N$, then stop.

B.1.1 Second step: computation of correlation functions

After this calculation the second step is to compute correlation functions using all the information x_n, b_{x_n} stored in the file.

The calculation of the energy as a function of l , allowing to obtain a plot such as the one in Fig.(8.2), can be therefore obtained without repeating the Markov chain for each different l :

- a) read the file (by splitting it into smaller pieces if it is too large to fit the computer memory).
 b) at a given iteration n compute all the necessary correcting factors up to $l \leq l_{max}$ using that:

$$G_{x_n}^{l+1} = G_{x_n}^l \times b_{x_{n-l}}$$

Compute the average energy using Eq.(8.20) by updating independently both the numerator

$$N^l = \sum_{n>n_0} G_n^l e_L(x_n)$$

and the denominator

$$D^l = \sum_{n>n_0} G_n^l$$

. For the numerator the local energy at iteration n is simply given by $e_L(x_n) = \Lambda - b_{x_n}$, where Λ is the constant shift of the Green function and b_{x_n} is just read from the file. This update can be done for each of the l_{max} independent averages by using the two vectors N^l and D^l . The total amount of time required is proportional therefore only to $l_{max} \times N$, which is usually irrelevant in many practical purposes.

- c) If average of correlation functions are required, and the forward walking (8.33) is necessary, compute the necessary correlation function at iteration x_{n-m} and update the corresponding numerator

$$N_m^l = \sum_{n>n_0} G_n^l O_{x_{n-m}} = \sum_{\bar{n}>n_0-m} G_{\bar{n}+m}^l O_{x_{\bar{n}}}$$

where for convenience we have introduced the index $\bar{n} = n - m$ running over the iterations where the correlation function $O_{x_{\bar{n}}}$ is actually computed. Once \bar{n} is selected and $O_{x_{\bar{n}}}$ is evaluated N_m^l can be updated as a function of both l and m with few operations, whereas the denominator D^l remains the same as in the calculation of the energy. It is convenient in this case to fix $m = l/4$ to a given value, in order to avoid to deal with a very large matrix N_m^l , since only the $m, l \rightarrow \infty$ is meaningful.

- d) If error bars are required, the use of the binning technique is convenient. The averages (b) and (c) are split in partial averages over smaller bins of length $M = N/k$ and the error bars over the whole average quantities can be easily evaluated.

With this kind of scheme, one can explicitly check the convergence in the power method, namely the convergence in l , essentially by no extra cost in computer time. Most of the computational time is indeed spent in the first Markov chain iteration.

Appendix C

O is a semipositive definite operator

We consider here any real wave function $\psi(x)$ and compute the expectation value of O over this state. We show in the following that $\langle \psi|O|\psi \rangle \geq 0$ for any ψ , implying that O is a semipositive definite operator.

By using the definition of O in Eq.(11.2) we get:

$$\langle \psi|O|\psi \rangle = \sum_{s_{x',x}>0} s_{x',x}(\psi/\psi_g)^2(x) - \sum_{s_{x',x}>0} s_{x',x}(\psi/\psi_g)(x')(\psi/\psi_g)(x) \quad (\text{C.1})$$

where $s_{x',x}$ has been defined in Eq.(10.18). In the RHS of the above equation the first term and the second one come from the diagonal matrix elements and the off-diagonal ones of the operator O , respectively. By using that $s_{x',x}$ is obviously symmetric, we can interchange the dummy variables $x \leftrightarrow x'$ in the first term and we can recast therefore the equation in an obviously positive one:

$$\begin{aligned} \langle \psi|O|\psi \rangle &= \frac{1}{2} \sum_{s_{x',x}>0} \frac{1}{2} s_{x',x} [(\psi/\psi_g)^2(x) + (\psi/\psi_g)^2(x')] + s_{x',x}(\psi/\psi_g)(x')(\psi/\psi_g)(x) \\ &= \frac{1}{2} \sum_{s_{x',x}>0} s_{x',x} [(\psi/\psi_g)(x') - (\psi/\psi_g)(x)]^2 \geq 0 \end{aligned} \quad (\text{C.2})$$

This concludes the main statement of this appendix.

Appendix D

E_{γ}^{FN} is a convex function of γ

This follows by writing $\gamma = p\gamma_1 + (1-p)\gamma_2$, for any γ_1, γ_2 and $0 \leq p \leq 1$, thus finding a variational lower bound for $E_{\gamma}^{FN} \geq pE_{\gamma_1}^{FN} + (1-p)E_{\gamma_2}^{FN}$ because the ground state energy E_{γ}^{FN} of H_{γ}^{FN} is certainly bounded by the minimum possible energy that can be obtained by each of the two terms in the RHS of the following equation: $H_{\gamma}^{FN} = pH_{\gamma_1}^{FN} + (1-p)H_{\gamma_2}^{FN}$. The above inequality represents just the convexity property of E_{γ}^{FN} .

Bibliography

- [1] R. Assaraf and M. Caffarel. *Phys. Rev. Lett.*, 83:4682, 1999.
- [2] R. Assaraf and M. Caffarel. *J. Chem. Phys.*, 113:4028, 2000.
- [3] R. Assarafa and M. Caffarel. Zero-variance zero-bias principle for observables in quantum monte carlo: Application to forces. *J. Chem. Phys.*, 119:10536, 2003.
- [4] C. Attaccalite and S. Sorella. *Phys. Rev. Lett.*, 100:114501, 2008.
- [5] R. Car and M. Parrinello. *Phys. Rev. Lett.*, 55:2417, 1985.
- [6] R. Car and M. Parrinello. *Phys. Rev. Lett.*, 55:2417, 1985.
- [7] R. Car and M. Parrinello. *Phys. Rev. Lett.*, 55:2471, 1985.
- [8] M. Casalegno, M. Mella, and A. M. Rappe. *J. Chem. Phys.*, 118:7193, 2003.
- [9] D. M. Ceperley and M. Dewing. The penalty method for random walks with uncertain energies. *J. Chem. Phys.*, 110:9812, 1999.
- [10] M. Holzmann C. Pierleoni D. M. Ceperley. Coupled electron ionmontecarlo calculations ofatomic hydrogen. *Phys. Rev. Lett.*, 2004.
- [11] S. Chiesa and D. M. Ceperley S. Zhang. Accurate, efficient, and simple forces computed with quantum monte carlo methods. *Phys. Rev. Lett.*, 94:036404, 2005.
- [12] N. D. Drummond and R. J. Needs. *submitted to Phys. Rev. B*.
- [13] J.G. Pasta E. Fermi and S.M. Ulam. Studies of non-linear problems. *LASL Report LA-1940*, 1955.
- [14] Bradley Efron. *The Jackknife, the Bootstrap and Other Resampling Plans*. Society for Industrial and Applied Mathematics, 1982.
- [15] C. Filippi and S. Fahy. *J. Chem. Phys.*, 112:3523, 2000.
- [16] C. Filippi and C. J. Umrigar. *Phys. Rev. B*, 61:R16291, 2000.
- [17] C. Filippi and C. J. Umrigar. Correlated sampling in quantum monte carlo: A route to forces. *Phys. Rev. B Rapid Communications*, 61:16291, 2000.

- [18] J.C. Grossman and L. Mitás. Efficient quantum monte carlo energies for molecular dynamics simulation. *Phys. Rev. Lett.*, 94:56403, 2005.
- [19] A. Harju, B. Barbiellini, S. Siljamaki, R. M. Nieminen, and G. Ortiz. Stochastic gradient approximation: An efficient method to optimize many body wave functions. *Phys. Rev. Lett.*, 79:1173, 1997.
- [20] J. M. Wozniak J. A. Izagiurre, D. P. Caterello and R. D. Skeel. Langevin stabilization of molecular dynamics. *J. Chem. Phys.*, 114(5):2090, 2001.
- [21] P. R. C. Kent, R. J. Needs, and G. Rajagopal. *Phys. Rev. B*, 59:12344, 1953.
- [22] I. Stich L. Mitás, J. Grossman and J. Tobik. Silicon clusters of intermediate size: Energetics, dynamics and thermal effects. *Phys. Rev. Lett.*, 84:1479, 2000.
- [23] M. W. Lee, M. Mella, and A. M. Rappe. *J. Chem. Phys.*, 122:244103, 2005.
- [24] Xi Lin, Hongkai Zhang, and Andrew Rappe. *J. Chem. Phys.*, 112:2650, 2000.
- [25] S. Moroni and S. Baroni. Reptation quantum monte carlo: A method for unbiased ground-state averages and imaginary-time correlations. *Phys. Rev. Lett.*, 82:4745, 1999.
- [26] O. Narayan and A. P. Young. Convergence of monte carlo simulations to equilibrium. *Phys. Rev. E*, 64:021104, 2001.
- [27] S. De Palo, S. Moroni, and S. Baroni. *cond-mat/0111486*.
- [28] C. Pierleoni and D. M. Ceperley. Computational methods in coupled electron-ion monte carlo simulations. *ChemPhysChem*, 6:1, 2005.
- [29] E. Schwegler T.Ogitzu S. A. Bonev and G. Galli. A quantum fluid of metallic hydrogen suggested by first-principles calculations. *Nature*, 431:669, 2004.
- [30] Friedemann Schautz and Claudia Filippi. *J. Chem. Phys.*, 120:10931, 2004.
- [31] T. Schneider and E. Stoll. Molecular-dynamics study of a three-dimensional one-component model for distortive phase transitions. *Phys. Rev. B*, 17(3):1302, 1978.
- [32] Martin Snajdr and Stuart M. Rothstein. *J. Chem. Phys.*, 112:4935, 2000.
- [33] S. Sorella. *Phys. Rev. B*, 64:024512, 2001.
- [34] S. Sorella. *Phys. Rev. B*, 71:R241103, 2005.
- [35] Z. Sun and W. A. Lester. *J. Chem. Phys.*, 97:7585, 1992.
- [36] S. Tanaka. *J. Chem. Phys.*, 100:7416, 1994.
- [37] N. Metropolis A.W. Rosenbluth M.N. Rosenbluth A.N. Teller and E. Teller. Equation of state calculations by fast computing machines. *J. Chem. Phys.*, 21:1078, 1953.
- [38] C. J. Umrigar. *Int. J. Quantum Chem. Symp.*, 23:217, 1989.

[39] C. J. Umrigar and Claudia Filippi. *Phys. Rev. Lett.*, 94:150201, 2005.

[40] C. J. Umrigar, K. G. Wilson, and J. W. Wilkins. *Phys. Rev. Lett.*, 60:1719, 1988.